The Dissertation Committee for Mark Edward Fountain Certifies that this is the approved version of the following dissertation:

SYNTHESIS AND STUDIES OF GADOLINIUM TEXAPHYRIN CONJUGATES AND MODEL PLATINUM THERAPEUTIC AGENTS

Committee:

Jonathan Sessler, Supervisor

Eric Anslyn

Sean Kerwin

John Richburg

C. Grant Wilson

SYNTHESIS AND STUDIES OF GADOLINIUM TEXAPHYRIN CONJUGATES AND MODEL PLATINUM THERAPEUTIC AGENTS

by

Mark Edward Fountain, B.A.; M.S.

Dissertation

Presented to the Faculty of the Graduate School of

The University of Texas at Austin

in Partial Fulfillment

of the Requirements

for the Degree of

Doctor of Philosophy

The University of Texas at Austin

August 2008

Dedication

To Michelle and Jennifer who made it possible. Also to dad, who taught us we could do anything we set our minds to.

"Theories should be as simple as possible, *but no simpler*."

- A. Einstein

"…the reflection moves, without argument , as the source."

- Byron Katie

Structure of the Dissertaion and Collaborators

I have chosen a non-traditional format for this disseration in which published papers and preliminary publishable manuscripts together contain relevant background information and form the text of the document. Chapters 2, 3, and 4 are free standing manuscripts with their own introductions, thus they contain some repetition of the information in the introduction.

Chapter 1, the introduction, provides a briefy overview of the Texaphyrin (MGd) synthesis and its conjugates. Additional information is available in the publication "Texaphyrin Conjugates. Progress Towards Second Generation Diagnostic and Therpaeutic Agents." previously published in *Macrocyclic Chemistry: Current Trends and Future Perspectives* (2005), and the publication "Gadolinium texaphyrin-methotrexate conjugates. Towards improved cancer chemotherapeutic agents," published in *Organic and Biomolecular Chemistry*.[1] [2] The remainder of the introduction details published literature which must be credited with the intellectual foundation of this dissertation. This introductory information is largely regarding significant biological chemistry considerations in tumor biology, localization, imaging, and platinum chemistry.

Chapter 2 consists of the manuscript entitled "Motexafin Gadolinium (MGd)-Fluorophore Conjugates: Synthesis and Imaging in A549 Lung Cancer Cells." being prepared for submission to the *Journal of Medicinal Chemistry*.

Chapter 3 consists of the manuscript entitled "Motexafin Gadolinium (MGd)-Malonato-Platinum compounds: synthesis of new platinum conjugates and comparison

with carboplatin in A549 lung cancer cells.“ also being prepared for submission to the *Journal of Medicinal Chemistry*.

Chapter 4 consists of the manuscript entitled “Synthesis of [1-(phenylmethyl)-3,4-diaminopyridinium chloride] dichloroplatinum and Activity in A549 Lung Cancer Cells.“ being prepared for submission to the *Journal of Inorganic Biochemistry*.

All synthetic work was performed by the author. Dr. Hassan Naqui and Dr. Martin Poenie of the University of Texas Department of Cell Biology performed the MGd-fluorophore conjugate cell imaging and toxicity studies, as well as the biological testing of the Pt-quaternary compounds. Biological testing of the MGd-Pt conjugates was performed by Dr. Darren Magda at Pharmacyclics and Dr. Hassan Naqui and Dr. Martin Poenie of the University of Texas Department of Cell Biology. The candidate was responsible for producing initial and intermediate drafts. It is important to stress the fact that Dr. Jonathan Sessler and Dr. Martin Poenie were responsible for polishing all final drafts of manuscripts, as well as this dissertation. Without their help in the writing process and logical flow, the clarity of points significant to a wider audience would have suffered greatly. Credit goes to all the people contributing so much of their time and help in the completing of this work. Errors and omissions, of course, remain the responsibility of the author.

SYNTHESIS AND STUDIES OF GADOLINIUM TEXAPHYRIN CONJUGATES AND MODEL PLATINUM THERAPEUTIC AGENTS

Publication No._____

Mark Edward Fountain, Ph.D.

The University of Texas at Austin, 2008

Supervisor: Jonathan Sessler

The experimental cancer therapeutic agent gadolinium texaphyrin (MGd) is a cationic paramagnetic expanded porphyrin currently being tested as an X-Ray sensitizing (XRS) agent, and is a compound with demonstrated tumor localization. Additionally MGd shows promise as a chemotherapeutic agent, both as a stand-alone agent, and showing activity in vitro with ascorbate via a novel ROS generating mechanism.[3] This dissertation reports the synthesis, characterization, and cell studies of novel MGd-fluorophore, and platinum therapeutic conjugates. Also discussed are cationic Pt agents having cytotoxic activity.

In this research we set out to answer three questions: *i*) can fluorescent conjugates of MGd be synthesized, with observable subcellular localization, different from that of MGd, *ii*) can MGd-Pt conjugates with observable Pt release be synthesized?,

and *iii*) can Pt compounds containing a cationic moiety be tuned to have efficacy comparable to traditional Pt therapeutic agents?

Two MGd-xanthene fluorophore conjugates were synthesized with the goal of using them to probe sub-cellular distribution. The anionic (FITC), and cationic (Rhodamine), fluorophore conjugates demonstrated nuclear and mitochondrial localization, respectively.

In an ongoing project designed to reduce non-specific agent toxicity, a platinum-releasing MGd therapeutic conjugate was synthesized. The MGd-amidopropylmalonato-Pt conjugate demonstrated efficacy equivalent to carboplatin, a classical "non-selective" agent as inferred from in-vitro studies with A549 lung cancer cells. Aqueous stability studies of this conjugate gave results in agreement with hydrolytic loss of Pt, reversible with added Pt-diaquo.

Finally, Pt complexes of amino-1-benzylpyridinium salts were synthesized and found to demonstrate significant cytotoxicity in screening studies. This latter positive development led to the suggestion that complexes of this type could consititute a new class of lipophilic-quaternary-cation Pt therapeutic agents. It is hoped that this series of putative Pt anti-cancer agents will prove useful as both stand-alone therapeutic agents and as the basis for producing conjugate with biolocalizing properties.

Table of Contents

Nomenclature

ACN – acetonitrile

BOC – *t*-butyl carbamate

FITC – Fluorescein isothiocyanate

Futile Redox Cycling – A catalytic oxidation-reduction cycle within cells, generating toxic reactive oxygen species. Also called redox cycling

M – Motexafin, the parent water solubilized texaphyrin ring. The coordinated metal cation is given as a suffix, e.g. MGd, MLu, etc.

MGd – Motexafin gadolinium, gadolinium texaphyrin

PDT – Photodynamic therapy

Rho – Rhodamine

ROS – Reactive oxygen species (i.e. $OH^{\cdot}$,O_2^{-} H_2O_2)

Trans Effect – Activation for substitution on Pt of the position trans to a ligand; halides especially activate the trans position for substitution

Tumor - An abnormal benign or malignant mass of tissue that is not inflammatory, arises without obvious cause from cells of preexistent tissue, and possesses no beneficial physiological function[4]

Chapter 1: Introduction

1.1 TEXAPHYRINS, CANCER AND PORPHYRINS

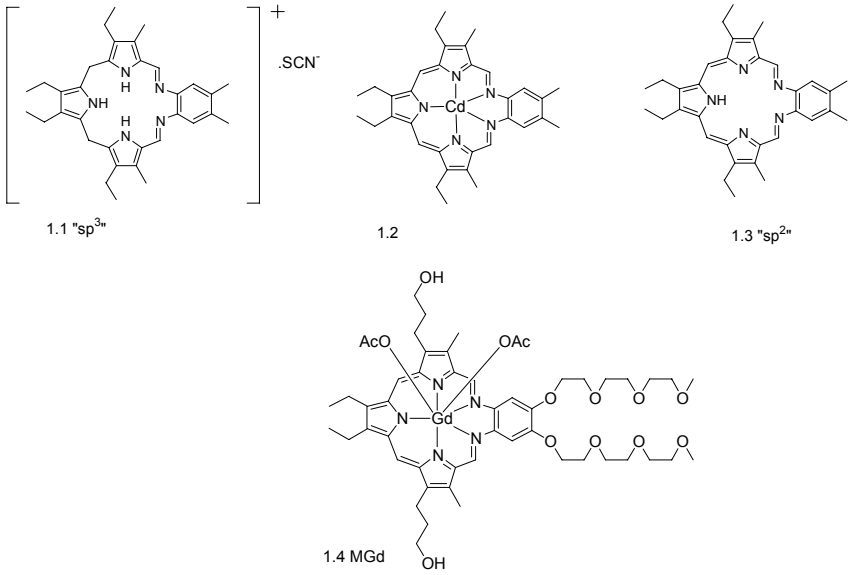

Figure 1.1. Gadolinium Texaphyrin MGd Analogs

In the 1980s Sessler and co-workers first synthesized the expanded-porphyrin "texaphyrin" ring system (Figure 1.1), **1.1** (abbreviated "M" – motexafin).[5] Initially characterized in the solid state as the HSCN salt **1.1**, the "sp^3" form, a 24-electron non-aromatic macrocycle, texaphyrin was later metallated and oxidized to the aromatic 22-electron pentadentate Cd metallated planar "sp^2"complex **1.2**.[6] Much later the unstable metal-free aromatic "sp^2" form **1.3** was also prepared.[7,8] The aromatic form proved to be a planar aromatic macrocycle. As such, this expanded structure with five fixed nitrogen atoms was considered likely to stabilize complexes with the larger lanthanide cations, including paramagnetic gadolinium(III) (MGd) **1.4**.[9] These expectations were, in fact, realized.

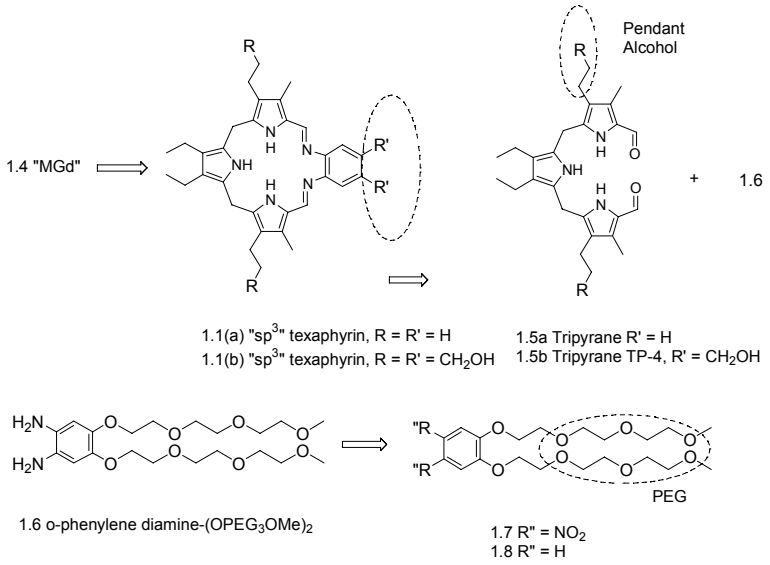

Scheme 1.1. Retrosynthesis showing water solubilizing modifications to MGd.

Due to the therapeutic potential of MGd as a Magentic Resonance Imaging (MRI) diagnostic agent and X-ray sensitizer (XRS), the original organic soluble peripherially-alkylated texaphyrin structure was modified to provide the water-soluble MGd analog **1.4**.[10] Shown retrosynthetically (Scheme 1.1), the "sp^3" texaphyrin ring can be considered as consisting of a tripyrrane fragment **1.5** and an *o*-phenylenediamine fragment **1.6** - **1.8**. The tripyrrane fragment, **1.5a** was modified to **1.5b**, containing two pendant hydroxypropyl groups. Subsequently, the *o*-phenylene diamine moieties were functionalized, ultimately to the bis-PEG_3OMe **1.6**. The oxygenated *o*-phenylene diamine **1.6** in turn was prepared from the stable dinitroveratrole-type compound **1.7** accessed specifically by nitration of veratrole **1.8**. Thus, the synthesis of MGd, consists of catalytic reduction of the dinitro compound **1.7** to the unstable diamine compound **1.6** (prone to oxidation). This was then followed immediately by cyclization with tripyrrane **1.5b**; this

gave the sp^3 texaphyrin **1.1(b)**. Metallation produced the water soluble MGd **1.4**, a compound currently in clinical testing. These functionalized MGd products also demonstrated improved Gd-complex stability as compared to their non-oxygenated analogs prepared earlier. Presumably this reflects the more electron rich nature of the modified texaphyrin ring.[11-13] Additional studies of MGd demonstrated useful redox chemistry, including generation of superoxide in the presence of ascorbate.[14,15] On this basis, MGd was evaluated as a potential dual action MRI contrast agent and radiation sensitizer.[16]

Preliminary animal and preclinical studies demonstrated tumor localization by MRI, and efficacy over controls as an x-ray sensitizer.[17-20] In clinical trials, the use of MGd as a radiation sensitizer gave rise to delays in the time to neurological progression of metastatic brain cancer, although not at the level of significance sufficient to warrant FDA approval.[21]

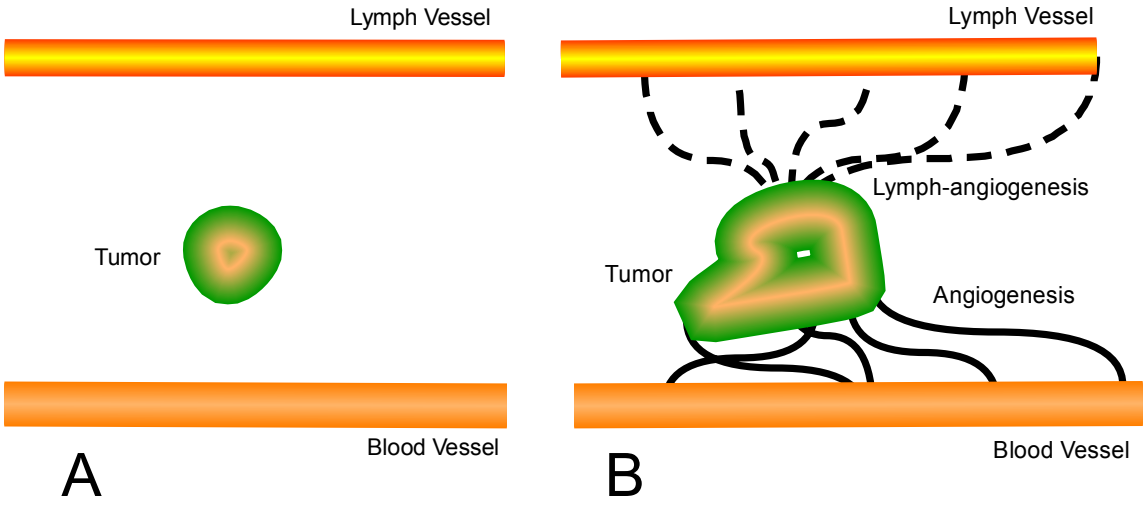

Figure 1.2 (A) Small tumor situated in tissue between blood vessel and lmphatic vessel. (B) Angiogenesis that increases the tumor's blood supply, and lymph-angiogenesis, which has been correlated with disease severity and metastasis.

1.2 TUMOR BIOLOGY, CHEMOTHERAPY AND PORPHYRINOIDS

The foundation of this work was the biological model of considering a tumor as an "organ" within the body. Thus targeting merely becomes a drug delivery exercise. Non-specific localization, giving undesired results, usually results in toxicity.

While the tumor is considered a population of autonomous cells, growing as rapidly as possible, additionally significant, these cells are also genetically unstable.[22] The tumor's genetic instability causes the constituent cells to become more heterogeneous and resistant to therapeutic treatment over time.[23] Additionally, the central region of the tumor usually remaining hypoxic, contains both slowly growing cells, and cells undergoing necrosis (accidental cell death). These more slowly growing tumor cells typically have a higher resistance to chemotherapeutic agents. Thus, often a "cocktail," consisting of a combination of several drugs, is given to overcome this treatment resistance.[24]

The body's blood circulation (Figure 1.2A) supplies a tumor with necessary oxygen and nutrients by diffusion from the blood vessels. With a normal blood supply, tumors typically become hypoxic on reaching 2-3 mm in diameter. A hypoxic tumor secreting hormones can stimulate new blood vessel development (angiogenesis).[25] These new, immature and highly permeable blood vessels (Figure 1.2B) improve the oxygen and nutrient diffusion to the tumor. This results in the accumulation of macromolecules in the tumor by the so-called Enhanced Permeability and Retention (EPR) effect, where a tumor, lacking a lymphatic drainage system, retains macromolecules.[26] The accumulated molecules include serum proteins and certain chemotherapeutic agents.[27,28] This effect has been used therapeutically to target liposomes to tumors.[29] While angiogenesis improves the tumor's incoming blood/nutrient supply, not all tumors have an improved

drainage (lymphatic) system. Recent literature describes tumors that, again by hormone secretion, stimulate the development of a lymphatic drainage systems. The extent of so called "lymph-angioigenesis" has been correlated with the disease severity (i.e. likelyhood of metastasis from the tumors).[30]

Effective drugs minimally must reach their target tissues. Chemotherapeutic agents are typically administered intraveinously. Administration directly to the circulatory system maximizes drug bioavailability and avoids early drug metabolism occuring in the GI tract and liver (first pass effect). Often the administration of therapeutic agents having poor tumor localization is accompanied by systemic toxicity. This systemic toxicity can be caused by the metabolism of these drugs in non-target tissues. Theoretically, drugs with selective localization will display reduced systemic toxicity due to lower non-target tissue metabolism. In accord with such thinking, chemotherapeutic agents that specifically localize in tumors have long been desired. The question has thus focused on how to achieve this effect. Enhanced localization at a target organ or site has been correlated with appropriate solubility, receptor binding, or rate of drug uptake within the target tissue.[31-39] While drugs with these attributes may initially be distributed throughout the body, localization is often see subsequently through some combination of organ, structural, or cellular affinity. Therapeutic porphyrinoids, in analogy to biological porphyrinoids, represent a class of compounds that demonstrate accumulation in tumors. Additinally, porphyrinoids have been used synergistically in photodynamic therapy (PDT) demonstrating cytotoxic activity by the generation of reactive oxygen species (ROS).[40] The texaphyrins are members of the "expanded porphyrin" class of macrocycles. These (larger) expanded porphyrins have demonstrated coordination of larger metals and allowed development of several additional experimental therapeutic agent that appear to be biologically well-tolerated.[41]

The porphyrinoids, (pyrrolic heterocycles containing four central nitrogen atoms), are widely distributed biologically, and are recognized for performing a variety of functions. These important redox-active molecules generally coordinate a core metal as in chlorophyll (Mg), cytochrome c (Fe), horseradish peroxidase (Fe), vitamin B-12 (Co), and heme (Fe). Taken in concert, these prosthetic groups help reduce CO_2 to sugar, oxidize molecules, transport electrons, decompose peroxides, catalyze molecular rearrangements, and transport oxygen, respectively.[42-47]

Porphyrinoid molecules **1.7** – **1.10**, (Figure 1.3,) have been used in Photodynamic Therapy (PDT) applications, **1.7** (n = 1) since 1912. They were shown, as early as 1924, to localize selectively in tumors, and have been utilized in cancer PDT applications since the 1930s.[48-50] Photofrin,® **1.7**, Figure 1.3, is solubilized as the anionic polycarboxylate, was the first clinically approved porphyrinoid PDT agent.[51,52] Photofrin,® a conceptual

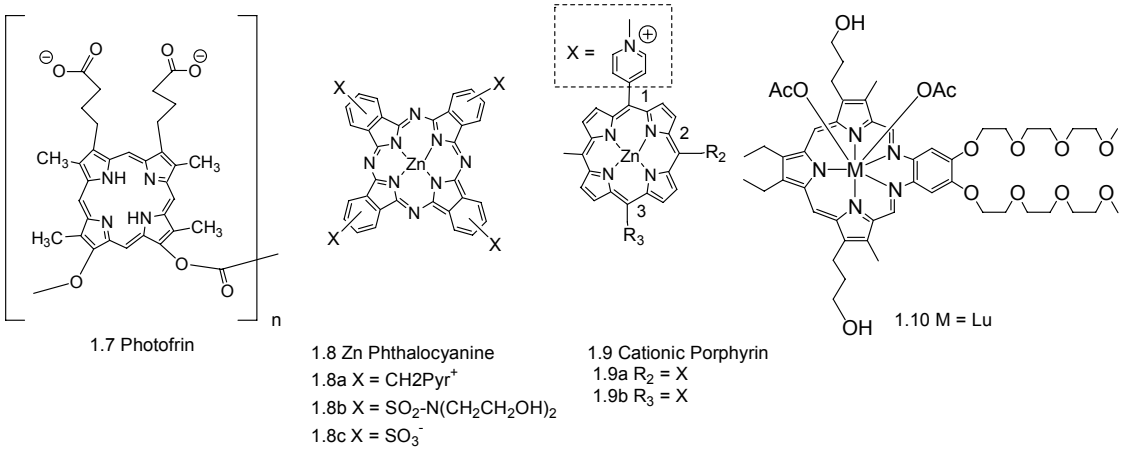

Figure 1.3 Therapeutic PDT: Photofrin **1.7**, Zn phthalocyanine **1.8**, cationic porphyrin **1.9a**, **1.9b**, and MLu **1.10.**

predecessor of MGd. is a complex mixture of porphyrin oligomers (active agent n = 2-3). It gained Canadian regulatory approval in 1993 after decades of clinical work starting in

the 1960s. The drug demonstrated severe photo-toxicity, leading subsequently to the more purified form Photofrin II.® It also inspired the synthesis of additional agents, whose syntheses and use has been extensively reviewed in the literature.[50,53-56]

The in vivo efficacy of Photofrin® **1.7** and its analogues has found to be correlated with lipophilicity and, to some extent, serum binding.[53,57-62] These lipophilic porphyrinoids are generally thought to be bound to serum albumin during circulation.[63] Supporting the hypothesis of serum uptake by tumors is the activity demonstrated by low density lipoprotein (LDL), a serum component that has been utilized to develop therapeutic conjugates.[64] Other serum binding effects have been observed in vivo, where non-toxic porphyrinoids displaced serum bound therapeutic porphyrinoids, resulting in higher efficacy.[65,66]

An additional study with oligoporphyrins - the higher molecular weight fraction of Photofrin® demonstrated higher tumor retention of the lipophilic oligomers (n = 4, 5, 7, 8).[67] Similarly, MGd **1.4**, on reacting with oxalate forms a coordination polymer, which was found to have improved tumor uptake relative to the monomeric form.[68]

One of the difficulties associated with developing porphyrinoid therapeutic agents is that some degree of water solubility is required for formulation along with a reasonable degree of lipophilicity to enhance activity as discussed above.[69] Solubility, in several recent cases, has been effected through the use of the amphiphilic methoxy ethoxy group, polyethylene glycol, termed "PEG" for short (see Scheme 1.1, **1.8**). This is due to many PEG functionalized porphyrinoids demonstrating both adequate water solubility and amphiphilic/lipophilic characteristics. It is believed that the non-toxic PEG embeds in membranes, as demonstrated from cell fusion studies, and assists in the cellular uptake of compounds that may otherwise lack toxic effects.[70,71] The amphiphilic PEG group has been used extensively as a solubilizing agent for both chemotherapeutic agents (e.g.

doxorubicin, Pt-malonates), as well as therapeutic conjugates.[72,73] This is particularly true in the porphyrinoid class, with examples including Hp-Pt and MGd-Pt conjugates.[72-76]

1.3 CELLULAR UPTAKE AND LOCALIZATION OF MATERIALS

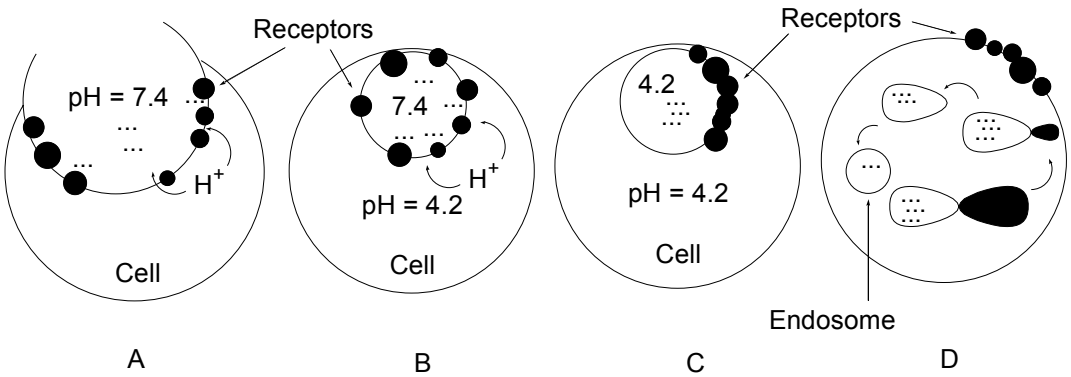

Figure 1.4 Endocytosis: A) Cave-like uptake structure, B) Vesicle acidification and substrate release, C) Receptor clustering, D) Receptor return to membrane leaving vesicle containing substrate molecules.

The uptake of material into cells is typically mediated by the continual process of endocytosis (Figure 1.4A – 1.4D). Cellular uptake of porphyrinoids is generally attributed to this "absorptive endocytosis," which has been referred to as a "fluid-phase" mechanism.[77] In this process, cave-like structures are formed, mediated by the protein caveolin, and the exogenous agent is engulfed along with a portion of the surrounding fluid (Figure 1.4A). Uptake can be non-specific. However, in some cases exogenous species taken in are receptor bound. In both cases internal chambers, called endosomes, (Figure 1.4B) are formed. During endocytosis, the formed endosome is acidified, with the pH changing from 7.4 to 4.2, (Figure 1.4B - C). This results in the release of the receptor bound compounds from the cellular receptors (Figure 1.4C), which are recycled to the cell membrane (Figure 1.4D). The pH within the endosomes is thought to become

progressively lower on moving further into the cell, a process that has has been suggested as a sorting mechanism in sub-cellular trafficking.[78]

As noted above, the internalized materials are initially contained in endosomes.[79] In normal cells, these endosomes process and distribute molecules to the cytoplasm or organelles. Alternatively the molecules can be re-excreted from the cell.[80] Lipophilic, amphiphilic and positively charged molecules, generally pass rapidly out of the endosomes. [81,82] Macromolecules that are too large to pass through the lysosomal membrane demonstrate retention until digested. Anions compartmentalized within the endosome, repelled by the negative charge on membrane phospholipids, may be retainied in the endosomes until excreted from the cell.[80]

As noted above, lipophilicity plays a significant role in the in vivo tumor localization of porphyrinoid therapeutic agents. While the localization and therapeutic activity of PDT agents **1.7-1.10**, has been extensively studied at the sub-cellular level, there are relatively few examples attributing therapeutic activity to (extracellular) tumor vasculature damage.[60,62,83-85] Due to the high reactivity of the reactive oxygen species (ROS) these agents produce, the damage to biomolecules they effect is localized. Nonetheless there is a general attempt is to develop ROS agents that stimulate the apoptosis pathway, resulting in "natural cell death." The cellular uptake and movement of these ROS generating PDT agents has been imaged utilizing fluorescence microscopy.

For instance porphycene dimer (PcD) **1.7** localizes at the cell membrane and in the lysosomes, and was found to be active therapeutically upon irradiation and to give rise to apoptosis.[49] From imaging studies it was found that (anioinic) porphyrin PDT agents demonstrate sub-cellular redistribution during and after therapeutic incubation, which may correlate with efficacy.[86]

One specific example is provided from fluorescence-based imaging studies involving Zn phthalocynanines (ZnPcy). The localized, charged (+/-) ZnPcy species (Figure 1.3 **1.8a, 1.8b)** were observed to relocalize on irradiation. The least toxic, (hydrophilic) uncharged derivative (**1.8c**), which demonstrated Golgi localization, showed a slight cytoplasmic distribution on irradiation, in agreement with the above mentioned lipophilicity-toxicity correlation.[87] In this case derivatives **1.8a**, **1.8b**, and **1.8c** with peripherial positive, negative, and neutral substitution demonstrated efficacy, with ED_{50} values of 0.27, 3.02, and 34.4 uM, respectively, being observed.

A number of cationic porphyrins have demonstrated specific sub-cellular localization, often mitochondrial, as well as DNA binding activity.[88] Using the cationic porphyrinoid PDT agents **1.9a** and **1.9b** differing sub-cellular localization and efficacy patterns have been observed.[89] Altering the position of the charge on the porphyrin ring periphery from 1,2 to 1,3 in PDT agents **1.9a** and **1.9b**, respectively, has led to alterations in the respective localization (mitochondria vs lysosomes) and efficacy (5:1 ratio) when used as PDT agents. The expanded porphyrin MLu **1.10**, while similar to MGd both structurally and in it's tumor localizing properties, is therapeutically active as a PDT agent.[90,91] Several additional porphyrin-type photosensitizers and their targets have been discussed in the recent literature.[92,93] Nonetheless their specific cellular uptake and sub-cellular distribution properties (SAR type correlations) are at present poorly understood. [49,94]

Historically, the high therapeutic activity of MGd has been thought to be due to mitochondrial uptake and generation of reactive oxygen species (ROS) such as H_2O_2 and hydroxyl radical ($OH^{\cdot}$) under therapeutic conditions, triggering apoptosis.[49] In fact high uptake of MGd in isolated mitochondria has been demonstrated. [95]

From the above studies, it can be concluded that lipophilic, cationic porphyrinoids generally demonstrate superior tumor uptake and organelle localization. Anionic porphyrinoid species are typically observed in lysosomes or near the cell membrane, and in the studies carriied out to date, demonstrate lower efficacy. Finally, hydrophilic compounds demonstrated the lowest activity.

1.4 CELLULAR IMAGING: PORPHYRINS, TEXAPHYRINS AND XANTHENES

Of the recent imaging studies involving therapeutic porphyrinoid species, a survey of the literature indicates 427 publications for PDT agents and 9 for radiation sensitizers. Most of the latter were concerned with Mn porphyrin or MGd. The relatively large number of biological fluorescent imaging studies carried out with porphyrins and related species reflects their specific uptake by abnormal tissue, long wavelength fluorescence (e.g. 650, 720 nm) properties, and adequate fluorescent quantum yield (0.09-0.12) all of which facilitate microscopy studies. [96,97]

The advent of confocal microscopy and charge coupled device (CCD) cameras with both higher sensitivity and the ability to perform spectral analysis of images has also made it easier to carry out localization studies and helped with differentiation of fluorescent species.[98,99] Commercial detectors also have good sensitivity in the $\geq$ 600 nm region that corrleates with that of typical porphyrin fluorescence. This is useful since fluorescent studies in biological systems using fluorophores that emit above 600 nm allows for analysis that is generally free of background interference, whereas in the 400-500 nm range fluorescence from endogenous species (e.g. the green fluorescent protein (GFP)) leads to a high background signal.[100] This, in turn, has made it possible to follow molecular trafficking events at the sub-cellular level in real time.[101]

The subcellular imaging of MGd is technically challenging due to photobleaching, an inherently low fluorescent quantum yield (2.8×10^{-3}), and a fluorescence emission maximum in the 700-800 nm region where detectors are relatively insensitive.[49] Imaging studies carried out using Interferometric Fourier Fluorescence Microscopy in EMT6 mammary sarcoma cells MGd allowed punctate localization at t = 4 hours after administation to be noted. The MGd distributed in lysosomes, endoplasmic reticulum, and mitochondria, as inferred from comparative organelle staining analysis. After 48 hours, MGd was seen in the nucleus in 15% of the cells.[102]

Weakly fluorescent porphyrinoids, such as MGd, can be imaged directly in cells; however, due to their low endogenous fluorescence, high sensitivity detectors and specialized image processing are required. Species that lack endogenous fluorophores must be conjugated to a fluorophore to utilize the aforementioned imaging technique. Such fluorescent labeling is, however, expected to provide species that may be used for detecting apoptosis, macromolecules, enzyme activity, and imaging the location of processes and molecules, etc. It is thus expected to help in the search for new cancer drugs.[92,103]

Non-fluorescent biomolecule imaging and localization is technically challenging; thus, fluorophores with significant fluorescence quantum yields are often appended to molecules of interest to improve detection. However, such modification may alter the charge on the conjugate or otherwise produce structural changes. The magnitude of metabolic changes from "normal," created by fluorescent tagged substrates is unknown. The tagged system, however, is observable.

The xanthene class of fluorophores (Figure 1.5) are endowed with high quantum yields (0.95-0.98). The dyes, FITC, fluorescein, and rhodamine have thus been widely used to prepare conjugates for biological molecule localization studies. The anionic

species, fluorescein, although a strong fluorophore, has been reported to be rapidly excreted from cells by anion pumps.[104] Rhodamine demonstrates both selective cancer-cell localization and PDT activity.[105-108] The cationic and slightly lipophilic Rhodamine 6G demonstrates localization to the mitochondria, whereas the highly lipophilic octadecyl rhodamine is retained in cell membranes.[109]

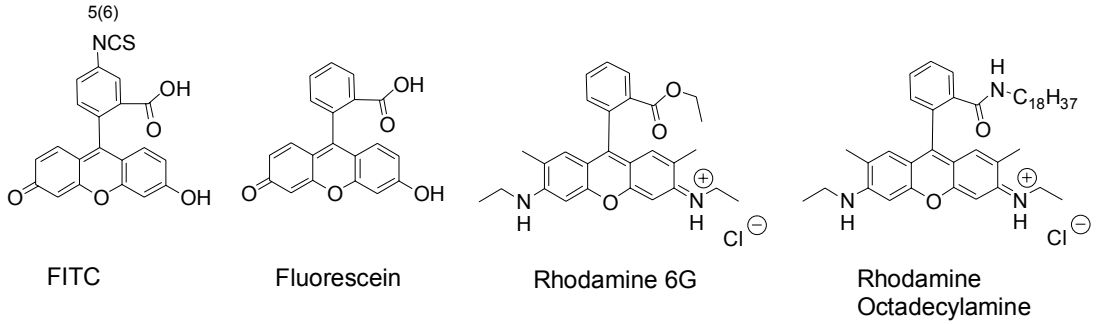

Figure 1.5 Xanthene fluorophores used in bioconjugation for imaging studies.

The xanthene isothiocyanates (i.e. FITC, RITC), are synthetically accessible and convenient to use. They react directly with amines and alcohols to form the corresponding thioureas and thiocarbamates, respectively. The reactive FITC has been used in DNA binding studies. It reacts directly with anilines to generate binding fluorophores.[110] Rhodamine 6G can be reacted with primary amines to give the amide directly.[111-114] Rhodamine 6G has also been reacted with linear diamines to give solubile fluorophores with a remaining free amine functionality that can be used for further conjugation to molecules of interest. [110] The cellular distribution and retention of these fluorophores is related to both the charge and lipophilicity of the molecule.

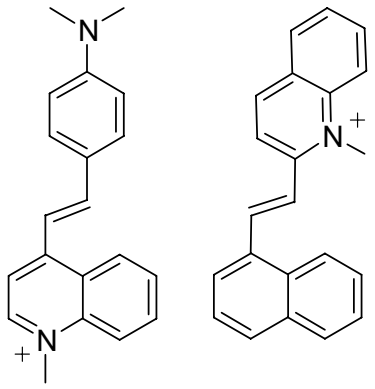

1.11 **1.12**

Figure 1.6 – Synthesized styryl quaternary cations demonstrating subcellular mitochondrial **1.11** and nuclear **1.12** localization.

In an elegant combinatorial study (Figure 1.6), 276 fluorescent styryl quaternary cations were synthesized. Of these, 119 demonstrated subcellular localization patterns.[115] In total, 53 demonstrated localization to the mitochondria or nucleus. Structure **1.11** is one of the 46 mitochondrially localizing compounds, while structure **1.12** is one of the seven nuclear localizing compounds. While, in this series, both compounds are structurally similar, more diverse compounds demonstrate mitochindrial uptake, whereas the range of nuclear localizing compounds is more limited. Both the mitochondria and nucleus possess dual membranes. These sites, from which apoptosis mechanisms are triggered, are important sub-cellular localization targets for therapeutic agents.

1.5 ROS GENERATION – PDT, X-RAY, AND REDOX CYCLING

As discussed above, the specific tumor targeting of porphyrinoids and Reactive Oxygen Species (ROS) generating agents is desirable to reduce systemic toxicity. At the subcellular level, the location of ROS generating agents is related to efficacy. Especially

in this context, the concept of catalytic therapeutic agents (not consumed in the generation of toxic species) is attractive.

The significance of sub-cellular localization of these agents is underscored by specific ROS species demonstrating high reactivity. For example, hydroxyl radical ($HO^{\cdot}$), has been reported as surviving under cellular conditions only long enough to travel c.a. 1% of the cancer cell length (0.1 nm/ 10 nm) before reacting with biomolecules.[49] Thus, the development of therapeutic agents specifically localizating to sites where ROS damage triggers apoptosis could, theoretically, increase efficacy.

Since 1900, therapeutic generation of (ROS) has been extensively studied, using both PDT agents and X-ray therapy. Catalytic porphyrinoid ROS generators are energetically driven by X-rays (MGd), light (PDT, i.e. Photofrin), or more recently, cellular redox systems (MGd).

X-ray + X-ray sensitizer (XRS) → $XRS^{\cdot} + e^{-}$

(loss of inner shell electrons)

($H_2O \rightarrow H_2O^{\cdot} + e^{-}$)

($H_2O^{\cdot} + H_2O \rightarrow OH^{\cdot} + H_3O^{+}$)

$OH^{\cdot} + OH^{\cdot} \rightarrow H_2O_2$

$OH^{\cdot} + H^{\cdot} \rightarrow H_2O$

Figure 1.7 Generation of ROS under X-ray conditions.

Porphyrinoid PDT agents provided the first effective method for ROS generation. Mechanistically PDT uses light to excite porphyrin molecules and generate singlet oxygen, which can serve a precursor for superoxide and ($OH^{\cdot}$) radicals.[49] The high absorption of UV light by biological tissues however, provides a limit to the usefulness

of PDT as a non-invasive technique. The extensive work devoted to producing new agents with suitable absorption features has been reviewed.[116] There continues to be work to develop two-photon techniques with far-UV/near-IR agents, giving tissue transparency and adequate energy for PDT generation of ROS.[49]

X-ray irradiation (Figure 1.7) is one of the most widely used cancer therapy techniques; mechanistically, exposure of atoms to high-energy X-rays results in the ejection of inner shell orbital electrons. These solvated electrons react directly with water, generating radical species. Most radiation damage is attributed to secondary reactions of free radicals.[117] Thus, radiolysis primarily produces H_3O^+, e^-, and $OH^{\cdot}$, initiating the cascade illustrated in Figure. 1.7.

With its low toxicity and high tumor affinity, MGd was considered as a possible XRT agent.[14] Initially it was proposed that the low affinity of MGd for $HO^{\cdot}$ radicals would make it an effective agent.[118] The radioenhancing properties of MGd have been evaluated in animal models and reviewed clinically.[118-121]

Ascorbate, in combination with MGd via redox cycling, demonstrates enhances toxicity and growth inihibition of uterine cancer cell line MES-SA as detected by MTT assay. This combination also enhances the radiation response in A549 and MES-SA cells, presumably as a result of oxidative stress induced by futile redox cycling.[3,122] The highly reactive ROS species generated can be detected by UV (benzidine) and dichlorofluorescein assays.[123] [15]

Ascorbate, considered "non-toxic" is attractive as an antioxidant, cancer therapy agent, and as an adjuvant. Also, ascorbate has been popularized by Linus Pauling; however, it remains controversial as a general dietary supplement, at least at the high dosage levels recommended by Pauling.[124-128] In fact, both efficacious and adverse effects have been reported for ascorbate. In Jurkat cells, H_2O_2 in the presence of ascorbate leads

to a 15-fold increase in DNA lesions, and an increase in both apoptosis and necrosis.[129] Jurkat-ascorbate adjuvant cell studies with the chemotherapeutic agents etoposide, melphalan, As_2O_3, and camptothecin demonstrated no effect for etoposide and melphalan. Decreased apoptosis was seen on exposure to As_2O_3, while camptothecin decreased apoptosis, but not necrosis.[130,131]

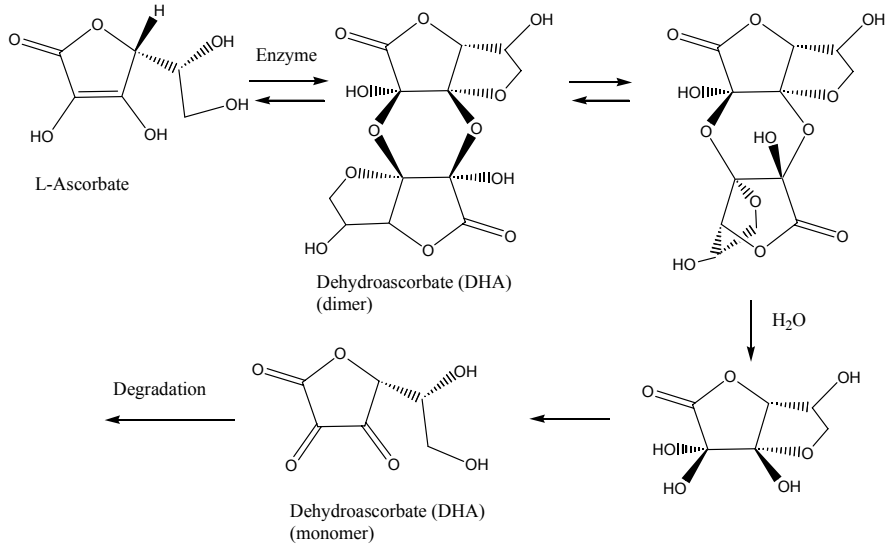

Scheme 1.2 Metabolic pathway for the decomposition of ascorbate via DHA dimer to DHA under biological conditions.

Complicating therapeutic use is the instability of ascorbate in aqueous solution (Scheme 1.2), a phenomenon that has been discussed in the pharmacology literature and specifically evaluated in cell studies.[132,133] A spectrophotometric study of the stability of ascorbic acid has implicated a decomposition pathway that leads to dehydroascorbate, ROS, and diketogulonic acid.[132] Studies also indicate that ascorbate is poorly taken up by cells. Multiple studies along these lines have used dehydroascorbate (DHA), a product of ascorbate oxidation, both because DHA is rapidly taken up by cell glucose transporters

and subsequently reduced to ascorbate, and because it is thought to preclude the generation of ROS in culture media.[130,131]

1.6 Development of Chemotherapeutic Agents: A Targeting Rationale.

Therapeutic cancer approaches have been researched for more than a century, beginning ca. 1900 with non-invasive PDT and X-ray therapy. The anticancer agent mustine was developed from "mustard gas" after WW I, reported in clinical trials as early as 1942. A more widely publicized story is that development follows the decreased white blood cell counts observed in survivors of the sinking of a ship laden with mustard gas, in Bari, Italy in 1943. Following this incident it was hypothesized that such agents could be used for treating leukemia. [134] The analog carmustine is still in use today, specifically for glioblastomas. The folate antagonist methotrexate was developed in the 1950s following the observation that cancer patients given folate suppliments fared worse than untreated patients. Cisplatin was an accidental discovery in the 1960s. More recently, tumor localizing antibody and porphyrinoid experimental agents have been developed. Current chemotherapy utilizes a list of approximately 60 clinical agents. [135] Few of these current cancer chemotherapy agents localize to tumors. As a consequence, systemic toxicity during treatment remains a significant limitation.

Due to the drawbacks of non-targeting therapeutic agents, considerable effort has been devoted to improving localization. A further incentive for such studies is that targeting can be used to overcome some common resistance mechanisms such as lowered uptake, increased excretion, or enhanced detoxification/reduced activation of untargeted prodrugs.[136,137] Typical conjugates consist of a biomolecule targeting agent, attached to a fluorophore for imaging, a cytotoxic agent for chemotherapy, or both.[138-140] Therapeutic

conjugates containing biotin, vitamins, and cholesterol have been evaluated as tumor-specific conjugates.[141,142] Some early tumor localizing conjugates were therapeutically inactive because the cytotoxic agent could not be cleaved from the targeting moiety.[143,144] Current conjugates often contain cleavable bonds designed to take into account such factors as are needed to release the chemotherapeutic agent under the anticipated therapeutic conditions.[145,146]

While a number of biomolecules and a few synthetic agents display selective tumor uptake as a result of fluid-phase or absorptive endocytosis, synthetic polymers such as PEG, while lacking a specific recognition unit can also provide for drug targeting agents, utilizing the EPR effect, as previously noted.[77]

In an effort to develop texaphyrin-based targeted agents, two approaches have been previously reported by this group. Both underscore the importance of chemotherapeutic agent release. The first series consisted of methotrexate (MTX) chemotherapeutic conjugates.[2] While activity was observed in conjugates utilizing a readily hydrolyzed ester linkage, the more hydrolytically stable amide linked conjugates were inactive. The second series consisted of Pt chemotherapeutic conjugates.[147] As will be clear from the discussion below, the latter have been less successful than the MTX conjugates.

1.7 CONJUGATES FOR TUMOR TARGETING AND PT RELEASE

Several Pt-conjugates have been reported in the literature, synthesized in an attempt to develop agents that target tumors and reduce the systemic toxicity often encountered with non-specific single agents. These experimental agents reflect a repeated

cycle of synthesis, discovery of limitations, and subsequent structural modifications leading to further synthetic attempts.

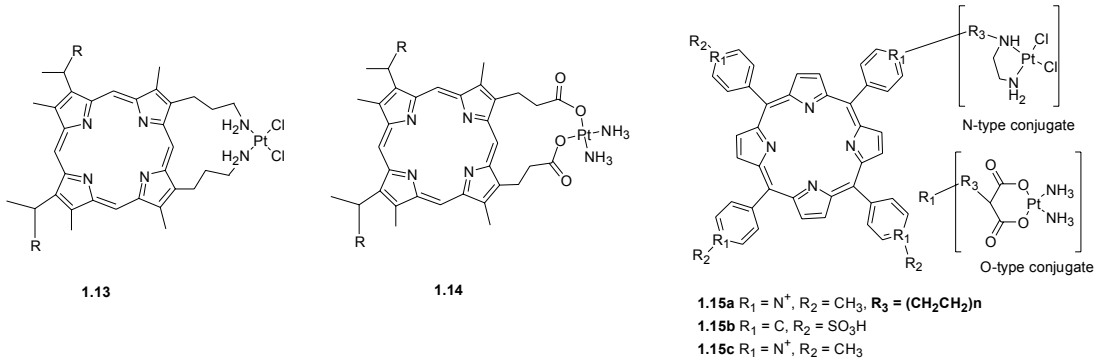

Figure 1.8 Porphyrin-Pt conjugates: non-labile (**1.13**, **1.15a**, **1.15c**: N-type conjugates), labile (**1.14**, **1.15c**: O-type conjugates).

Of particular interest to us were the porphyrin-Pt conjugates, (Figure 1.8).[74] Structures **1.13** and **1.14** were based on a lipophilic hematoporphyrin (Hp) motif of porphyrins solubilized with ionic charges or PEG solubilizing substituents.[74,148-151] Series **1.15a - c** was based on tetraphenyl porphyrin motif, solubilized with ionic charges.[152,153] In these cases, the non-labile N-Pt conjugates **1.13** and "N-type conjugates," generally lacked activity whereas the ester-Pt conjugates **1.14** and "O-type conjugates" were more active. In O-Pt conjugates (**1.15b**, **1.15c**), solubilization with PEG350 or PEG 550 led to activity, as did the use of a relatively lipophilic PEG_2 conjugate. In series **1.14** appending long-chain (n = 17) PEG substituents was found to improve the activity in cell studies, albeit only to a point equivalent to that displayed by cisplatin. [150,154] Activity was also observed for the cationic O-Pt conjugates (solubilized with either $CH_2N(CH_3)_2$ or $CH_2N(CH_3)_3^+$). Cationic O-type Pt conjugate **1.15c** displayed the highest activity of the TPP series.

This research group previously synthesized, shown in Figure 1.9, MGd-PEG-diaminoplatinum and aminosuccinato-platinum conjugates **1.16 - 1.18**.[147] Unfortunately, these systems demonstrated low activity when subject to in vitro biological testing. In conjugates **1.16** and **1.17**, attachment was effected via piperazine. From previous SAR studies of several N-side conjugates, possible spatial limitations for the interaction of the Pt(II) centers with DNA were proposed to account for the low activity of **1.16** and **1.17**. In the case of the aminosuccinate species, **1.18**, the poor performance could be ascribed to possible rearangement as discussed below.

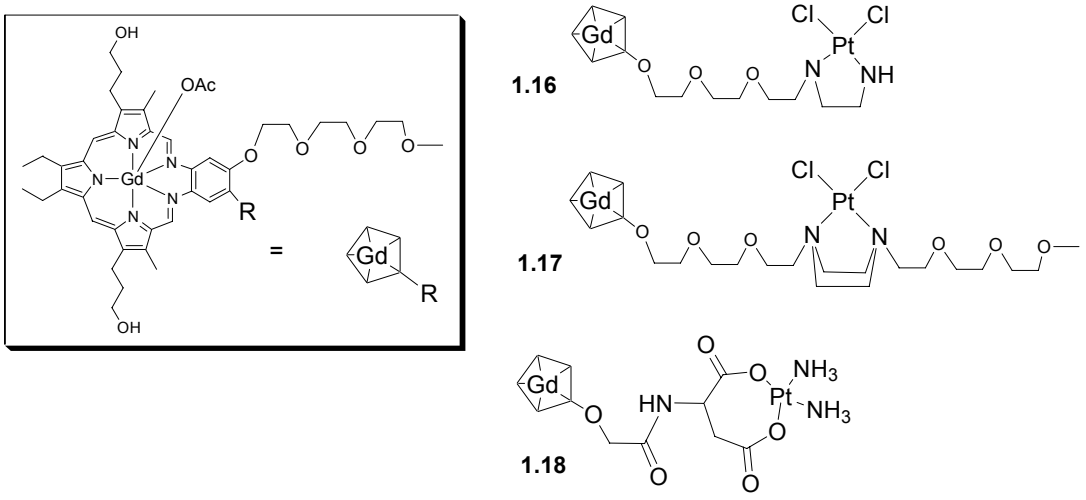

Figure 1.9 Texaphyrin-Pt conjugates: non-labile (**1.16**, **1.17**), labile (**1.18**)

Other researchers have developed PEG solubilized malonato-Pt conjugates. In these compounds (Fig. 1.10) a malonate moiety is attached to the PEG portion with a propyl spacer **1.19**,[155] or a direct amidomalonate connection **1.20**,[75] is utilized. The species produced in this way demonstrated efficacy. Interestingly, while **1.19** demonstrated activity, the same compound lacking folate, a non-targeted PEGylated

conjugate, formed more DNA adducts than **1.19**.[155] An amidomalonate-Pt conjugate **1.20**, containing a Nuclear Localizing Sequence (NLS) to facilitate transport of the molecule to the cell nucleus, demonstrated rapid hydrolysis, this premature platinum release ($t_{1/2}$ = 1 hour) limited the therapeutic usefulness.[75] A polymeric formulation of this amidomalonate type of conjugate however, has demonstrated a release rate suitable for therapeutic purposes.[75,156]

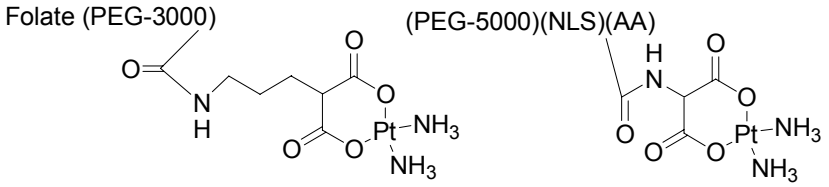

1.19 **1.20**

Figure 1.10 Conjugates for targeted Pt-release

The classes of Pt conjugates most reported in the literature (Figure 1.11) are non-labile diamino coordinating species **1.21**, and the labile aminomalonates **1.22**, amidomalonates **1.23**, lipophilic alkyl (or PEG) malonates **1.24**, and aspartate complexes **1.25**. These species have been conjugated to alkanes, long-chain PEG, steroids, bio-molecules, enzyme inhibitors, and DNA intercalators.[73,157,158]

The first synthesized non-labile (Pt-N) conjugates **1.21** generally demonstrated poor efficacy when compared to cisplatin. The subsequent platinum aminomalonates **1.22**, while considered more labile, have been reported to rearrange, giving an amine-bound (Pt-N) platinum species **1.22a**. Separately, these compounds demonstrated poor anticancer activity.[159-162] The amidomalonates **1.23** were prone hydrolysis, the specifics of the reaction proving to be quite complex.

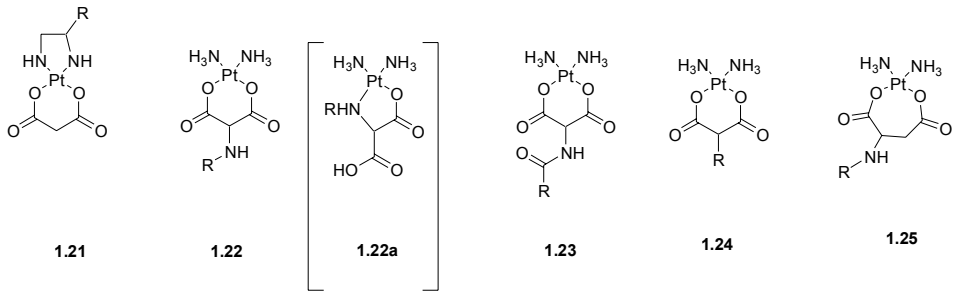

Figure 1.11 Types of Pt-complexes used experimentally and as conjugates : N-side (**1.21**), O-side (**1.22 - 1.25**)

Analogues of the clinically approved carboplatin, the Pt alkyl malonates **1.24**, undergo displacement of platinum under aqueous conditions. Alterations in the substitution at the malonate β-carbon have been demonstrated to lead to changes in efficacy. [73,163-166] The lability of the carboxylates has been shown to be important in regulating the stability of these Pt drugs.[167] The most active porphyrin conjugates were those of the O-Pt type that released the therapeutically active diaquo-type species from malonates structurally analogous to **1.24**.[154]

1.8 PLATINUM THERAPEUTIC AGENTS

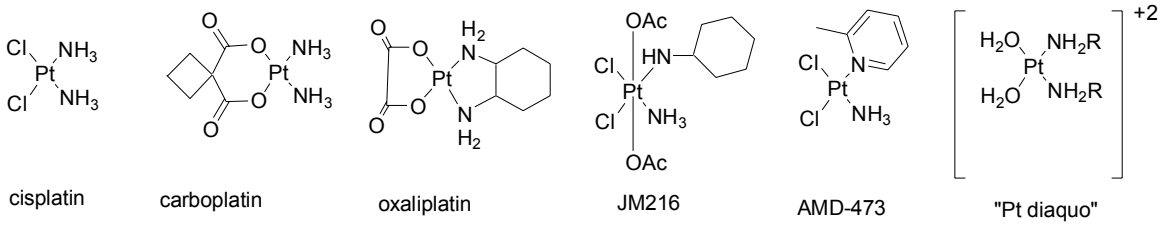

Figure 1.12 Clinical Pt therapeutic agents cisplatin, carboplatin, oxaliplatin, JM216, AMD-473, and the active form "Pt diaquo".

Inorganic cisplatin (Figure 1.12) is a DNA-modifying agent that forms interstrand and intrastrand crosslinks and acts as an inhibitor of both bacterial and mammalian cell (tumor) growth.[168-170] One of the original inorganic drugs, cisplatin was approved by the FDA in 1978. Although cisplatin is used worldwide for the treatment of testicular and ovarian cancer, its use is accompanied by significant kidney toxicity, and some tumors demonstrate resistance.[168,169,171-173] Extensive study has elaborated mechanisms of action, profiles, specificity, applications, and patterns of resistance. Some SAR patterns have been put forward.[174] Numerous analogues of cisplatin have been synthesized (fig. 1.12), including carboplatin initially and more recent analogues such as the diaminocyclohexane (DACH) derivative oxaliplatin, Pt(IV) diacetate JM216 and picoline derivitive AMD-473, etc.[175-178] These latter species show particular promise in overcoming resistance. All of the platinum(II) compounds discussed here contain labile (Cl or CO_2^-) ligands, which give "diaquo," type species on hydrolysis. The non-labile (NH_2R) ligands and their significance will be discussed later.

In 1989 the FDA approved the clinical use of the second generation drug carboplatin, a complex that demonstrates lower kidney toxicity compared to cisplatin.[179] Developed more recently, the third-generation drug oxaliplatin received European approval in 1999, and US approval in 2004. This species has proved useful in treating resistant colorectal cancer. Both carboplatin and oxaliplatin differ from cisplatin, being more lipophilic with cyclobutane-malonate and diaminocyclohexane (DACH) as labile and non-labile ligands for the bound Pt(II) centers, respectively. Different systemic toxicity is observed in the latter analoges; carboplatin may cause deafness, while oxaliplatin has been reported to cause nervous system damage.[180]

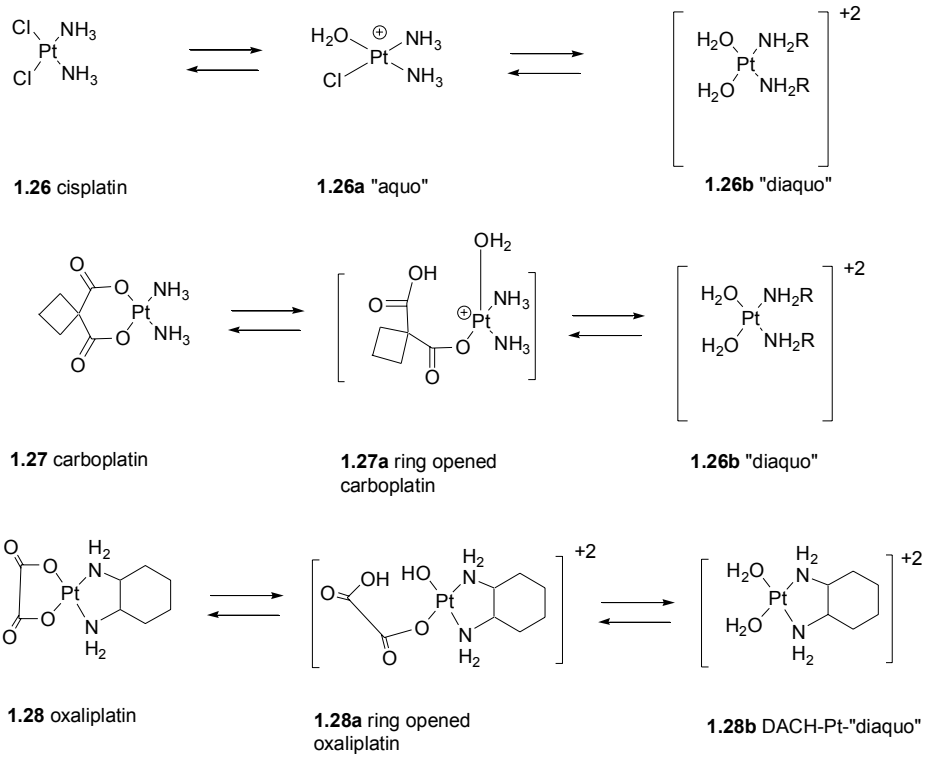

Figure 1.13 Hydrolysis equilibrium for active Pt therapeutic agents.

The clinically approved drugs cisplatin, carboplatin, and oxallipaltin (Figure 1.13) have therapeutic activity, attributed mechanistically to hydrolytic loss of the non-nitrogen ligands (chloride or carboxyl), giving initially the mono-aquated species **1.26a**, **1.27a**, and **1.28a** respectively. The mono-aquated species, on completion of hydrolysis generate the reactive DNA-binding "diaquo" species **1.26b** and **1.28b**.[167,178,181-184] All three parent compounds are thus formally prodrugs; the half-life of the prodrugs decreases across the series. Thus cisplatin is stable in both phosphate buffered saline (PBS), and plasma. Inside the cell, cisplatin demonstrates equilibration of the three above forms, **1.26**, **1.26a**, and **1.26b** to a ratio of 44%: 30%: 26%, attributed in part to the lowered chloride level (c.a. 100 mM extracellular, 3-20 mM intracellular). Carboplatin and oxaliplatin undergo hydrolysis, with $t_{1/2}$ = 244 hours and 1.5 hours respectively in saline, decreasing to $t_{1/2}$ =

30 hours and 0.25 hours in plasma. Carboplatin hydrolysis (CBDCA loss) has been postulated to occur through neutral, acid, and base catalyzed mechanisms.[167] This rate of hydrolysis, which has been extensively studied, is affected by pH, chloride ion concentration in the case of cisplatin, and other nucleophiles.[185-188]

The "diaquo" species produced by hydrolysis is highly reactive toward biological nitrogen, especially in reaction with cellular DNA, with which it reacts to form GG dimers.[189] The platinum drugs are known to be reactive with thiol-type compounds such as glutathione (GSH), in addition to DNA.[190] In the context of Pt agents, resistant cells are known to excrete GSH-Pt species.[191] Cellular resistance to X-ray irradiation has also been correlated with augmented GSH levels.[192]

Several platinum-carboxylate analogues of carboplatin, readily synthesized from the commercially available carboxylic acids demonstrate significant therapeutic activity. The lipophilic malonates,[165] Pt-blues (phthalates),[193] and polycarboxylates (i.e. citrate)[194-196] have all been previously reported to demonstrate efficacy in cell culture, and in some cases to display reduced systemic toxicity in animal studies, compared to cisplatin. It was thus thought these kinds of species would prove useful as Pt releasing linkers that could be attached to MGd.

1.9 EXPERIMENTAL N-SIDE SUBSTITUTED PLATINUM ANALOGUES

While the third-generation drug oxaliplatin is an approved N-side substituted Pt compound that demonstrates activity in resistant tumors, efforts continue to be devoted to preparing yet improved analogues (Figure 1.14). Lead compounds of this general nature include the above transplatin analogue,[197]the JM-216 bis-succinate analog,[198] and three pyridine analogs.[199-201] Several of these, notably in the pyridine family, demonstrate activity against resistant tumors. These compounds being more polar than oxaliplatin may

also have higher solubility and improved (or altered) uptake/retention profiles, and possibly be cationic at cellular pH.

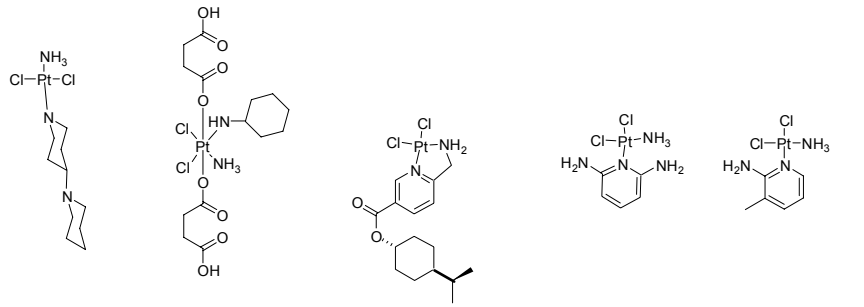

Figure 1.14 Recent experimental cisplatin analogues.

Previous Pt compounds modified on the inert N-side have served to demonstrate that the highest activity is seen when NH_3, 1,2-diaminocyclohexane (DACH), small alkylamines, and o-phenylene diamine are used to effect the modification.[175,202-204 205] The structures in Fig. 1.14, containing small lipophilic N-side ligands, demonstrate in vitro activity in agreement with the SAR predictions. Due to the low water solubility of these (alkyl-N)$_2$-Pt complexes, various solubilizing modifications, such as oxygenation, have typically led to lower efficacy, heptaplatin being a notable exception.[206,207] Evaluation of these compounds only served to reinforce the lipophilicity and efficacy correlation.

The above mentioned experimental Pt therapeutic drugs (Figure 1.14) are thought to act as DNA binding agents. The nucleus and mitichondria, both contain DNA and both are compartmentalized within double membranes. For activity as DNA binding agents, any Pt therapeutic drugs must reach this compartmenttalized DNA. The lipophilicity and efficacy correlation observed in the cell uptake, retention, and PDT studies of the previously mentioned rhodamine and porphyrin cationic species appeared similar to the

trends observed in Pt therapeutic drugs. We hypothesized that the coordination of Pt to lipophilic cationic molecules could produce therapeutically active Pt agents.

1.10 CATION MOVEMENT THROUGH MEMBRANES

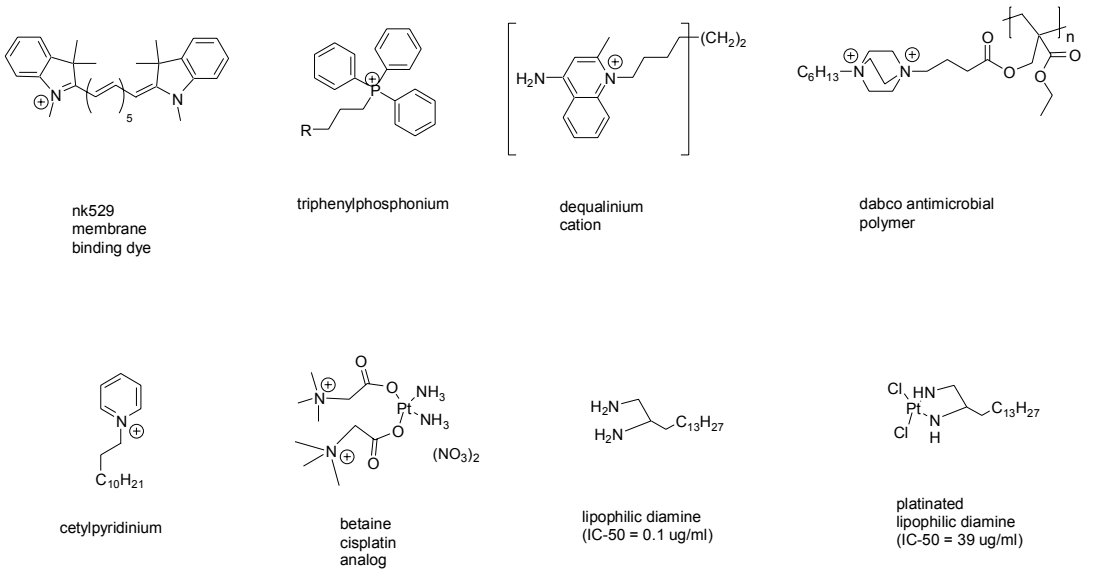

Figure 1.15 Cationic compounds demonstrating biological activity.

From numerous imaging studies it is clear that lipophilic cations (Figure. 1.15) embed in and move through cellular membranes. Delocalized lipophilic cations (DLC) are known to act as transport agents or toxins and have been proposed for therapeutic use. For example NK-529,[208] is a fluorescent dye demonstrating localizing (embedding) in cell membranes while triphenylphosphonium cation,[209-211] demonstrates mitochondrial localization and has been proposed as a therapeutic agent carrier. Toxic membrane damaging detergent type cations include dequalinium chloride,[212-214] C6-DAP,[215] and cetylpyridinium,[216] which are used as a herbacide, polymeric antibacterial agent, and

topical disinfectant, respectively. Therapeutically significant, the aforementined rhodamine has demonstated activity in multiple drug resistant (MDR) tumors[217] while an experimental betaine-Pt compound demonstrates improved efficacy over cisplatin in cell studies. [218]

The above mentioned lipophilic quaternary cationic compounds do not specifically target tumors and are either highly toxic or inert, thus they have not generally been used therapeutically. If these cations could be conjugated to a targeting moiety, such complexes hold potential for localizing in tumors and and subsequently in target organelles.

1.11 SUMMARY AND CONCLUSIONS

The experimental expanded porphyrin MGd is currently being tested as a therapeutic radiation sensitizer. In the case of both MGd, and the porphyrinoids being used or developed for PDT, in vitro tumor localizing activity is typically found to be correlated with lipophilicity. At the sub-cellular level, highest activity is typically found for cationic molecules. The porphyrinoids and some xanthenes have been utilized as PDT agents. The fluorescence of these compounds has enabled studies of sub-cellular localization, which, in turn, are aiding in efforts to develop SAR correlations for various therapeutic agents that function with catalytic generation of ROS. Due to its low quantum-yield, sub-cellular localization studies of MGd have required special techniques.

Recently the porphyrinoids have begun to attract attention for use as localizing moieties in conjugates since they could permit the specific uptake or retention of drugs in tumors. Such conjugates are particularly likely to be attractive if they could be designed such that they could release the therapeutic agents in question.

Three platinum therapeutic agents are in wide use; however, they suffer from non-specific toxicity. Extensive work to develop conjugates has been undertaken. However,

activity has been demonstrated in only a few cases. Significant problems appear to plague this approach, involving both molecular (ligand) rearrangements and untoward release rates of Pt. Novel non-labile N-side Pt agents have also been recently developed and appear to have higher solubility than the clinically approved oxaliplatin. This N-side substitution may improve the solubility of these agents and increase efficacy. Some lipophilic cations are also known to demonstrate excellent cell toxicity. Unfortunately, metallation generally diminishes their efficacy. From this background we set out to develop improved therapeutic agents.

Chapter 2: Motexafin Gadolinium (MGd)-Fluorophore Conjugates

2.1 INTRODUCTION

The texaphyrins, e.g., motexafin gadolinium (MGd; **1.4**) are members of the "expanded porphyrin" class of macrocycles. These particular expanded porphyrins have demonstrated an ability to coordinate larger metal cations and to concentrate in tumors. The additional ability of MGd to generate Reactive Oxygen Species (ROS) under X-ray irradiation has resulted in extensive study as an experimental therapeutic agent.[41] While in vivo localization studies using MGd as an Magnetic Resonance Imaging (MRI) agent have proven successful, the subcellular fluorescence imaging of MGd is technically challenging.[102] In subcellular fluorescence studies of porphyrinoid PDT agents which lack the technical challenges of MGd, varying the molecular charge of the PDT agent has demonstrated alteration in both toxicity and subcellular localization.[89] We hypothesized that the synthesis of fluorescent xanthene – MGd conjugates with different molecular charges would facilitate evaluation of charge and subcellular localization correlation using fluorescent imaging.

The therapeutic activity of MGd has been ascribed in part to mitochondrial uptake and generation of reactive oxygen species (ROS), such as H_2O_2, via a process of redox cycling, thereby triggering apoptosis.[219] In fact, the uptake of MGd in isolated mitochondria has been demonstrated.[95] Further, ascorbate, in combination with MGd, was found to engender enhanced toxicity and growth inihibition of uterine cancer cell line MES-SA as detected by MTT assay. This ascorbate-MGd combination was also found to enhance the radiation response in A549 and MES-SA cells, as were subsequently other endogenous electron donors, such as ribonucleotide reductase.[3,122,220]

The localized generation of ROS, which generally act over short distances,[49] provides an incentive to map out the subcellular localization properties of MGd.

The subcellular imaging of MGd is technically challenging. This reflects the fact that MGd contains a paramagnetic, gadolinium(III) center and has an inherently low fluorescent quantum yield (0.0028%),[221] a fluorescence emission maximum in the 700-800 nm region where detectors are relatively insensitive, and inherent propensity to undergo photobleaching.[102] In spite of these limitations, cellular imaging studies of MGd in EMT6 mammary sarcoma cells could be carried out using liquid Nitrogen cooled CCD sensors and image processing to resolve the signals (Interferometric Fourier Fluorescence Microscopy).[102] This resulted in detection of punctuate fluorescence after incubating the cells for 4 hours in the presence of MGd. In this study MGd distributed in lysosomes, endoplasmic reticulum, and mitochondria, as inferred from comparative organelle staining analysis. After 48 hours, MGd was seen in the nucleus in 15% of the cells.[102]

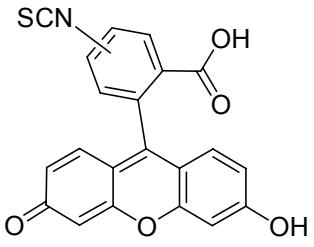

2.3 FITC

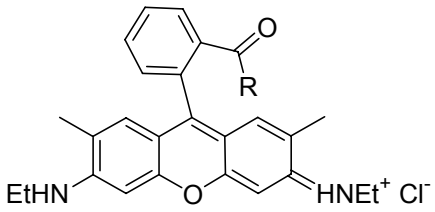

2.4 Rhodamine 6G, R = OEt
2.5 Octadecyl Rhodamine, R = $NHC_{18}H_{37}$

Figure 2.1. Fluorophores FITC **2.3**, Rhodamine 6G **2.4**, and Octadecyl Rhodamine **2.5**.

While the above study confirmed that MGd can be imaged directly in cells, it also served to underscore the potential benefits of MGd analogues that might be more fluorescent and hence easier to track at the subcellular level using conventional

fluorescence microscopy. In an effort to address this need, we now wish to report the synthesis and characterization of two new texaphyrin fluorophore conjugates, namely the FITC- and Rhodamine-linked MGd derivatives **2.1** and **2.2**.

The xanthene dyes (Figure 2.1), FITC **2.3** and Rhodamine 6G **2.4** have been widely used to prepare conjugates for biological molecule localization studies.[104] Because the fluorescein and rhodamine ions have opposite charge and because any structural modification could be potential important, we were curious to see what effect, if any, appending a FITC or rhodamine fluorophore had on the subcellular biolocalization properties of MGd. Rhodamine, as a lipophilic delocalized cation has well known tendency to accumulate in mitochondria due to their negative membrane potential.[222] We were also curious whether such modifications would alter the basic *in vitro* localization. Thus, as detailed below, key objectives of the present study were to develop synthetic methods for generating fluorescent conjugates, and determine their subcellular localization properties.

2.2 EXPERIMENTAL

Previous efforts to elaborate the texaphyrin core with, e.g., redox active or other therapeutic agents, have led to the development of two functionalization strategies. The first involves the direct attachment of the modifying group to one of the hydroxypropyl substituents, while the other involves replacing one of the glycol groups on the ortho-phenylenediamine portion of the texaphyrin skeleton with a tether to which the agent in question is attached. We felt both strategies could be applied successfully to the development of texaphyrin fluorophore conjugates. With this consideration in mind, the FITC and rhodamine derivatives **2.1** (MGd-FITC) and **2.2** (MGd-Rho) were chosen as

specific synthetic targets. As detailed below, the first of these was prepared via the direct functionalization of a preformed MGd core, whereas the second required the preparation of an *o*-phenylenediamine precursor and subsequent synthetic elaboration of the texaphyrin macrocycle.

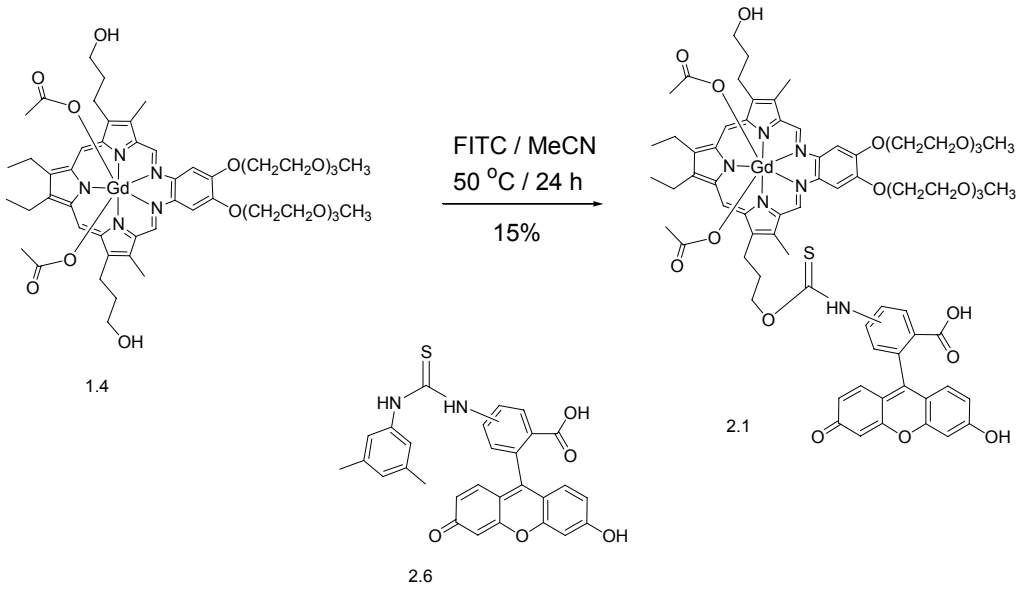

Scheme 2.1. Synthesis of FITC-MGd conjugate **2.1** and control compound **2.6**.

As shown in Scheme 2.1, conjugate **2.1** could be prepared starting from MGd **1.4** and FITC **2.3** (available as an 85:15 mixture of the 5 and 6 substituted isomers). Mixing these two species in hot acetonitrile gave the expected MGd mono-FITC conjugate **2.1**.[223] Purification of product **2.1** was effected on a reverse phase tC-18 RP Sep-Pak column. HPLC analysis of the purified product was consistent with the presence of two MGd-FITC thiocarbamate conjugates, in the expected isomer 85:15 ratio dictated by the 5(6)-FITC starting material(UV_{472}: 93.08% = 12.56% + 80.52% at T_r = 8.63 min, 9.57 min, respectively). The material was additionally characterized by HRMS and elemental analysis. The FITC conjugate **2.1** demonstrated water solubility of less than 0.01 mg/ml

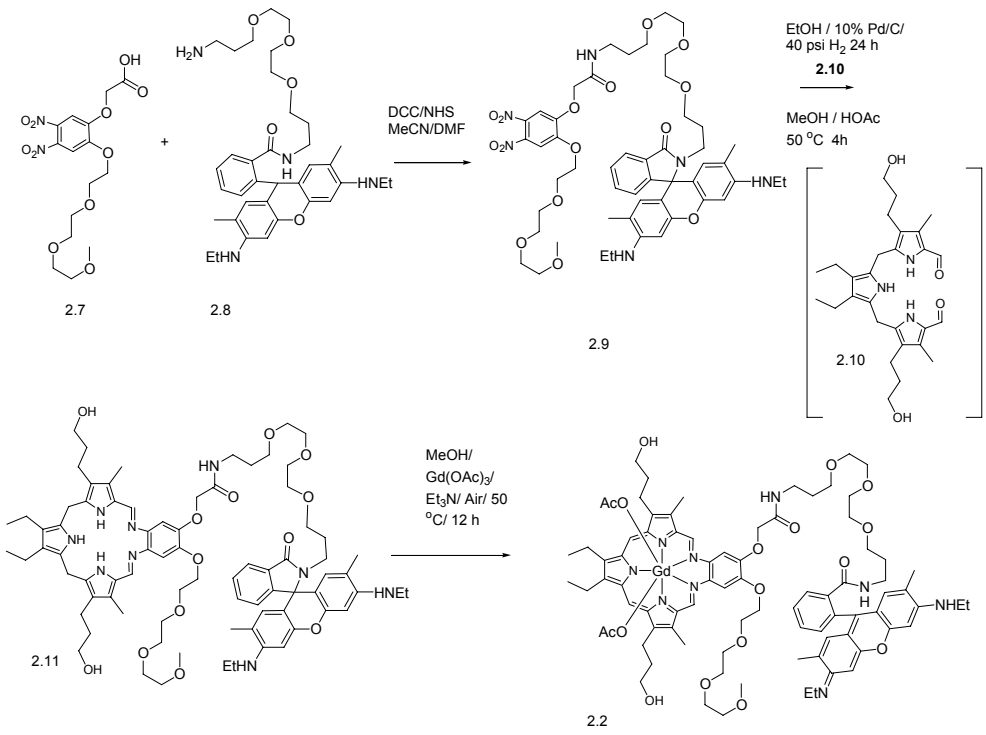

Scheme 2.2 Synthesis of MGd-Rhodamine conjugate, **2.2**.

(UV470 basis in deionized water). As a control for the imaging studies, the published 3,5-dimethylaniline-FITC urea **2.6** was also prepared.

The synthesis of compound **2.2**, was effected starting from a solubilized dinitrobenzoic acid derivitive **2.7**, and the leuko form of a highly water soluble derivative of rhodamine 6G, **2.8**, both prepared by published procedures.[111,147,224] Thus the synthesis of **2.9** was effected by activation of **2.7** as the NHS derivative, mediated by DCC, followed by reaction with **2.8** (1.2 equiv.) as the leuko form. After stirring 24 hours the reaction was quenched in water, extracted into methylene chloride, and purified by flash chromatography on mildly deactivated silica gel (CH_2Cl_2/MeOH/NH_3) to give the amide **2.9**. The nitro groups of **2.9**, were then catalytically reduced (Pd/C, H_2) in methanol, to produce the unstable diamine. The methanolic solution was then filtered

through Celite to remove the catalyst and immediately reacted with dialdehyde **2.10** at 50 ^{o}C in the presence of acetic acid catalyst to give the cyclized "sp^3" texaphyrin intermediate **2.11**. The solution was evaporated to give a red oil. Separately, a solution of $Gd(OAc)_3$ (1.5 equiv.) in methanol with triethylamine (11 equiv.) was saturated with air by sparging for 10 minutes. To this solution was added the "sp^3" texaphyrin intermediate **2.11**, redissolved in a minimal amount of methanol. The resulting solution was heated to 50 ^{o}C for 12 h to give the crude metallated conjugate **2.2**. Purification was effected in two stages. First the crude material was purified by flash chromatography on deactivated silca gel (CH_2Cl_2/MeOH/HOAc). The product-containing fractions were combined, evaporated, and further purified by reverse phase chromatography on tC18 SPE cartridges. HPLC analysis of the purified product demonstated predominantly a single product (UV_{472}: 95.18%, T_r = 12.85 min). The material was additionally characterized by HRMS and elemental analysis.

2.3 SPECTROSCOPIC AND PHOTOPHYSICAL STUDIES

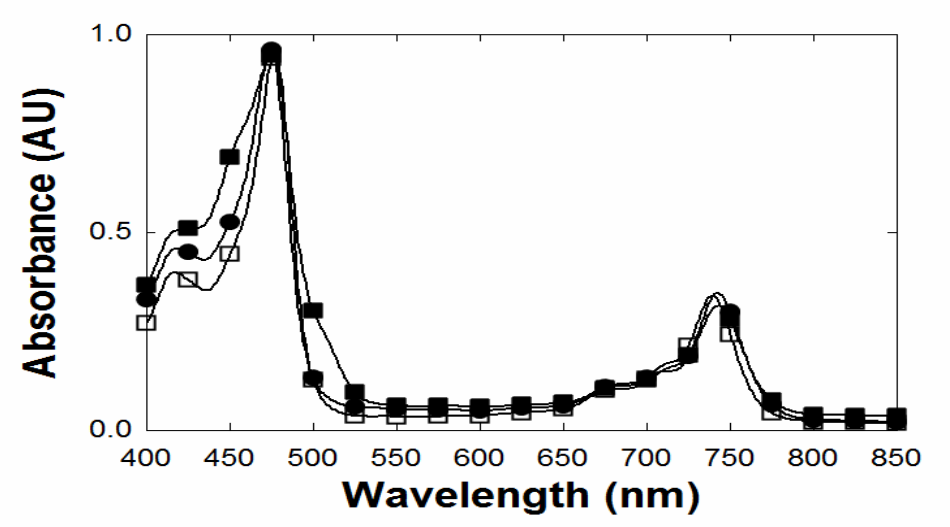

Figure 2.2. Electronic spectra of MGd **1.4** (□) and its fluorescent derivatives MGd-FITC **2.1** (■)and MGd-Rhodamine **2.2** (●) as recorded in methanol.

The fluorophore conjugate intermediates were additionally characterized by UV-visible and fluorescence spectroscopy for determination of extinction coefficient and quantum yield. This latter was important because MGd contains a paramagentic Gd(III) center that could potentially quench the fluorescence of an appended fluorophore.

The electronic spectra of the MGd-FITC and MGd-Rho conjugates, **2.1** and **2.2**, recorded in methanol, are shown in Figure 2.2. As can seen by inspection of this figure, there is little difference in the spectra of the conjugates compared to that of MGd. The expected texaphyrin-derived Soret and Q bands were observed at ca. 470 and 750 nm, respectively. Although some broadening in these bands is seen, no features specifically ascribable to the FITC and rhodamine subunits were observed

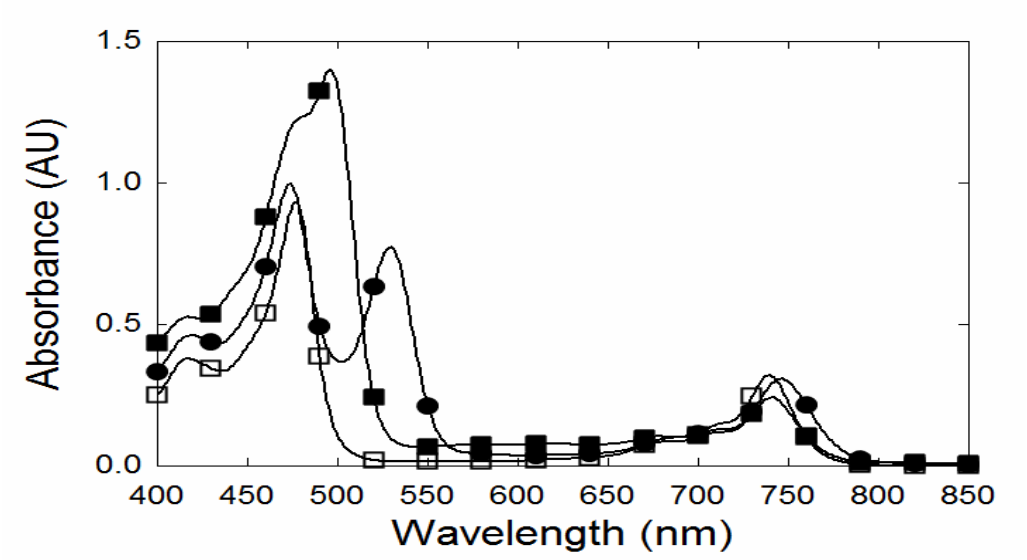

Figure 2.3. Electronic spectra of MGd **1.4** (□), MGd-FITC **2.1** (■) (+NaOH), and MGd-Rhodamine **2.2** (●) (+HCl) as recorded in methanol.

The methanol solutions of **2.1** and **2.2** used to record the UV-visible spectrum were found to lack any significant absorbance that can be attributed to the attached fluorophores. This is not unexpected since both fluorophores are in their non-ionized form and in this state they do not absorb strongly. To these solutions was added dilute base (MGd-FITC **2.1**) or acid (MGd-Rho **2.2**). This gave much more strongly absorbing species, as can be seen in Figure 2.3, in agreement with conversion of the xanthenes to their ionized forms. For instance, the intensity of the absorbances at 470 and 495 nm in the spectrum of the FITC conjugate **2.1** (also recorded in methanol) were seen to increase to ca. 149% and 80%, respectively, as compared to the unionized 470 nm absorbance illustrated in Figure 2.4. Likewise, a methanolic solution of the MGd-Rho conjugate **2.2** was seen to turn red upon acidification amd there was the appearance of a new 530 nm peak in the electronic spectrum, characteriztic of rhodamine, at c.a. 80% of the intensity of the 470 nm MGd absorbance observed for the unionized form in Figure

2.4. Thus the ionized xanthene conjugates **2.1** and **2.2**, absorbing at 495nm and 530 nm were in agreement with the reported 500 nm and 530 nm respectively for ionized fluorescein and rhodamine.

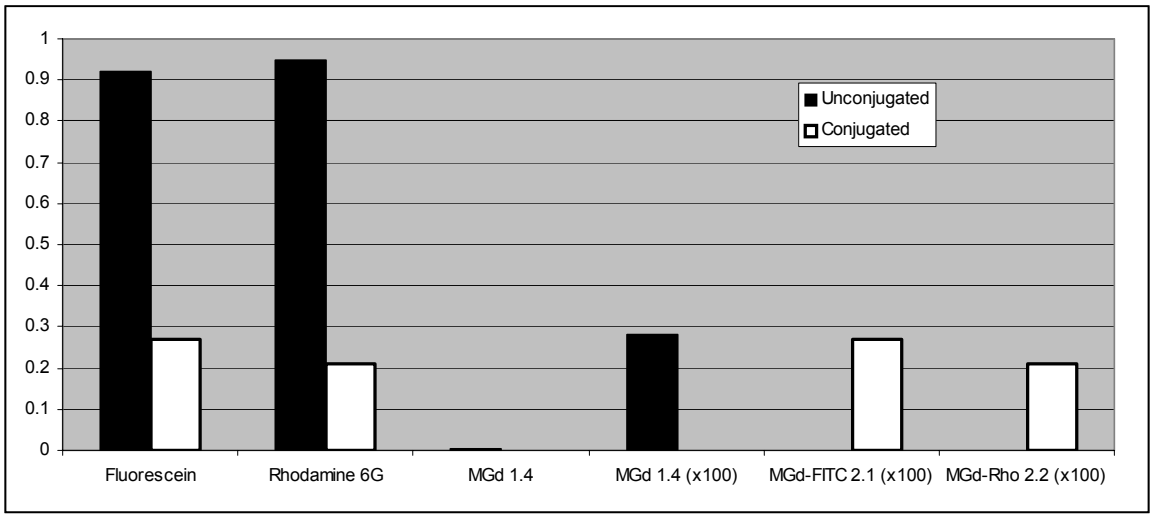

Figure 2.4. Quantum Yield determination for unconjugated (black bars) and conjugated (white bars) fluorophores: Fluorescein, Rhodamine, MGd , and their conjugates as recorded in methanol.

The quantum yields of MGd-FITC and MGd-Rho (Figure 2.4) were determined by utilizing standards with known quantum yields (sodium fluorescein Φ_f = 0.92, Rhodamine 6G, Φ_f = 0.95, MGd $\Phi_f = 2.8 \times 10^{-3}$).[225,226] Using an otherwise uncorrected fluorimeter and a published procedure,[227] the quantum yields of all fluorophores were determined in comparison with literature compounds, at reported excitation wavelengths .[227-231] Due to the difference in the Φ_f, measurements were performed at 50 μM (2 nm slit width) and 200 μM (0.5 nm slit width) for the xanthene and MGd fluorophore Φ_f, respectively. The published fluorescence excitation wavelengths of MGd, fluorescein and rhodamine (473nm, 456nm, and 480 nm respectively) are grouped closely together.[225,232]

We hypothesized that co-excitation of the fluorophores was thus possible for the conjugates.

The results of the quantum yield (Φ_f) determination for the conjugates revealed a significant decrease in the Φ_f for the appended fluorophores (Φ_f = 0.27 and 0.21 for FITC and Rhodamine conjugates, respectively). Smaller variations were ascribable to the fluorescence of the MGd core (Φ_f = 2.7 x 10^{-3} and 2.1 x 10^{-3} for the MGd - FITC and MGd - Rhodamine conjugates, respectively). Specifically, the MGd-derived fluorescence Φ_f in the MGd-FITC, and MGd-Rho conjugates **2.1** and **2.2**, decreased to 76% and 83% of that recorded for free MGd, **1.4**. In contrast, the Φ_f of the FITC and rhodamine fluorophores in the conjugates **2.1** and **2.2** were only 25% and 20%, respectively, of the corresponding non-conjugated values. The Φ_f results obtained for the conjugated xanthene fluorophores is in broad agreement with Φ_f = 0.13 – 0.18 reported for fluorescein-peptide conjugates,[227] thus the decrease in Φ_f may not be simply a result of proximity to Gd.

2.4 IMAGING AND CYTOXICITY STUDIES IN A549 CELLS

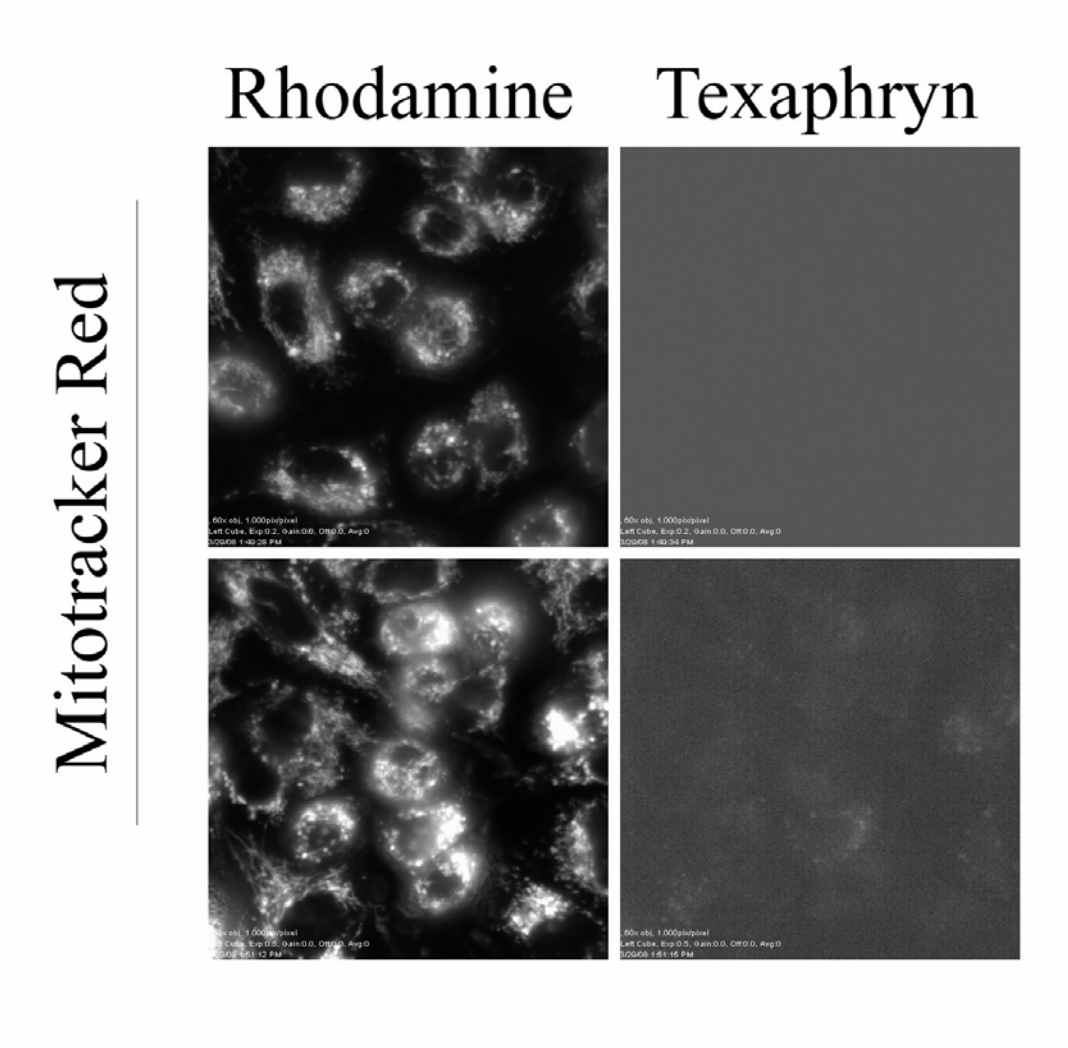

Figure 2.5. Legend: Rhodamine leakover control study showing two different photographs of A549 cells that were loaded with Mitotracker Red, a rhodamine derivative. The images on the left side are taken using the "Rhodamine" filter set whereas the images on the right side are taken using the MGd filter set.

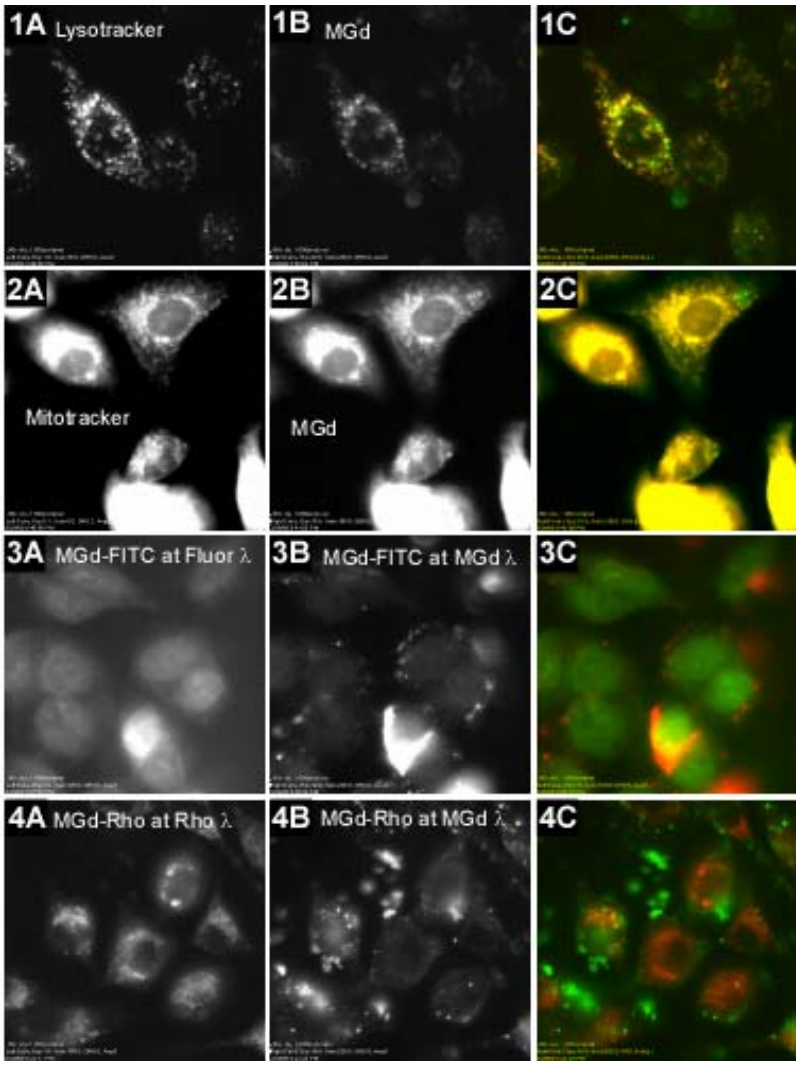

Figure 2.6. Legend: Intracellular localization of MGd and its conjugates. 1A-C are images of A549 cells loaded with Lysotracker and unconjugated MGd. 1A shows an image taken using the Lysotracker filter set whereas 1B is a fluorescence image taken using the MGd filter set. 1C shows the overlay of the Lysotracker image (red) and the MGd image (green). 2A-C are images of A549 cells loaded with mitotracker and unconjugated MGd. 2A shows an image of mitotracker obtained using the rhodamine filter set whereas 2B shows a fluorescence image of the same cell using the MGd filter set. 2C shows the overlay with mitotracker (red) and MGd (green). 3A-C are images of A549 cells loaded with the MGd-FITC conjugate using the fluorescein (3A) or MGd (3B) filter sets. 3C shows the overlay of the fluorescein filter image (green) and the MGd filter image (red). 4A-C are images of A549 cells loaded with MGd-Rho conjugate using the rhodamine or MGd filter sets. 4a shows a fluorescence image using the rhodamine filter set whereas 3B shows an image of the same cell obtained using the MGd filter set. 4C shows the overlay of the rhodamine image (red) and the MGd image (green).

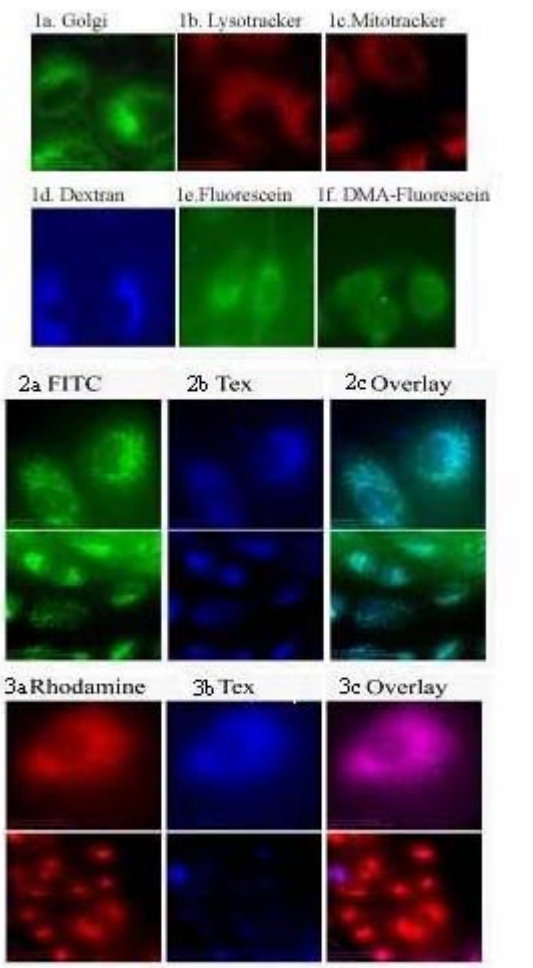

Figure 2.7. Legend: Colorized fluorescence microscopy photographs of A549 cells incubated with organelle stains, MGd and MGd-conjugates. 1A-F are control organelle stains. Fluorescence images of cells incubated with MGd-FITC **2.1**, were taken using the FITC filter set (2a) and the MGd filter set (2b). Image 2c shows an overlay of 2a and 2b. Fluorescence images of cells incubated with MGd-Rho **2.2**, were taken using the Rhodamine filter set (3a) and the MGd filter set (3b). Image 3c shows an overlay of 3a and 3b.

The texaphyrin conjugates were incubated with A549 lung cell lines to study their uptake and distribution patterns. Initially, imaging of MGd-FITC **2.1** was attempted using confocal microscopy due to the higher resolution of these instruments, but in this case, no signal could be obtained from MGd alone; only the xanthene portion was detectable. Since an important goal of this study was to obtain colocalized images of MGd fluorescence and rhodamine or fluorescein fluorescence in their respective conjugates, all further studies were carried out using wide field microscopy.

Fluorescence imaging studies were performed using a wide-field fluorescence microscopy and ccd camera. The imaging studies were performed using commercial fluorescein and rhodamine filter sets to image the xanthene portion of the conjugates. The MGd imaging was performed using a custom excitation filter (470 nm +/- 20 nm excitation filter and 700+ nm long pass emission filter), obtained from Chroma.® This filter was chosen to reduce emission from either the rhodamine or fluorescein components of the conjugates and allow selective imaging of the texaphryn fluorescence or the texaphryn component of the rhodamine and fluorescein conjugates. In a control bleedover experiment using Mitotracker (Figure 2.5), only a small amount of fluorescence attributable to rhodamine species was observed when using the MGd imaging custom filter. Additional images of the A549 cells using fluorescent organelle stains (Figure 2.6, 1a-f) were obtained to act as localization controls, fluorescein controls 1e and 1f utilized fluorescein and 3,5-dimethylaniline-FITC to demonstrate localization of unconjugated fluorescein species. Dual labelling images of the A549 cells using MGd and fluorescent organelle stains (Figure 2.7, 1a-c, 2a-c) were obtained as additional controls.

The study in Figure 2.6 and showed that MGd **1.4**, MGd-FITC **2.1** or MGd-Rho **2.2** at 5 μM was rapidly internalized by cells. Specifically, cellular uptake of MGd and Lysotracker; MGd and Mitotracker, MGd-FITC **2.1**, and MGd-Rho **2.2** is demonstrated in the control dual labeling studies (Fig. 2.6, 1A-1C through 4A-C respectively). In the dual labeling studies with MGd, Lysotracker, and Mitotracker (image 1A, 1B and 2A, 2B), differential punctate distribution was observed. In the conjugate studies with **2** and **3**, some particulates were observed in the media, presumably precipitated conjugate, fluorescent only with the long pass filter.

MGd and its fluorescein conjugate both show a tendency to accumulate in the lysosomes as indicated from long pass filter images 1B and 2B, respectively. This image is more intense with the fluorescein conjugate. The images generated from the two fluorophores of the MGd-fluorescein conjugate show lysosomal colocalization, with some differences depending on the filter set used. In images of dividing cells (Figure 2.6, 3a-c and Figure 2.7, 2a-c (bottom photos)) generated from the two fluorophores of the MGd-fluorescein conjugate show nuclear colocalization, with some differences depending on the filter set used. Using the MGd filter set, weak nuclear fluorescence is observed (Figure 2.6, 3b) along with the punctate cytoplasmic distribution, typical of the MGd compounds as in image in Figure 2.7, 1B. The MGd-fluorescein image overlay shows a nuclear pattern of localization, different from either fluorescein alone or the dimethylaniline-FITC control.

The images from the two fluorophores of the MGd-Rho conjugate also differ depending on the filter set. When using the rhodamine filter set, intense cytoplasmic staining is observed. Using the MGd filter set, weak cytoplasmic fluorescence is observed (image Figure 2.7, 4B), along with intense punctate spots. A likely explanation is that rhodamine fluorescence is pH, and thus, organelle dependent. This was also observed in

the particulates with no rhodamine fluorescence detected colocalizing with either intracellular or extracellular punctate spots. From these images it appears that MGd and its rhodamine conjugate can gain entry to mitochondria. This is in agreement with a number of compounds bearing a delocalized positive charge which tend to accumulate in mitochondria. The rhodamines are often employed as a vital stain for this organelle. Thus rapid localization is thus demonstrated by both these conjugates, conjugate **2.1** appearing in the lysosomes, and in the nucleus of dividing cells, while **2.2** is observed in the mitochondria.

2.6 DISCUSSION

In this paper we have described the synthesis of two fluorescent MGd conjugates. The first of the these, the FITC-based system **2.1**, was prepared from MGd via a direct coupling procedure, whereas the corresponding rhodamine conjugate, **2.2**, required a more directed synthesis procedure. Both conjugates were characterized using standard means. The subcellular localization properties were then tested using fluorescence microscopy and MTT assays. We have confirmed our hypothesis that the two conjugates, differing in xanthene fluorophores and charge, could demostrate differential cellular distribution.

2.7 Experimental Section

Materials. Unless otherwise noted, all reagents were obtained from commercial suppliers and used without further purification. Solvents were dried over molecular sieves except dichloromethane, which was dried over CaH_2. Methanol used in sp^3-texaphyrin syntheses was degassed by purging with argon for 5 minutes. Methanol used in the sp^2-texaphyrin syntheses (MGd cyclization and metallation) was oxygenated by purging with air for 5-10 minutes, with additional purging being carried out during the reaction period for large scale preparations. The intermediate tripyrrane-dialdehyde **2.10** (2,5-bis[(5-formyl-3-hydroxypropyl-4-methylpyrrol-2-yl) methyl]-3,4-diethylpyrrole) was supplied by Pharmacyclics, Inc. The (2-{2-[2-(2-Methoxy-ethoxy)-ethoxy]-ethoxy}-4,5-dinitro-phenoxy)-acetic acid **2.7** was prepared by literature methods.[147] The $Gd(OAc)_3.xH2O$ was supplied by Strem Chemical Company.

Chromatography. Merck type 60 (230-400 mesh) silica gel was used for column chromatography. For small-scale work-up Sep-Pak cartridges were purchased from Waters in 0.5-20 gram sizes of C-18 or silica. TLC was carried out using the conditions noted below using Whatman K6F aluminum backed silica gel plates.

HPLC analyses. HPLC analyses were performed on a Beckman or Shimadzu Analytical/Preparative HPLC system with a Zorbax XDB 5 μM 5 x 100 mm column. A 0.1% TFA (or 33mM NH_4OAc) aqueous phase against acetonitrile (ACN) gradient (10-95% over 15 minutes followed by 5 minutes at 95% acetonitrile) was used for analysis of

the MGd fluorophore conjugates. All ^{1}H, and ^{13}C NMR spectra were measured with a Varian 300 MHz or Varian Mercury 400 (400 MHz.) spectrometer in $CDCl_3$, D_2O, CD_3OD or D_7-dmf. The NMR chemical shifts are reported in ppm relative to the solvent. Low resolution and high resolution electrospray mass spectrometry (ESI MS) were performed with a Thermo Finnigan LTQ and Qq-FTICR (7 Telsa) instruments, respectively. Mass spectrometry (LRMS, HRMS) was carried out by the University of Texas at Austin Mass Spectrometry Facility. Elemental analyses were performed by Midwest Microlabs Inc. Electronic spectra were recorded on a Beckman DU-7 spectrophotometer.

Fluorescence and Quantum Yield: Measurements were performed according to published procedures.[227] Briefly, the electronic spectra were measured and the absorbance adjusted to c.a. 1.0 AU (0.9-1.1). The quantum yields were then measured on a Jobin Ybon fluorimeter. The xanthene $\Phi_{f\ FITC}$ was measured at 50 μM, 0.5 nm slit width, $\lambda_{ex/em}$ 456/470-650 nm, The xanthene $\Phi_{f\ Rho}$ was measured at 50 μM, 0.5 nm slit width, $\lambda_{ex/em}$ 480/500-700 nm, the MGd Φ_f was measured at 200 μM, 2 nm slit width, $\lambda_{ex/em}$ 473/650-850 nm. The fluorescence emission for each was integrated over the noted range and compared to the commercial xanthene fluorophore or MGd.

Chromatography: TLC, Flash, and SPE

TLC - Silica gel TLC of organic soluble samples commonly used EtOAc/hexanes or DCM as the eluents. The water solubilized PEGylated intermediates were chromatographed using 9:1 DCM:MeOH with HOAc or NH_3 to further deactivate the silica gel unless otherwise indicated. Silica gel chromatography of the texaphyrins required 9:1:0.1 DCM:MeOH:HOAc as the eluent.

Flash Chromatography - For the MGd mono-substituted complexes chromatography was typically performed by loading up to 1000mg MGd as a DCM

solution on 75 cc pre-packed silica gel (1" diameter column) and eluting with 200-400 ml DCM, followed by 200-400 ml DCM/0.1-0.2% HOAc containing 5% MeOH, followed by the same solution at 10-40% MeOH. This elutes the first small red and pale green impurities. The main fraction is eluted with 400-800 ml DCM/HOAc solution containing 15% MeOH. Relevant fractions are collected as 100-200 ml aliquots. Relevant fractions can be re-chromatographed on 100 cc silica gel by diluting to 5% MeOH and loading directly onto the column. Elution with DCM/0.1% HOAc at 10% MeOH removes the trace red and green impurities and the main product fractions are removed at a gradient of 15-40% MeOH in DCM/HOAc with 400-600 ml solvent.

SPE - The MGd conjugates could also be purified on RP-tC18 SPE (Waters Sep-Pak) columns using gradients of MeOH or ACN against aqueous buffer (33mM NH_4OAc).

Synthesis of MGd-FITC (carbamate). 2.1 To a solution of MGd (1130 mg, 0.98 mM) in ACN (150 ml) was added fluorescein isothiocyanate (FITC) (380 mg, 0.98 mMol). The solution was stirred at 50 ^oC for 72 hours, followed by evaporation to provide the crude product (1.31g, 91%). Purification of 1000 mg was effected by dissolving the solid in DCM/MeOH (25 ml, 9:1) and adding acetonitrile/0.1 M NH_4OAc buffer/HOAc (80 ml 4/1/1) followed by evaporation at 60 ^oC to remove the DCM. The residual solution was filtered to remove the insoluble material and the filtrate was diluted with water (1:1). This aqueous solution was divided into 3 portions and each loaded on a C-18 SPE column (10 g). Each loaded column was first washed with acetonitrile/buffer/water (4/1/1), to remove impurities, followed by acetonitrile/buffer (3:2) to remove MGd. The MGd-FITC product was then eluted with acetonitrile/buffer (4:1). The resulting product solutions were combined, diluted with buffer (1:1) and reloaded on the C-18 SPE column. The column was washed with water (20 ml),

acetonitrile (30 ml), and the product was then eluted with 98/2 (MeOH/HOAc). Evaporation, tituration with Et_2O, and drying under high vacuum provided a green solid (234 mg, 15 %). HPLC (472 nm): 93.08%, a mixture of the 5(6) isomers. (T_r = 8.63; 12.56%); (T_r = 9.57; 80.52%). MS (EI) (M-2 OAc)+ 1418. HRMS(EI)+ calculated for $C_{69}H_{76}Gd[158]N_6O_{15}S$ (M-2 OAc) 1418.4330, found 1418.4314. UV (dilute into MeOH/ 2% HOAc) λ_{max} (log ε): 283 (4.53), 414 sh. (4.57), 474 (4.93), 740 (4.46). $\Phi_{f\ MGd}$ = 0.0021 (200 μM, 2 nm slit width, $\lambda_{ex/em}$ 473/650-850 nm), $\Phi_{f\ FITC}$ = 0.27 (50 μM, 0.5 nm slit width, $\lambda_{ex/em}$ 456/470-650 nm). Anal. Calcd for MGd-FITC·$5H_2O$: C 57.05%; H 5.38%; N 5.47%; S 2.09%. Found: C 57.26%; H 5.23%; N 5.17%; S 2.03%. The extreme line broadening due to the paramagnetic Gd precluded NMR analysis of the MGd conjugates. However, HPLC analyses, MS studies, and UV-Vis spectroscopic studies were carried out.

Synthesis of Rhodamine amide 2.8, *N*-(3-{2-[2-(3-Amino-propoxy)-ethoxy]-ethoxy}-propyl)-2-(6-ethylamino-3-ethylimino-2,7-dimethyl-3H-xanthen-9-yl)-benzamide. This compound was prepared according to a modification of a published procedure[111,224,227]. Briefly, to a solution of Rhodamine 6G (1.88 g, 3.9 mMol) in DMF (75 ml was added 4,7,10 Trioxa-1,13-tridecanediamine (3.0 ml, 13.6 mMol). The resulting solution was held at 60 ^oC for 24 hours. Evaporation of the DMF and purification by flash chromatography over basic alumina (DCM/MeOH gradient 0-15%) provided the product (1.82 g, 75%) as an oil.

By HPLC analysis the material eluted as two peaks, agreeing with a protonated (10.78 min, high 529 nm UV absorption) and non-protonated (11.47 min.) form, the ratios interconverting dependent upon pH (respective HPLC retention times and UV spectra are identical).

HPLC (529 nm): T_r 10.78 min = 66.53%, 11.47 min = 25.45% (the total area % of protonated and non-protonated forms as noted above was 91.98%); OH^- pre-treatment: 10.78 min = 50.18%, 11.47 min = 38.54% (total 88.72%). TLC: (silica-5/1/0.05 DCM/MeOH/NH3) Rf=0.5. ^{1}H NMR (400 MHz, ^{6}d-DMSO/D_2O) 1.25 (6H, t), 1.60-1.72 (4H, m), 1.84 (6H, s), 3.04 (2H, t), 3.10-3.26 (10H, m), 3.40-3.57 (15H, m), 6.17 (2H, s), 6.31 (2H, s), 6.93 (1H, m), 7.48 (1H, m), 7.82 (1H, m). MS (CI) (M+2H)+ 618. HRMS(CI) calculated for $C_{36}H_{49}N_4O_5$ 617.3703, found 617.3709

Synthesis of Dinitrobenzene-Rhodamine amide 2.9, N-(3-{2-[2-(3-Amino-propoxy)-ethoxy]-ethoxy}-propyl)-2-(6-ethylamino-3-ethylimino-2,7-dimethyl-3H -xanthen-9-yl)-benzamide. To a solution of **2.7** (0.5 g, 1.24 mMol) in DMF (5 ml) and N-hydroxysuccinimide (0.14 g, 1.2 mMol) was added DCC (0.25 g, 1.2 mMol) in DCM (2 ml). The reaction was stirred for 30 minutes, after which **2.8** (0.76 g, 1.23 mMol) was added. The solution was was stirred overnight. Purification of the product was effected by flash silica gel chromatography (9/1/0.05 DCM/MeOH/NH_3) twice to provide the product **2.9** (0.39 g, 32%). Material could also be purified on tC-18 SPE cartridges with TFA(0.1%)/ACN gradient (80/20 to 20/80) and the purified fractions partitioned between DCM and 5% aq. $NaHCO_3$. The DCM solution was dried over K_2CO_3 and evaporated to give a clear oil. HPLC (528 nm): T_r = 12.87min, 14.92 min (total 96.12%); 28.20%, 67.92% respectively; T_r (pre-treatment with 3N HCl):12.75 min = 93.70% TLC: Rf=0.6 (5/1/0.05 DCM/MeOH/NH_3). ^{1}H NMR(400 MHz, $CDCl_3$) δ 1.32 (6H, t, 7.2 Hz), 1.40 (2H, p), 1.80 (2H, p), 1.89 (6H, s), 3.13-3.24 (8H, m), 3.35 (2H, s), 3.36-3.37 (2H, m), 3.43 (2H, q, J = 6.2 Hz), 3.48-3.54 (12H, m), 3.60-3.65 (4H, m), 3.68-3.70 (2H, m), 3.90 (2H, t, J = 4.4 Hz), 4.34 (2H, t, J = 4.8 Hz), 4.62 (2H, s), 6.21 (2H, s), 6.32 (2H, s), 7.02 (1H, m), 7.18 (1H, t, J = 5.5 Hz), 7.41-7.45 (3H, m), 7.53 (1H, s), 7.88 (1H, m). MS (CI) (M)+ 1003. HRMS(CI) calculated for $C_{51}H_{67}N_6O_{15}$ 1003.4664, found 1003.4627. Anal.

Calcd for $C_{51}H_{67}N_6O_{15}$: C 61.00%; H 6.73%; N 8.37%. Found C 54.74%; H 5.37%; N 5.95%.

Synthesis of sp^3-texaphyrin-rhodamine conjugate 2.11 A solution of **2.9** (0.39 g, 0.39 mMol) in EtOH (50 ml) with H_2O (2 ml) and 10% Pd/C (0.1 g), was hydrogenated for 24 hours. The resulting solution with the addition of conc. HCl (1 ml) was filtered through celite and the cake washed with ethanol. The filtrate was added to a solution of **2.10** (0.19 g, 0.40 mMol) in MeOH (100 ml) under argon. The solution was held at 50 ^oC for 12 hours, turning deep red as the reaction progressed. Evaporation gave the sp^3TxRh.3HCl **2.11** product (0.57 g, 98%). MS (EI) (M+2H)+2 695. HRMS(EI) calculated for $C_{79}H_{106}N_9O_{13}$ 1388.7910, found 1388.7890. UV (MeOH/ 2% HOAc) λ, max.: 371, 492 sh, 529.

Synthesis of MGd-rhodamine conjugate 2.2. A solution of the above **2.11** (0.24 g, 0.16 mMol), Et_3N (0.25 ml, 11 equiv.) and $Gd(OAc)_3$ (0.10 g, 1.5 equiv.) in MeOH (100 ml) was saturated with air, by sparging for 10 minutes, and heated to 50 ^oC in air for 12 hours. The resulting solution was evaporated to dryness to give 0.31 g, of a solid. Purification was effected by flash silica gel chromatography (DCM/1% HOAc with a MeOH gradient: 0-25% to remove impurities, 40% MeOH to elute the product) to give a green solid. The material was further purified by dissolving the sample in a solution of 6 ml ACN and 0.5 ml HOAc, dilution 1:1 with NH_4OAc buffer (0.1 M NH_4OAc pH=4.3) and loading on a C-18 SPE cartridge (10g). The column was washed with 20-40% ACN to remove impurities and the product was eluted with 60% ACN / 40% NH_4OAc buffer. This solution was diluted 1:1 with buffer, again loaded onto the C-18 column and eluted with 75% ACN, the resulting solution was evaporated and dried in high vacuum. Dissolving in 1 ml MeOH, dilution with 4 ml water and dialysis against water (1000 mwco) gave no change in the conductivity of the water (NH_4OAc sublimes under high

vacuum). Final evaporation gave a green solid **2.2** (45 mg, 7%). HPLC (472): RT 12.85 min; 95.18%. Acidification with HCl (3N, 1% v/v) resulted in the appearance of two peaks in the HPLC, in agreement with conversion of the leuko form, presumably to the colored ioinized form: HPLC (472): RT 12.60 min; 49.69%: RT 15.10 min; 45.70%. MS (EI) (M – OAc)+ 1600, (M – 2 OAc +H)+ 1542. HRMS(EI) calculated for $C_{79}H_{101}N_9O_{13}Gd$[155] 1538.6745, found 1538.6749. UV (MeOH/ 2% HOAc) λ_{max} (log E): 308 (4.41), 420 sh. (4.58), 470 (4.94), 743 (4.48). Φ_{fMGd}= 0.0023, (200 μM, 50 μM respectively); MGd (λex = 473, λem = 650-850), Φ_{fRho} = 0.21 (λex = 480, λem = 500-700). Anal. Calcd for $C_{83}H_{106}N_9O_{17}Gd$: C 60.09%; H 6.44%; N 7.60%; O 16.39%. Found C 60.40%; H 6.51%; N 7.67%; O 16.26%}

Synthesis of 3,5-dimethylaniline-FITC (thiourea), 2.6 5-[3-(3,5-Dimethyl-phenyl)-thioureido]-2-(6-hydroxy-3-oxo-3H-xanthen-9-yl)-benzoic acid.[110] To a solution of 3,5-dimethylaniline (80 mg, 0.66 mM) in EtOH (6 ml) was added FITC (250 mg, 0.64 mMol). The solution was stirred at 25 ^{o}C for 24 hours. The solution was partitioned between HCl (40 ml, 3N) and DCM:MeOH (100 ml, 9:1), washed with water, brine, and dried over $MgSO_4$. Evaporation followed by flash chromatography purification over silica gel to provide the product (60 mg, 18%). HPLC (445 nm): T_r 12.77 min. 98.36%. ^{1}H NMR(400 MHz, d^6- DMSO) δ 2.23 (s, 6H), 6.56 (s, 4H), 6.66 (s, 2H), 6.79 (s, 1H), 7.02 (s, 2H), 7.16 (d, 8.0 Hz, 1H), 7.75 (d, 8.4Hz, 1H), 8.10 (s, 1H), 9.97 (s, 1H) 10.08 (d, 1H), 10.11 (s, 2H). MS(CI) (M-H)- 509. UV (DMSO solution diluted into MeOH) λ_{max} (log ε): 277 (5.54), 453(4.97), 479 (4.96). UV (DMSO solution diluted into MeOH, 2% (by volume) 0.1 N NaOH added) λ_{max} (log ε): 284 (5.52), 496(5.89).

Electronic Spectra and Quantum Yield Determination: The electronic spectra of the MGd-fluorophore conjugates **2** and **3** at 1.17 x 10^{-5} M and 1.15 x 10^{-5} M respectively in methanol solution containing acetic acid (0.35 M) gave a UV absorption of 1.0 (±

10%). Conversion to the fluorescent zwitterionic forms was effected by altering the pH of the methanolic solutions (with 0.1% v/v; 0.1 N NaOH and 3 N HCl respectively). These solutions were then diluted for the fluorescence studies. The quantum yields of the MGd and xanthene portions of the conjugates respectively were determined at 2×10^{-7} M (2 nm slit width) and 5×10^{-8} M (0.5 nm slit width) respectively.

Imaging Studies and Cytotoxicity Measurements in A549 Lung Cancer Cells

Fluorescence microscopy was performed using a Nikon Diaphot 200 microscope with fluorescein and rhodamine filter cubes. MGd fluorescence was observed using a custom filter set (Chroma Technology Corp.) Consisting of a D470/40x excitation filter, a 495dclp dichoric mirror, and an E700lp emission filter.

The human lung carcinoma cell line A-549 was obtained from ATCC and cultured in DMEM supplemented with 10% FBS and streptomycin/penicillin mixture. Cell lines were maintained as monolayer cultures in plastic culture flasks grown at 37^{o}C in a humidified atmosphere of 5% CO_2/95% air.

Chapter 3: Motexafin Gadolinium (MGd)-Malonato-Platinum compounds.

3.1 INTRODUCTION

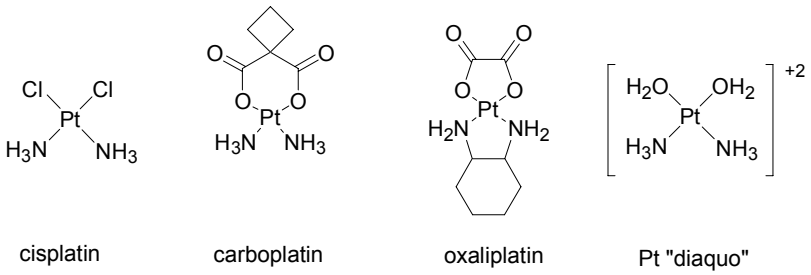

Figure 3.1 Structure of Pt therapeutic agents cisplatin, carboplatin, oxaliplatin, and active form "Pt diaquo."

Although cisplatin (Fig. 3.1) is used worldwide for the treatment of testicular and ovarian cancer, its use is accompanied by significant kidney toxicity.[168,169,171-173] Carboplatin and oxaliplatin are also widely used cancer therapeutic agents but they also show systemic toxicity due to non-specific tissue distribution. The MGd-Pt conjugates previously prepared have demonstrated poor efficacy in cell studies.[147] As MGd demonstrates both low toxicity and high tumor specificity in vivo, we hypothesized that MGd-Pt conjugates with more "carboplatin-like," coordination, e.g. malonates, could prove more active than the MGd-Pt conjugates to date.

Many strategies have been used to increase their tumor specificity, including structural modifications to the compound or by conjugation to antibodies, folate, PEG, and porphyrins. In addition, considerable effort has been directed at improving the performance of these compounds in terms of their ability to deliver active forms of Pt to cells.[147,155,233] Extensive study has elaborated mechanisms of action, profiles, specificity,

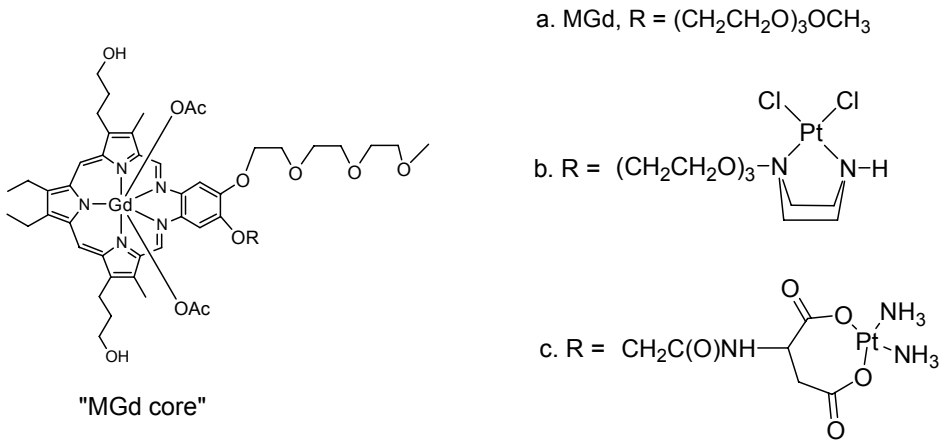

Figure 3.2 Structure of the "MGd core," MGd (**a)**, amino-Pt conjugate (b), and aspartate conjugate (c).

applications, and patterns of resistance. These three approved drugs have therapeutic activity, attributed mechanistically to hydrolytic loss of the non-nitrogen ligands (chloride or carboxyl), giving initially a mono-aquated species. The mono-aquated species, on completion of hydrolysis and loss of the O-side ligand, generates the reactive DNA-binding "Pt diaquo" species.[167,178,181-184]

Several Pt-conjugates have been reported in the literature, attempting to reduce the systemic toxicity often encountered with single agents. In an effort to improve the delivery of Pt to cells, we have developed Pt-conjugates of expanded porphyrins (e.g., MGd) illustrated in Fig. 3.2, which are attractive due to their specific uptake into tumor cells.[20,234] The texaphyrins are members of the "expanded porphyrin" class of macrocycles and have demonstrated coordination of larger metals. This has in turn allowed development of what appear to be several biologically well-tolerated experimental therapeutic agents.[41] These MGd-Pt conjugates were designed to take advantage of the tumor specificity for Pt delivery; with the MGd moiety potentially also acting as a radiation sensitizer.[147]

We have previously described the synthesis of MGd-Pt conjugates (Fig. 3.2) utilizing a PEG spacer for solubility and piperidine (**b**), or aminosuccinate(**c**) for Pt coordination. In conjugate (**b**), attachment was effected via piperazine. From previous SAR studies of several N-side conjugates, possible spatial limitations for the interaction of the Pt(II) centers with DNA were proposed to account for the low activity observed. In the case of the aminosuccinate species (**c**), the poor performance could be ascribed to possible premature Pt release. Unfortunately, these MGd-Pt systems demonstrated poor solubility and low activity when subject to in vitro biological testing. Here we report the synthesis of a new MGd-Malonate-Pt analog, **3.1**. The cytotoxicity of this analog was compared to carboplatin. In Appendix A we also report the development of an experimental general synthetic strategy to simplify the preparation of additional analogues.

3.2 SYNTHESIS OF MGD-PLATINUM CONJUGATE

Reviewing the historical success of the Pt malonates,[179] [235,236] and the PEG solubilized malonato-Pt conjugates recently prepared[73,155,237] inspired us to work along similar lines. We started from solubilized acid **3.2**, previously reported by this group to prepare MGd-Pt conjugates.[147] The aminopropylmalonate-di-t-butyl ester **3.3**, was prepared via the published procedure.[155] Coupling was effected by activation of the solubilized acid **3.2**, mediated by DCC, followed by the addition of aminomalonate **3.3** to give amide **3.4a**.

The deprotection of the malonate diester was performed at the dinitro stage. Removal of the t-butyl groups, generally considered to be facile, could not be effected by treatment with neat TFA, formic acid, or TMS-triflate.[238,239] Ultimately, 90/10 TFA/H_2O, utilized in peptide deprotection, proved successful.[240] The free acid **3.4b** was then

subject to catalytic reduction, cyclization with dialdehyde **1.5b**, and oxidative metallation with $Gd(OAc)_3$, to give the MGd malonate **3.5a** as the dominant product, with less than 20% of the mono-decarboxylation product being observed.

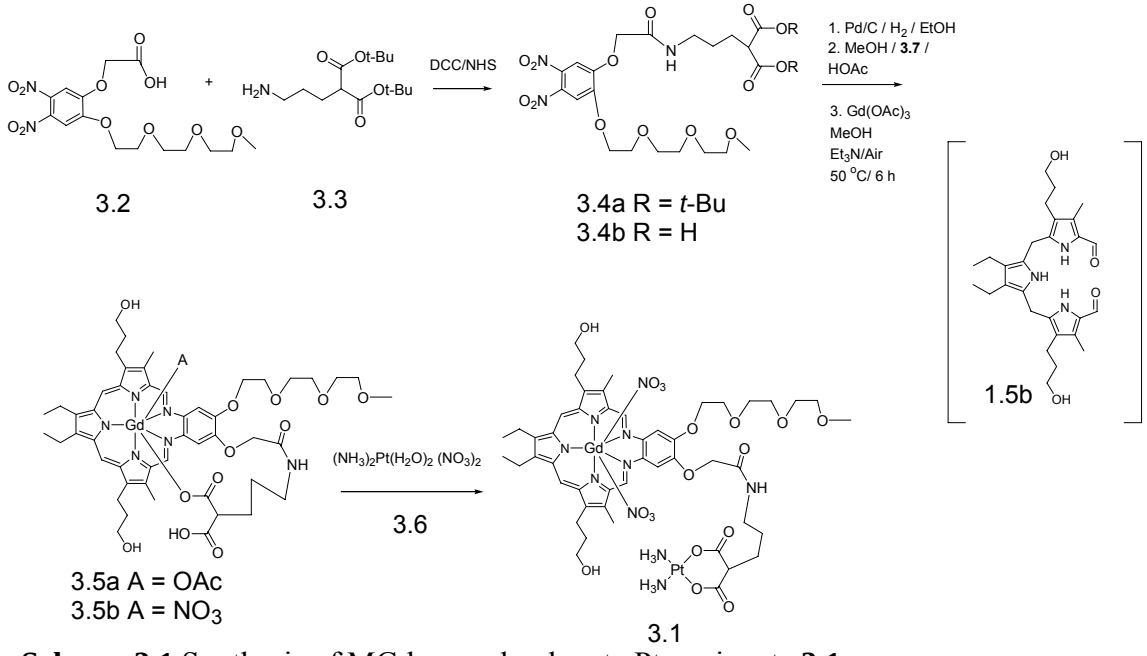

Scheme 3.1 Synthesis of MGd-propylmalonate Pt conjugate **3.1**.

With the MGd malonate in hand we proceeded to the platination. Initial attempts to platinate MGd-malonate **3.5a** with Pt "diaquo" **3.6** proved unsuccessful. Literature reports of the reaction of Pt-diaquo with acetate prompted us to exchange the MGd acetate anion for nitrate by loading on a tC-18 Sep-Pak column and eluting with $NaNO_3$ buffer to remove the NH_4OAc buffer used in the initial purification. Here the goal was to remove both ammonia and acetate, species that readily coordinate to platinum.[188]

A methanol solution of the resulting texaphyrin (nitrate) complex **3.5b** was mixed with an aqueous solution containing one equivalent of diaquo Pt and left to stir for 24 hours. Quenching the reaction by pouring into water gave a green solid, **3.1**. Analysis by

UV spectroscopy and LCMS provided support for a species that was consistent with the platinated-MGd product. By HPLC analysis the platinated MGd product eluted faster than the MGd-diacid. As anticipated, aqueous solutions of the conjugate appeared to release Pt over time, as supported by HPLC analysis. The HPLC of aqueous solutions of the platinated-MGd demonstrated decreasing levels of the platinated material and increasing levels of the MGd-diacid **3.5b**. This proved to be a reversible process, meaning the original HPLC trace corresponding to **3.1** could be regenerated by the addition of an excess of the Pt-diaquo complex. The conjugate was stable in both high concentrations of nitrate (0.5-1.0 M, aq.) and in methanol solution. Purification was effected on reverse phase tC-18 with Methanol/KNO_3 buffer. Desalting on the reverse phase tC-18 column by washing the bound material with water prior to elution with methanol gave the product which was evaluated for hydrolytic stability and tested against A549 cells.

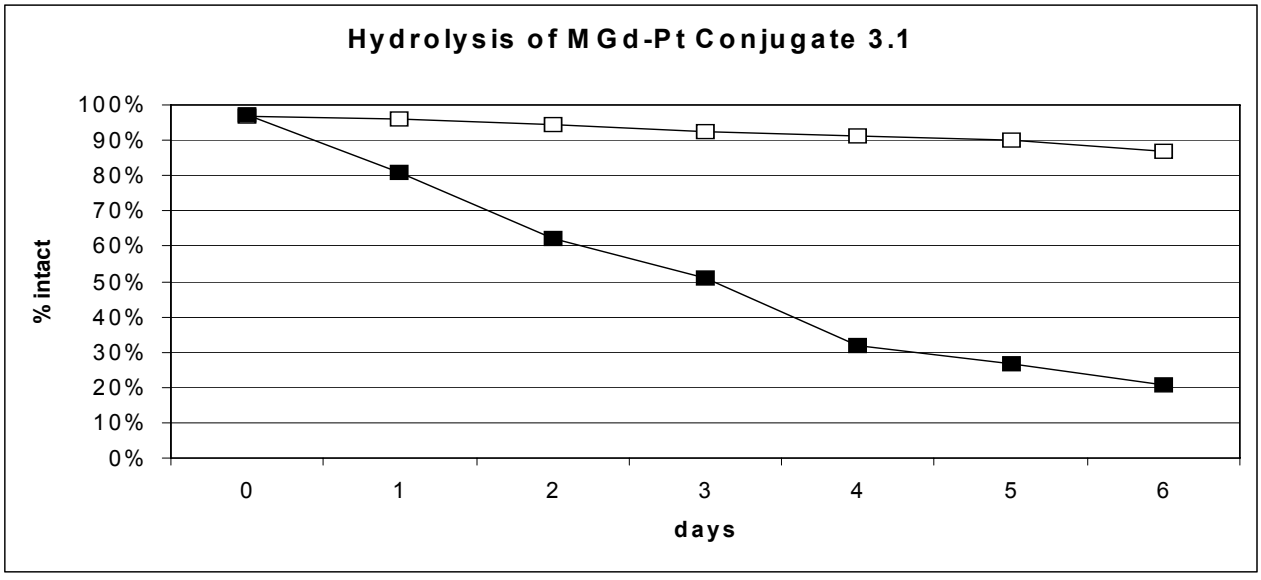

Figure 3.4 Hydrolysis Study of MGd-Pt conjugate **3.1** in methanol and phosphate buffered saline (PBS). Methanol (**3.1** □), PBS (**3.1** ■). Hydrolysis rate (loss of % intact) is inferred from HPLC analysis.

3.6 AQUEOUS STABILITY STUDY OF MGD-PT CONJUGATES

During purification of MGd-Pt conjugate **3.1**, the conjugate demonstrated reversible loss of Pt-diaquo. Presumably this loss was through hydrolysis. The loss was found to be reversible by the addition of Pt-diaquo. The half life of platinum loss for the conjugate in water was estimated at ca. 48 h, similar to the carboplatin hydrolysis rate.

In HPLC studies, the hydrolytic profile of conjugate **3.1** demonstrated $t_{1/2}$ = 3 days (additional, tertiary malonate model conjugates: noted in appendix A containing a PEG_2 linker, and a propyl linker conjugate were also prepared and both demonstrated an aqueous hydrolysis profile with $t_{1/2}$ = 9 days, the PEG conjugate Pt loss was confirmed as reversible on the addition of Pt-diaquo) The hydrolytic profile of conjugate **3.1** was reversible.Stirring the hydrolysis solution of **3.1** for one day at room temperature with excess "diaquo-Pt" resulted in regeneration of the peak at the original retention time for conjugate **3.1**, with a corresponding decrease in the peak seen to increase during the

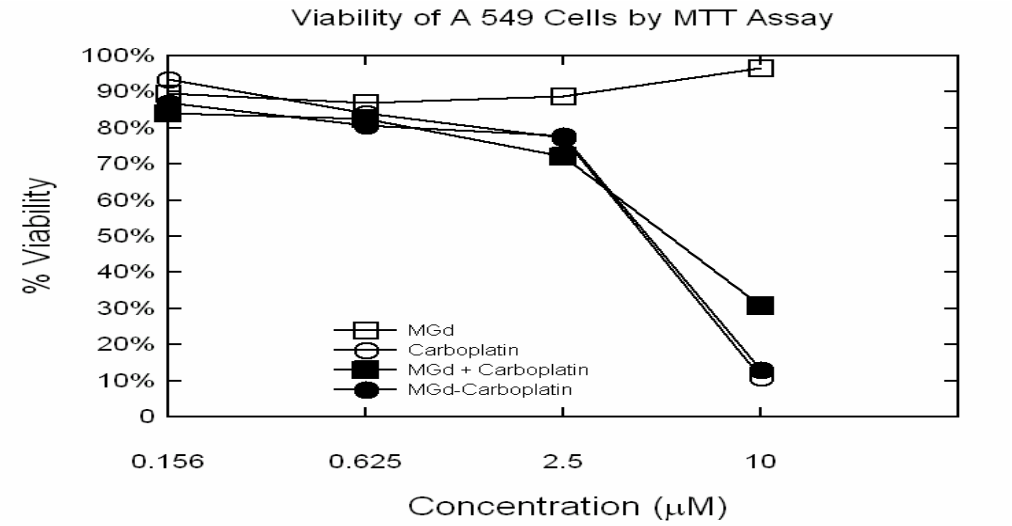

Figure 3.5 Cell studies with A549 Cells and Carboplatin, MGd and MGd-Pt conjugate **3.1**.

hydrolysis study.

Toxicity testing (Fig. 3.5) in A549 cells by MTT assay demonstrated efficacy equivalent to non-targeting carboplatin.

3.7 CONCLUSION

In an effort to exploit the tumor localizing ability of MGd a Pt conjugate containing a malonate coordinating moiety was synthesized. This compound demonstrated a hydrolysis rate similar to that of carboplatin. This conjugate also demonstrated efficacy against the A549 lung cancer cell line, similar to Carboplatin. Thus, we have confirmed our hypothesis that a MGd-Pt conjugate utilizing a malonate coordinating moiety demonstrate improved activity over the previous Gd-texaphyrin platinum conjugates.

3.8 EXPERIMENTAL METHODS

General Procedures

Unless otherwise noted, all reagents were obtained from commercial suppliers and used without further purification. Solvents were dried over molecular sieves except dichloromethane which was dried over CaH_2.Toluene and methanol used in sp^3-texaphyrin syntheses was degassed by purging with argon for 5 minutes. Toluene and methanol used in the sp^2-texaphyrin syntheses (MGd cyclization and metallation) were oxygenated by purging with air for 5-10 minutes, with additional purging being carried out during the reaction period for large scale preparations. The diacid **3.2** was prepared as previously repoprted.[147] The intermediate **1.5b** (2,5-bis[(5-formyl-3-hydroxypropyl-4-methylpyrrol-2-yl) methyl]-3,4-diethylpyrrole) was supplied by Pharmacyclics, Inc. Inorganic reagent $Gd(OAc)_3$.xH2O,was supplied by Strem Chemical Company. The $(NH_3)_2PtI_2$ (DIP) used was kindly supplied by Johnson Matthey Biomedical Materials.

Chromatography Merck type 60 (230-400 mesh) silica gel was used for column chromatography. For small-scale work-up Sep-Pak cartridges were purchased from Waters or Fisher in 0.5-20 gram sizes of C-18, alumina or silica. TLC was carried out using the conditions noted below using Whatman K6F aluminum backed silica gel plates, unless otherwise noted. Alternatively glass backed C-18 plates were used.

HPLC HPLC analyses were performed on a Beckman System Gold or Shimadzu Analytical/Preparative HPLC system equipped with PDA detector and a Zorbax XDB 5 μM 5 x 100 mm column. An ammonium acetate buffer (30 mM, pH = 4.3) / acetonitrile (ACN) gradient (30-99% ACN over 20 minutes) was used for the analysis of the non-Pt MGd compoounds. A 0.1% TFA / ACN gradient (10-99% over 15 minutes unless otherwise noted) was used for analysis of the MGd platinum conjugates. The MGd-Pt

conjugate HPLC analysis was performed on the C18 column with 0.1% TFA and acetonitrile as the eluent and detection at 472 nm.

NMR All ^{1}H, and ^{13}C NMR spectra were measured with a Varian Mercury 400 (400 MHz.) or Varian Inova 500 (500 MHz.) spectrometer in $CDCl_3$, D_2O, CD_3OD or D_7-dmf. The NMR chemical shifts are reported in ppm relative to the solvent. Low resolution and high resolution electrospray mass spectrometry (ESI MS) were performed with a Thermo Finnigan LTQ and Qq-FTICR (7 Telsa) instruments, respectively. Mass spectrometry (LRMS, HRMS) was carried out by the University of Texas at Austin Mass Spectrometry Facility. Elemental analyses were performed by Midwest Microlabs Inc. Electronic spectra were recorded on a Beckman DU-7 spectrometer.

General Methods: Chromatography: TLC, Flash, SPE and HPLC

TLC - Silica gel TLC of organic soluble samples commonly used EtOAc/hexanes or DCM as the eluents. The water solubilized PEGylated intermediates were chromatographed using 9:1 DCM:MeOH with HOAc or NH_3 to further deactivate the silica gel unless otherwise indicated. Silica gel chromatography of the texaphyrins required 9:1:0.1 DCM:MeOH:HOAc as the eluent.

Flash Chromatography - For the MGd complexes chromatography was typically performed by loading up to 1000mg MGd as a DCM solution on 75 cc pre-packed silica gel (1" diameter column) and eluting with 200-400 ml DCM, followed by 200-400 ml DCM/0.1-0.2% HOAc containing 5% MeOH, followed by the same solution at 10-40% MeOH. This elutes the first small red and pale green impurities. The main fraction is eluted with 400-800 ml DCM/HOAc solution containing 15% MeOH. Relevant fractions are collected as 100-200 ml aliquots. Relevant fractions can be re-chromatographed on

100 cc silica gel by diluting to 5% MeOH and loading directly onto the column. Elution with DCM/0.1% HOAc at 10% MeOH removes the trace red and green impurities and the main product fractions are removed at a gradient of 15-40% MeOH in DCM/HOAc with 400-600 ml solvent.

SPE - The MGd conjugates could also be purified on RP-tC18 SPE (Waters Sep-Pak) columns using gradients of MeOH or ACN against aqueous buffer (33mM NH_4OAc for esters and fluorophores, 10-100 mM KNO_3 or 0.1% TFA for other compounds), using NH_4OAc or KNO_3 buffers and acetonitrile or MeOH as the organic phase.

Pt-diaquo complex preparation: [200] $(NH_3)_2Pt(H_2O)_2^{+2}(NO_3)_2^-$ A solution of $(NH_3)_2PtI_2$ (0.42 g, 1 equiv.) and $AgNO_3$ (0.28 g, 2 equiv.) was dissolved in water (c.a. 10 ml) and stirred overnight in the dark. The solution was then centrifuged to pellet the silver iodide. The clear supernatant was removed and diluted as necessary.

Experimental

Synthesis of 2-(3-Amino-propyl)-malonic acid di-tert-butyl ester. **3.3**[155] To a solution of 3-phthalimidopropyl-di-*t*-butylmalonate (6.06 g, 15 mMol) in EtOH (75 ml) was added hydrazine (1.4 ml, 50% aq.). The solution was held at 70 ^oC for 3 hours. On cooling to ambient temperature and stirring overnight a flocculent white precipitate had formed. The EtOH was evaporated and the residue dissolved in DCM (2 x 100 ml). Washing with NaOH (250 ml, 0.5 N), drying with $MgSO_4$ and evaporation gave an oil (3.74 g, 91%) The oil can be further purified by flash chromatography over silica gel (EtOAc, MeOH gradient 0-12%). TLC: EtOAc: MeOH 8:1 R_f = 0.6 (detection with EtOH solution of 0.1% ninhydrin, 1% decylaldehyde). ^1H NMR($CDCl_3$ 300 MHz) δ1.42 (m, ~18 H), 1.52 (bs, 2H), 1.83 (q, 2 H), 2.72, (t, 2H) 3.12 (s, 1H). MS (CI) (M+H)+ 274.

Synthesis of 2-[2-(2-{2-[2-(2-Methoxy-ethoxy)-ethoxy]-ethoxy}-4,5-dinitro-phenoxy)-acetylamino]-malonic acid di-t-butyl ester. 3.4 To a solution of acid **3.2** (5.61 g, 14 mMol) in DCM (200 ml) with NHS (1.65 g, 14 mMol) was added DCC (3.6 g, 1.2 equiv.). The resulting solution was stirred briefly before the addition of the amine **3.3** (3.74 g, 13.7 mMol) and the resulting solution was left to stir overnight. The solution was then filtered and evaporated. The product was purified by flash chromatography over silica gel (EtOAc:hexanes 1:1) to provide the product, an unstable oil which undergoes decomposition under chromatography conditions(3.24 g, 36 %). HPLC (329nm): T_r 14.87 min, 91.24%. TLC(9:1 DCM: MeOH): R_f = 0.2. MS (EI) (M+H)+ 660. HRMS(EI) calculated for $C_{29}H_{46}N_3O_{14}$ 660.2980, found 660.2978. ^{1}H NMR(400 MHz, $CDCl_3$) δ 1.45 (s, 18 H), 1.60 (m, 2H), 1.81 (m, 2 H), 3.13 (t, J=7.2 Hz, 1 H), 3.36 (m, 5 H), 3.53 (m, 2 H), 3.53 (m, 2 H), 3.61-3.67 (m, 4 H), 3.72 (m, 2 H), 3.93 (m, 2 H), 4.37 (m, 2 H), 4.62 (s, 2 H), 7.00 (broad t, 1 H), 7.52 (s, 1 H), 7.52 (s, 1 H). ^{13}C NMR(100 MHz, $CDCl_3$) δ 25.6, 26.9, 2707, 38.6, 53.2, 58.8, 68.8, 69.2, 69.7, 70.3, 70.4, 70.7, 81.4, 109.2, 110.2, 136.0, 137.8, 149.4, 151.9, 166.2, 168.5. Anal. Calcd for $C_{29}H_{45}N_3O_{14}$: C 52.80%; H 6.88%; N 6.37%. Found C 46.13%; H 5.96%; N 5.32%.

Synthesis of MGd-malonate 3.5a The di-t-butyl protected dinitro malonate **3.4**, 1.69 g. (2.56 mMol) was stirred for 1 h. in 15 ml 90% TFA, 10% H_2O which cleanly deprotected the malonate (90+% by tlc and NMR) to give the diacid. The resulting solution was evaporated, then evaporated with 50 ml chloroform. The residue in MeOH(50 ml) was hydrogenated using Pd/C (0.42 g, 10% wet) catalyst at 40 psi for 18 hours. The solution was filtered through Celite and added to 1.28 g (2.66 mMol) **1.5b** in 50 ml MeOH and HCl (0.5 ml, 3N). The solution was held at 50 ^{o}C for 3 h. Complete by tlc, the solution was evaporated. Metallation: The residue was dissolved in MeOH (100 ml) with 1.10 g. $Gd(OAc)_3$ (1.05 equiv.) and 4 ml Et_3N. The solution was held at 50 ^{o}C

for 2 hours, complete by tlc. The solution was quenched with HOAc (4 ml) and evaporated. The residue was dissolved into 10 ml buffer (NH_4Oac, 33 mM, pH 4.3) and loaded onto a t-C-18 SPE cartridge (10 g). Elution with 80:20 ACN:buffer gave the product. This solution was diluted with buffer, again loaded onto the column, washed with water and eluted with MeOH. Evaporation and titration with Et_2O gave the product (0.18 g, 6.2 %)

HPLC (472nm): Tr 4.28 min 96.24%. MS (EI) (M – 2 OAc)+ 1084. HRMS(EI) calculated for $C_{49}H_{62}GdN_6O_{12}$ 1084.3667, found 1084.4425. Anal. Calcd for $C_{51}H_{65}GdN_6O_{14}$: C 53.57%; H 5.73%; N 7.35%. Found C 53.07%; H 5.73%; N 7.55%.

Synthesis of MGd-Pt 3.1. Starting from **3.5a** (230 mg, mMol) was dissolved in MeOH (10 ml) and diluted with KNO_3 (40 ml, 100 mM) and loaded on a C-18 SPE cartridge (10 g). The **3.5b** (NO3) was eluted off with MeOH (15 ml). The MeOH solution was mixed with $(NH_3)_2Pt(H_2O)_2^+$ (2 equiv.) and allowed to react in the dark for 48 hours. The resulting solution was diluted with an equal volume of KNO_3 (40 mM) and loaded on a C-18 SPE cartridge (10 g). Elution with KNO_3 (40 mM)/MeOH: 60/40 removed impurities. The product was eluted from the SPE cartridge with KNO_3 (40 mM)/MeOH: 40/60. The product was desalted by dilution 1:1 with KNO_3 (40 mM), reapplying to the SPE cartridge was followed by washing with HNO_3 (10mM) and eluting with MeOH containing 5% HNO_3 (10mM). The product was precipitated by the addition of Et_2O and centrifugation to give the green solid (84 mg, 9%).

HPLC (470 nm): Tr 7.36 min 95.97%. MS (EI) (M – NO_3)+ 1374. HRMS(EI) calculated for $C_{49}H_{66}GdN_9O_{15}GdPt$: 1373.3567; found: 1373.3574. UV: 419 (sh) 4.98e4, 474 1.19e5, 742 3.43e4. Anal. Calcd for $C_{49}H_{67}GdN_{10}O_{18}GdPt$: C 40.97%; H 4.70%; N 9.75%. Found C 40.67%; H 4.81%; N 9.46%.

Cytotoxicity Measurements in A549 Lung Cancer Cells

The human lung carcinoma cell line A-549 was obtained from ATCC and cultured in DMEM supplemented with 10% FBS and streptomycin/penicillin mixture. Cell lines were maintained as monolayer cultures in plastic culture flasks grown at 37^{o}C in a humidified atmosphere of 5% CO_2/95% air. The cytotoxic activity was measured by MTT assay. A 96-well plate was dispensed with 50 ul of cell suspension (4 x 10^3 cells/well). After the cells had settled (24 hours), the test compounds at equivalent concentrations (UV470 basis for MGd and the MGd-conjugate) were dissolved in media and sterilized by gamma irradiation, then 50 uL added. After incubation for 48 hours at 37^{o}C in 5% CO_2 the media was removed and cells washed once with serum-free DMEM containing no indicator. The cells were then incubated for 2-4 hours with MTT (1 mg/ml) in serum-free media. The media was removed and the cells were lysed with 50 ul isopropanol. The UV absorbance was measured at 595 nm against untreated wells and the IC_{50} values were calculated.

Chapter 4: Quaternary Amine Platinum Therapeutic Agents

4.1 INTRODUCTION

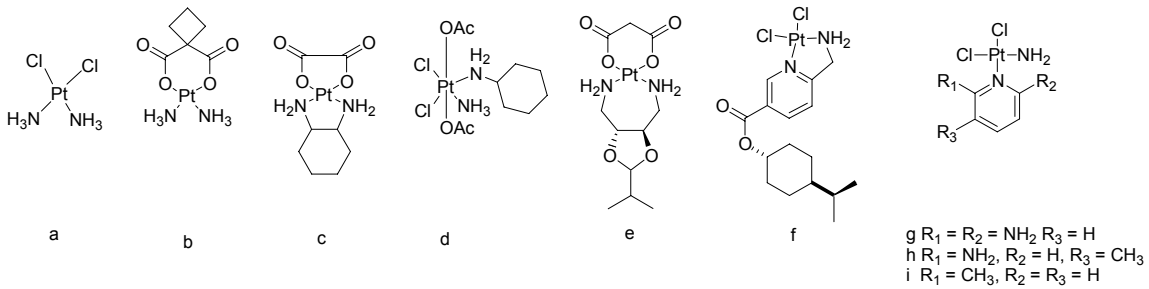

Figure 4.1. Platinum therapeutic agents: (a) cisplatin, (b) carboplatin, (c) oxaliplatin, (d) JM-216, (e) heptaplatin, (f) terpene-pyridine analog, (g - i) aminopyridine analogs

Cisplatin and carboplatin, are first and second generation therapeutic anticancer agents; however, they suffer from tumor resistance and non-specific toxicity. Third-generation oxaliplatin is an approved Pt compound with more lipophilic N-side substitution, and several experimental lipophilic N-side Pt therapeutic agents have been subsequently developed (Figure 4.1d-i). Oxaliplatin demonstrates therapeutic activity in resistant tumors; however, it suffers from low water solubility and neurotoxicity, thus efforts continue to develop improved platinum analogues.[180] We hypothesized that cationic, lipophilic N-side Pt therapeutic agents could retain the activity associated with lipophilicity, while the cationic charge, (analogous to Figure 4.1 g-i) appears to assist in efficacy.

Extensive structure activity relationship (SAR) studies of Pt compounds have shown that the highest activity is obtained with platinum is coordinated with alkylamines such as 1,2-diaminocyclohexane (DACH), small alkylamines, or o-phenylene

diamine.[175,202-205] Generally these (alkylamine)$_2$-Pt complexes exhibit low water solubility and so far modifications such as such as oxygenation, intended to make these compounds more soluble, have typically led to lower efficacy, heptaplatin being a notable exception.[206,207]

The structures in Figure 4.1,[197,199-201,241] containing small lipophilic N-side ligands, demonstrate in vitro activity. These finding are in agreement with structure activity relationship (SAR) studies, in which therapeutic activity has been correlated with small lipophilic ligands on Pt.[242],[202,204] The experimental pyridine family analogs (**g** - **i**) demonstrate activity against resistant tumors. These compounds, being more polar than oxaliplatin, may also have higher solubility and improved (or altered) uptake/retention profiles. These agents are also possibly cationic at cellular pH. Thus, the experimentally observed activity of the above pyridine-Pt compounds is in broad agreement with the lipophilicity and efficacy correlation proposed in SAR studies.

The above Pt therapeutic agents are thought to act as agents that bind to DNA and damage DNA. Cellular resistance to Pt anti-cancer agents is thought to involve excretion of the active Pt agent out of the cell, perhaps complexed to glutathione or other cellular molecules.[243,244] Thus, cellular retention of Pt therapeutic agents is an important consideration in the design of these compounds.

As noted previously, key objectives of the present study were to *i*) investigate the toxicity of lipophilic-cationic compounds and their lipophilic-cationic-Pt derivitives in cancer cells, *ii*) develop and utilize synthetic and testing methodologies that allow rapid synthesis and screening of lead candidates, and, *iii*) develop lead Pt compounds from these initial studies. In this context, we were inspired specifically by delocalized lipophilic cations (DLC), species which demonstrate cellular uptake and retention.

From numerous imaging studies it is clear that lipophilic cations can either embed in the membrane such as is the case for voltage sensitive dyes (e.g. NK-529[208]), or they can be transported through cellular membranes and accumulate in organelle such as mitochondria that have a negative membrane potential.[115] Delocalized lipophilic cations (DLC) are known to act as transport agents or toxins and have been proposed for therapeutic use. Therapeutically significant, the mitochondria localizing rhodamine also has demonstated activity in multiple drug resistant (MDR) tumors.[217] Separately, triphenylphosphonium cation demonstrates mitochondrial localization and has been proposed as a therapeutic agent carrier.[209-211] Further support for the lipophilicity/ retention hypothesis is demonstrated by a combinatorial study of fluorescent styryl quaternary cations in which 53 of 119 compounds synthesized were observed localized in the nucleus or mitochondria by fluorescence microscopy.[115]

Some lipophilic cations are also known to demonstrate significant cell toxicity,

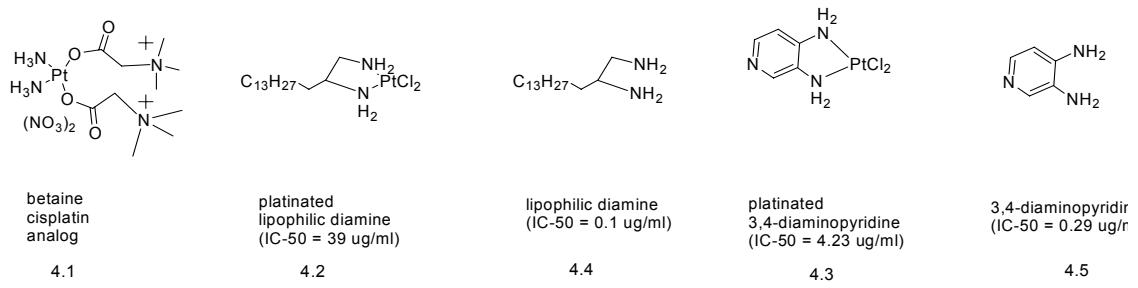

Figure 4.2. Cisplatin analogs: betaine **4.1**, lipophilic diamine-$PtCl_2$ **4.2**, precursors **4.4**, 3,4-diaminopyridine-$PtCl_2$, **4.3**, and ligand precursor **4.5**.

acting as detergents that damage cell membranes. Toxic cations include dequalinium chloride,[212-214], C6-DAP,[215] and cetylpyridinium,[216] which are used as a herbacide, polymeric antibacterial agent, and topical disinfectant, respectively. The above mentioned lipophilic quaternary cationic compounds do not specifically target tumors

and appear to act as either highly toxic detergents, or are inert, thus they have not generally been used therapeutically.

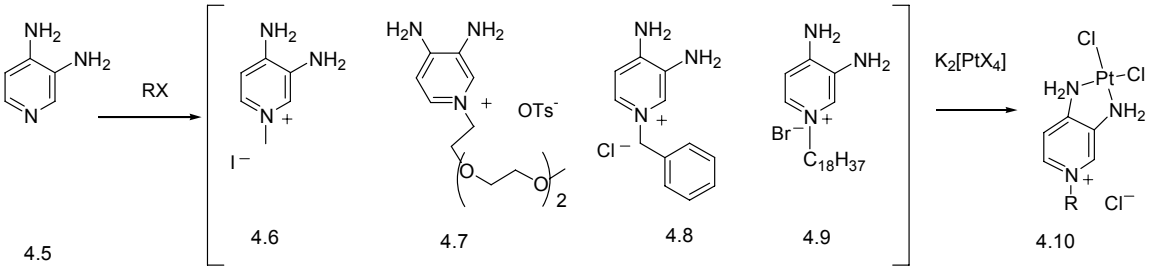

Scheme 4.1. Synthesis of quaternary diaminopyridines and Pt complexes.

The experimental cationic betaine-Pt compound **4.1** [218] (Figure 4.2) demonstrates improved efficacy over cisplatin in cell studies, presumably through DNA damage. We hypothesized that Pt therapeutic agents, with robust attachment of DLCs could result in agents both soluble and efficacious. An interesting anomoly is demonstrated by the experimental lipophilic diamine Pt complexes **4.2** and **4.3.** These species have a 400-fold and 15-fold lower toxicity, respectively as the Pt complex, compared to the amine ligand precursors **4.4** and **4.5**.[245 246] While presumably such Pt agents would possess improved cellular retention, possibly overcoming resistance mechanisms such as export of the active Pt species, unfortunately, metallation has diminished their efficacy. From this background we set out to develop improved therapeutic agents.

4.2 RESULTS

We hypothesized that quaternarization of 3,4-diaminopyridine **4.5**, (Scheme 4.1) would simultaneously inactivate the pyridine nitrogen against reactivity with Pt species,

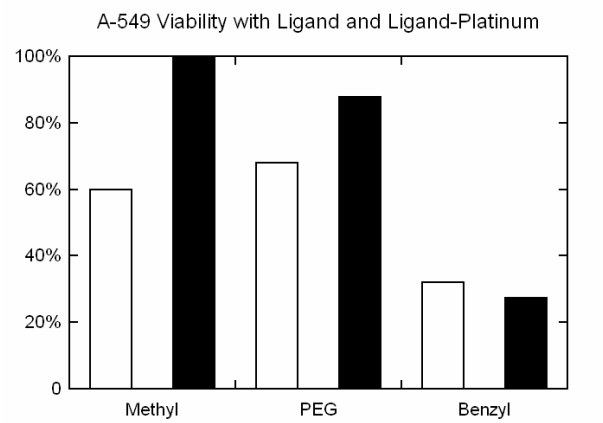

Figure 4.3 A549 cell viability by MTT assay following 96 h incubation with quaternary ligands (white bars) and their Pt complexes (black bars) at 20 μM.

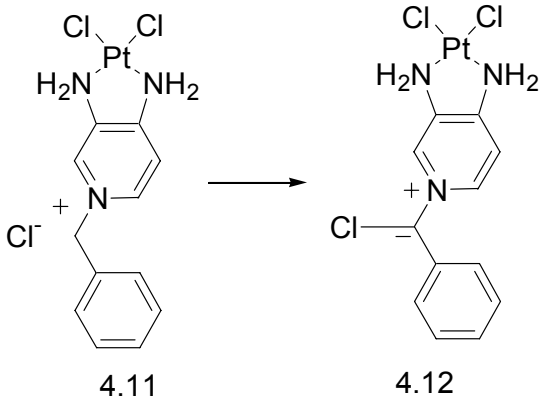

Scheme 4.2 Quaternary Pt salt **4.11** demonstrating highest cytotoxic activity and possible degradation product **4.12**.

and improve the solubility of these compounds. The synthesis of the methyl and benzyl quaternary derivitives having been previously reported, reaction of pyridine **4.5** with alkyl halides under either room temperature or microwave assisted conditions, gave the N-quaternary compounds **4.6** - **4.9**. The high nucleophilicity of the pyridine nitrogen gave selective quaternization, producing a product with ^{1}H NMR data consistent with only the desired isomer.[247] Although chromatography has been reported for these quaternary salts using highly polar conditions, the reaction selectivity allowed purification by recrystallization. These quaternary aminopyridine species are expected to be cationic at cellular pH. These aromatic cationic "diamine" compounds were thus designed to give non-labile coordination to Pt(II), a flat ring to fit the steric requirements for DNA intercalation, and we anticipated tuning the quaternary substitution to optimize properties.

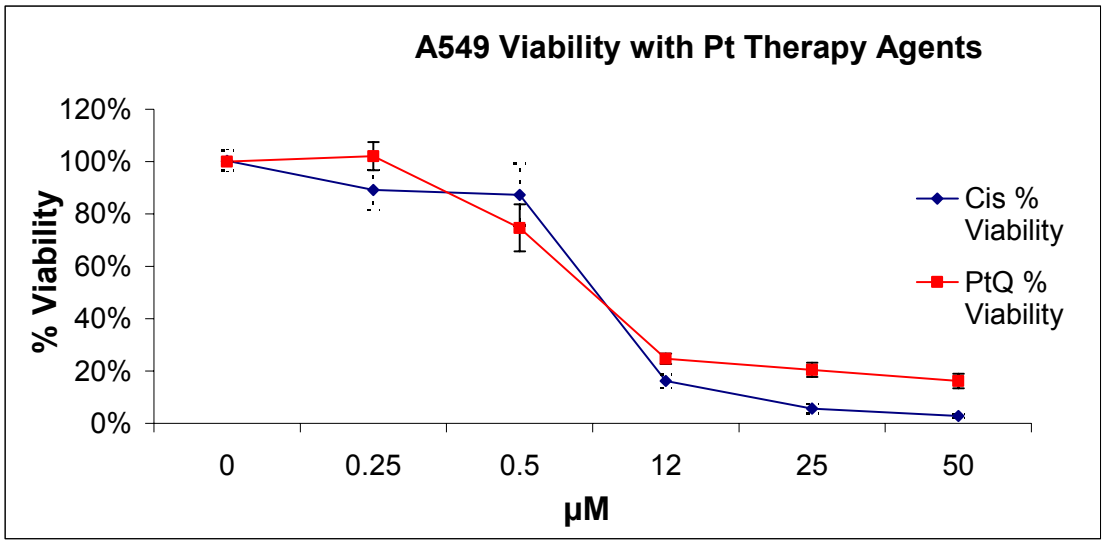

Figure 4.4 Evaluation of cytoxicity of cisplatin and **4.11** (PtQ) in the A549 lung cancer cell line by MTT assay.μM

With the quaternary amines salts in hand, the in situ screening method of Ziegler was used (Scheme 4.1).[200] Briefly, K_2PtCl_4 was activated in situ with excess iodide. In situ reaction with the amines generated the putative bis-coordinated Pt-complexes of type **4.10**. The solutions of the complexes were prepared with a 1:1 ratio of Pt to ligand. Addition of DMF dissolved the resulting complexes, and the excess halide was removed by reaction with $AgNO_3$. Centrifugation, followed by addition of KCl and evaporation gave the complexes.

4.3 CYTOTOXICITY STUDY

The products solutions were evaluated for toxicity using a standard MTT assay (Figure 4.4). Both the ligands **4.6** – **4.8** and their putative Pt conjugates, after dissolving in minimal dimethylacetamide, were evaluated for toxicity in the A549 cell line (Fig. 4.3)

at 20 μM concentration.[248] The resulting solutions were also assayed for total Pt content by ICP-MS. The insolubility of the C18 salt **4.9** precluded biological testing. While this methodology allowed rapid screening, the toxicity of the ligands and $AgNO_3$, as well as the detoxifying effect of Pt coordination needed to be accounted for. Loss of the Pt-complexes during the halide precipitation was also of concern.

Toxicity experiments with $AgNO_3$ demonstrated no significant toxicity over controls. The Pt-L toxicity was evaluated on the basis of Pt content, to correct for ligand toxicity. The results obtained in this way (Fig. 4.3) confirmed that the benzyl Pt compound **4.11** was the most active in this series. This series broadly parallels **4.2 – 4.5**, toxicity decreasing on metallation and toxicity increasing with lipophilicity across the series, until intersecting with **4.11**.

The synthesis of **4.11**, was scaled up by reacting the quaternary pyridine salt **4.8** in methanol directly with an aqueous solution of K_2PtCl_4. This reaction initially (1 h stirring) gave a flocculent pink precipitate. On standing 2-3 weeks in the dark, tan orange spherical crystals were produced that were unfortunately not suitable for X-ray diffraction studies. LC-MS and HRMS analyses for the orange crystals were consistent with structure **4.11**. The aqueous solutions of this material slowly changed color from pale yellow to blue, assigned as being a structure incorporating water ligand on the Pt. Such an arrangement is in agreement with LCMS studies of fresh and aged solutions, which revealed the existence of two discreet compounds. In fresh solutions, **4.11** exhibited T_r = 5.29 minutes, M+ = 465. Over time the LCMS of the solution changed to a new product with T_r = 4.15 minutes, M+ = 500. The LCMS values agree with the assignment of the initial cationic orange compound **4.11** as the late eluting product, and the slowly formed blue compound as the early eluting product, as the higher molecular weight compound, proposed structure **4.12**. This proposed structure incorporates an extra

chloride, as the benzyl ylide in agreement with the MS data. The proposed zwitterionic structure is in agreement with a product eluting more rapidly by HPLC, having less lipophilic character. The analogous simpler Pyridinium chlorophehylmethylylide has been previous reported, prepared by alternate means.[249] Fresh solutions of **4.11**, more stable in DMSO, less so in water, gave predominantly the longer retained M^+ = 464 LCMS peak, the M^+ = 500 increasing over time. Toxicity studies of solid **4.11** in the A549 lung cancer line by MTT assay demonstrated efficacy comparable to cisplatin, with LD_{50} = 6 μM following 96 h exposure.

4.4 CONCLUSION

To study putative N-side lipophilic cations, a series of increasingly lipophilic catioins and their putative platinates were synthesized. As the ligands themselves demonstrated significant toxicity, efficacy screening of the in-situ synthesized conjugates for efficacy was based on Pt content to account for the ligand toxicity bias. The benzyl diamino-Pt compound was then specifically synthesized and characterized. It demonstrated efficacy equivalent to cisplatin against A549 cancer cells. This confirms our hypothesis that cationic lipophilic Pt compounds can retain therapeutic activity.

4.5 EXPERIMENTAL SECTION

Materials. Unless otherwise noted, all reagents were obtained from commercial suppliers and used without further purification. Solvents were dried over molecular sieves. Inorganic K_2PtCl_4 was supplied by Aldrich and Strem Chemical Company.

HPLC Analyses. HPLC analyses were performed on a Shimadzu Analytical/Preparative HPLC system equipped with a PDA detector. An ODS C18aq column (100 x 4.6 mm, YMC) using 0.1% TFA and MeOH gradient (10% - 95% organic) as eluent, a flow rate of 0.5 ml/min, with detection at the noted wavelength.

NMR Spectroscopy. All ^{1}H, ^{13}C and ^{195}Pt NMR spectra were measured with a Varian Mercury 400 (400 MHz.) or Varian Inova 500 (500 MHz.) spectrometer in $CDCl_3$, D_2O, CD_3OD or D_7-dmf. The NMR chemical shifts are reported in ppm relative to the solvent except in the case of ^{195}Pt (relative to K_2PtCl_4 in D_2O). Low resolution and high resolution electrospray mass spectrometry (ESI MS) were performed with a Thermo Finnigan LTQ and Qq-FTICR (7 Telsa) instruments, respectively. Mass spectrometry (LRMS, HRMS) was carried out by the University of Texas at Austin Mass Spectrometry Facility.

Elemental Analyses. Elemental analyses were performed by Midwest Microlabs Inc. Platinum analysis was performed by Thomas Kreschollek of the Holcombe Research Group at the University of Texas at Austin using ICP-MS and commercial Perkin-Elmer platinum standards. Samples for ICP-MS were dissolved in dilute nitric acid.

Synthesis. The general procedures for preparing the intermediates and compounds are as follows.

Synthesis of the Quaternary pyridine ligands: The quaternary pyridine salt was prepared according to the published procedures.[250] Briefly, the aminopyridine and the appropriate alkyl halide were stirred at room temperature for 24 h in acetonitrile. If no precipitate was visible, the solution was either heated to 70 ^{o}C for 2-12 hours, or placed in a in a microwave reactor at 70 ^{o}C for 2-60 minutes. The solid products were isolated by filtration. All products were analyzed by NMR spectroscopy and demonstrated features in agreement with a single product, in agreement with previous sysnthesis of the methyl and benzyl derivitives.

Synthesis of the Pt-diaquo: The $(NH_3)_2Pt(H_2O)_2^{+2}(NO_3)_2^{-}$ was prepared according to published procedures. [179] Briefly $(NH_3)_2PtI_2$ (0.42 g, 1 equiv.) and $AgNO_3$ (0.28 g, 2 equiv.) was dissolved in water (c.a. 10 ml) and stired overnight in the dark. The precipitated solid removed by contrifugation and the clear supernatant was removed and diluted.

Synthesis of the Quaternary pyridine-diaminoplatinum dihalide (in situ preparation): The amine ligand was metallated according to the high throughput procedure of Ziegler.[200] Briefly, K_2PtCl_4 (200 mM, 50 μL) was activated by the addition of KI (800 mM, 50 μL) and was mixed in equimolar quantities with a methanolic solution of the amine quaternary salt (200 mM, 150 μL), and held for 1-4 h at 37 ^{o}C. The resulting solution was then treated with $AgNO_3$ (200 mM, 500 μL)and methanol (500 μL) and the precipitate removed by centrifugation. The supernatant was removed, treated with dilute HCl and again centrifuged. Methanol was added to redissolve precipitated product. The resulting solutions were evaporated, folowed by dilution with minimal dimethylacetamide, followed by toxicity evaluation (20 μM concentration) by cell assay. The same dimethylacetamide solution was assayed for Pt content by ICP-MS.

Synthesis of the Pyridinium, 3,4-diamino-1-methyl-iodide. 4.6[251] To a solution of the amine (0.5 g, 4.6 mMol) in acetonitrile (4 ml) was added MeI (0.7 g, 4.9 mMol). The solution was left to stir overnight. Filtration and washing with acetone gave the product as a white solid (0.66 g, 57%). HPLC(298nm): Tr 3.44 min, 99.71 %. ^{1}H NMR(400 MHz, d^{6}- DMSO) δ 3.84 (3H, s), 5.50 (2H, bs), 6.68 (1H, d, J = 6.8 Hz), 7.28 (2H, bs), 7.50 (1H, d J = 1.7 Hz), 7.70 (1H, dd J = 6.8, 1.7 Hz). ^{13}C NMR(100 MHz, $CDCl_3$) δ 45.5, 107.4, 125.7, 132.9, 135.5, 147.7. MS (EI) (M-I)+ 124.

Synthesis of the Pyridinium, 3,4-diamino-14-{2-[2-(2-Methoxy-ethoxy)-ethoxy]-ethyl}-benzene-1,2-diamine. 4.7 To a solution of the amine (0.5 g, 4.6 mMol) in ACN (4 ml) was added $MeOPEG_3OTs$ (1.6 g, 5.0 mMol). The solution was heated in a microwave reactor (80 ^{o}C, 15 min). Cooling, filtration and washing with acetone gave the product as a tan solid (1.82 g, 71%). HPLC (302nm): Tr 5.58 min, 90.30 %. ^{1}H NMR(400 MHz, d^{6}- DMSO) δ 2.27 (3H, s), 3.20 (3H, s), 3.37(2H, m) 3.43 (4H, m), 3.49 (2H, m), 3.70 (2H, t J = 4.8 Hz), 4.23 (2H, t J = 5.1 Hz), 5.49 (2H, bs), 6.69 (1H, d, J = 6.5 Hz), 7.01 (2H, d J = 8.5 Hz), 7.35 (2H, bs), 7.45 (2H, d J = 7.9 Hz), 7.58 (1H, s), 7.74 (1 H, dd J = 6.8, 1.4 Hz). ^{13}C NMR(100 MHz, d^{6} – DMSO) δ 26.2, 62.6, 63.5, 74.5, 75.0, 75.2, 76.7, 130.9, 133.5, 137.5, 143.2, 151.0, 153.0. MS (EI) (M-OTs)+ 256. HRMS(EI) calculated for $C_{12}H_{22}N_3O_3$ 256.1656, found 256.1659. Anal. Calcd for $C_{19}H_{29}N_3O_6S$: C 53.38%; H 6.84%; N 9.83%. Found C 53.46%; H 6.65%; N 10.07%.

Synthesis of the Pyridinium, 3,4-diamino-1-(phenylmethyl)-chloride. 4.8[250]. To a solution of the amine (1.1 g, 8.7 mMol) in MeOH (15 ml) was added BzCl (0.99 g, 9.0 mMol). The solution was left to stir for three days. The solution was added to EtOAc (200 ml) and the product initially oiled, then crystallized. The solid was isolated by centrifugation and washed with acetone to give a white solid (1.02 g, 48%). HPLC (308 nm): Tr 12.36 min, 96.97%. ^{1}H NMR(400 MHz, d^{6}- DMSO) δ 5.31 (2H, s), 5.68(bs

NH_2), 6.78 (1H, d, J = 6.8 Hz), 7.31-7.44 (5H, m), 7.59 (1H, d J = 1.7 Hz), 7.94 (1H, dd J = 6.5, 1.7 Hz). ^{13}C NMR(100 MHz, $CDCl_3$) δ 60.8, 107.4, 123.7, 128.7, 129.3, 129.7, 133.5, 134.8, 136.4, 148.4. MS (EI) (M-Cl)+ 200. HRMS(EI) calculated for $C_{12}H_{14}N_3$ 200.1189, found 200.1188.

Synthesis of the Pyridinium, 3,4-diamino-1-octadecyl-bromide. 4.9 This compound was prepared according to the general procedure above. To a solution of the amine (0.62 g, 5.7 mMol) in ACN (2 ml) was added octadecyl bromide(1.93 ml, 5.7 mMol). The solution was heated in a micorwave reactor (120 ^oC, 40 minutes). Filtration and washing with acetone gave the product as a white solid (0.97 g, 39%). HPLC (304 nm): Tr 17.96 min, 95.67%. ^1H NMR(400 MHz, d^6- DMSO/D_2O/MeOH) δ 0.83 (3H, t J = 7.1 Hz), 1.21 (30, bs), 1.69 (2H, t J = 6.9 Hz), 4.05 (2H, d J = 7.2 Hz), 5.50 (2H, bs), 6.69 (1H, d J = 6.7 Hz), 7.35 (2H, bs), 7.59 (1H, s), 7.77 (1H, d J = 6.7 Hz). ^{13}C NMR(100 MHz, d^6- DMSO) δ 14.6, 21.5, 22.8, 29.4, 29.6, 29.7, 29.9, 32.0, 58.14, 107.5, 124.2, 133.1, 134.7, 148.0. MS (EI) (M-Br)+ 363. UV: λ = 232, 304 Anal. Calcd for $C_{23}H_{44}BrN_3$: C 62.43%; H 10.02%; N 9.50%. Found C 62.51%; H 10.22%; N 9.50%

Synthesis of the putative Platinum-Amine complexes (in situ). The reaction was carried out as noted above. The products were complex mixtures by HPLC analysis. The dried samples were dissolved in dimethylacetamide and diluted with PBS for biological testing. Samples were assayed for Pt by ICP-MS. Low resolution ESI analysis of the L-Pt complexes gave results in agreement with predictions for the Pyridinium-Pt complexes with loss of ligand anion (methyl (M+ calculated 389, observed 388), PEG_3 (M- = 555), and benzyl (M+H = 466)).

Synthesis of the [1-(phenylmethyl)-3,4-diaminopyridinium chloride] dichloroplatinum. 4.11 (Preparative Scale) A solution of K_2PtCl_4 (0.44g mMol, 200mM) in water was added to a solution of diaminopyridine (0.27g, 200 mM) in

methanol. A volume of methanol equal to that of the pyridine solution was then added and the resulting solution allowed to stand in the dark for 2 weeks. The initially white-pink precipitate turned to orange spherical crystals under a flocculent blue-green precipitate. The fluffy blue green precipitate was removed by decantation and tituration of the orange solid with the mother liquor. The resulting orange solid was isolated by filtration and washed with methaol to give **4.11** (0.247g, 49%). HPLC (278nm): Tr 6.88 min, 97.12% LCMS ESI: T_r(M): 5.30 min (464.16). LCMS (EI) (M-H)+ 464, (M+ Cl)+ 500. HRMS(EI) calculated for $C_{12}H_{14}N_3Cl_2{}^{194}Pt$: 464.0192; found: 464.0194. HRMS(EI) calculated for $C_{12}H_{14}N_3Cl_3{}^{194}Pt$: 499.9901; found: 499.9906. ^{1}H NMR(400 MHz, d^7-DMF) δ 3.67 (s, 2H), 5.78 (s, 2H), 7.38 (d, 1H), 7.58-7.65 (m, 7H), 8.19 (s, 4H), 8.51 (d, 1H, J = 1.7 Hz),8.60 (p, 2H, J = 7.2, 1.7 Hz). ^{13}C NMR (100 MHz, d^7- DMF) δ 61.0, 111.0, 126.3, 128.1, 129.1, 129.4, 135.7, 136.6, 140.3, 153.5. ^{195}Pt NMR(86 MHz, d^7-DMF) δ (K_2PtCl_4 standard, 110 mg/ml in D_2O) 2887 ppm (small 3327 ppm peak). ^{195}Pt NMR(86 MHz, d^7- DMF) **4.11** (15 mg/ml d^7-DMF 2613 ppm. UV: λ_{max} = 278. Other hplc studies: Solid **4.11**, T_r = 5.30 min, 92% assay converts to: **4.12**, blue solution, on standing T_r = 3.97 min 82%. Anal. Calcd for $C_{12}H_{14}N_3Cl_3Pt$: C 28.73%; H 2.81%; N 8.38%. Found C 28.41%; H 2.84%; N 8.14. CH correlation by NMR: (C ppm/H ppm): 61.4/5.6; 111.4/7.3; 126.6, 129.0, 129.5, 129.7/~7.5; 136, 137/8.3; 140.6/8.4; 153.8/no H

Cytotoxicity Measurements in A549 Lung Cancer Cells

The human lung carcinoma cell line A-549 was obtained from ATCC and cultured in DMEM supplemented with 10% FBS and streptomycin/penicillin mixture. Cell lines were maintained as monolayer cultures in plastic culture flasks grown at 37^{o}C in a humidified atmosphere of 5% CO_2/95% air. The cytotoxic activity was measured by MTT assay. A 96-well plate was dispensed with 50 ul of cell suspension (4 x 10^3

cells/well). After the cells had settled (24 hours), the test compounds at equivalent concentrations were dissolved in DMSO and sterile filtered, then 5 uL added. After incubation for 48 hours at 37^{o}C in 5% CO_2 the media was removed and cells washed once with serum-free DMEM containing no indicator. The cells were then incubated for 2-4 hours with MTT (1 mg/ml) in serum-free media. The media was removed and the cells were lysed with 50 ul isopropanol. The UV absorbance was measured at 595 nm against untreated wells and the IC_{50} values were calculated.

Chapter 5: Conclusion and Future Directions

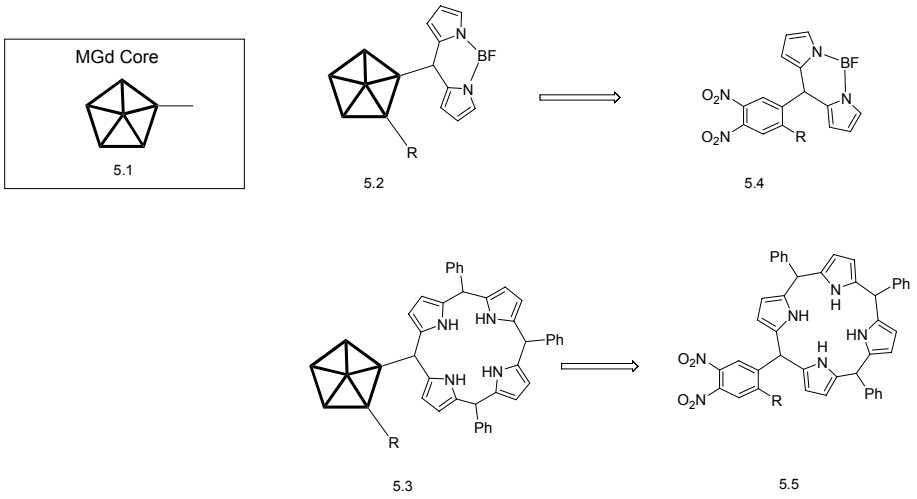

Figure 5.1 MGd BODIPY **5.2** and porphyrin **5.3** conjugates

In preliminiary studies the lipophilic and fluorescent conjugates were developed attempting to understand localization and efficacy correlations. At the cellular level, in these studies MGd and its analogues were observed to distribute diferentially. We viewed these efforts as an early step in the development of more useful conjugates.

In the course of the fluorescent studies, the MGd-Rho conjugate was observed to localized in the mitochondria of A549 cells, the MGd-FITC conjugate localized in the nucleus. The A549 cell line in toxicity studies with ascorbate adjuvant, as compared to the ascorbate sensitive Jurkatt leukemia cell line, demonstrated significantly lower sensitivity to MGd and it's fluorescent conjugates. The A549 cell line as compared to the ascorbate sensitive Jurkatt cell line, required 20-fold higher ascorbate levels and X-ray

irradiation before significant toxicity was observed.[129] In both cases however, apparent synergy was observed.

The conjugation of MGd to fluorophores with higher quantum yield hasboth technically simplified the imaging process of "MGd" as lower concentrations are more easily observed, and has demonstrated that these fluorescent conjugates have a different sub-cellular distributon. A reasonable extension of this work (Fig. 5.1) is to develop additional MGd fluorescent conjugates containing BODIPY **5.2** and porphyrin **5.3** moieties, based on a pyrrole motif. These can be envisioned as arising from published dinitro-BODIPY derivative **5.4**, and dinitroporphyrin **5.5** (the mononitro derivative having been reported), respectively. The resultant MGd-conjugates **5.1** and **5.2** are expected to be fluorescent. Preliminary experiments utilizing the aforementioned synthetic intermediates have provided samples with spectral and LCMS properties in agreement with those expected for the above structures **5.2** and **5.3**. An additional reason to synthesize these compounds is that they may also possess redox properties differing from the MGd compounds prepared to date. Altering the redox properties of MGd has been another ongoing project within the Sessler group, in an effort to improve the therapeutic efficacy of MGd.

Separately, continuation of the MGd-Pt conjugate synthetic efforts reported here have resulted in the preparation of two new conjugates, with spectral data in agreement with **A1** (see Appendix A) as well as a simpler, anologous "propyl" linked conjugate which demonstrated solubility issues. Attempting to utilize the biolocalization of MGd, the first water soluble MGd-platinum conjugate **3.1** synthesized in the course of this study demonstrated equivalent toxicity to carboplatin. This PEG solubilized conjugate

did not suffer from the low solubilility issues of previous MGd-Pt conjugates. The other conjugates, model compound in Appendix A, while less soluble, were proof in principle of a route that appears to enable both rapid synthesis and wide structural variation. Additionally gratifying was the preliminary aqueous stability study of conjugate **A1**, which demonstrated by HPLC the conjugate decreasing over time, reversing on the addition of Pt-diaquo. The HPLC traces of the study in Appendix A indicated more rapidly dissappearance for the tertiary malonate conjugate **3.1** than for the quaternary conjugate **A1**.

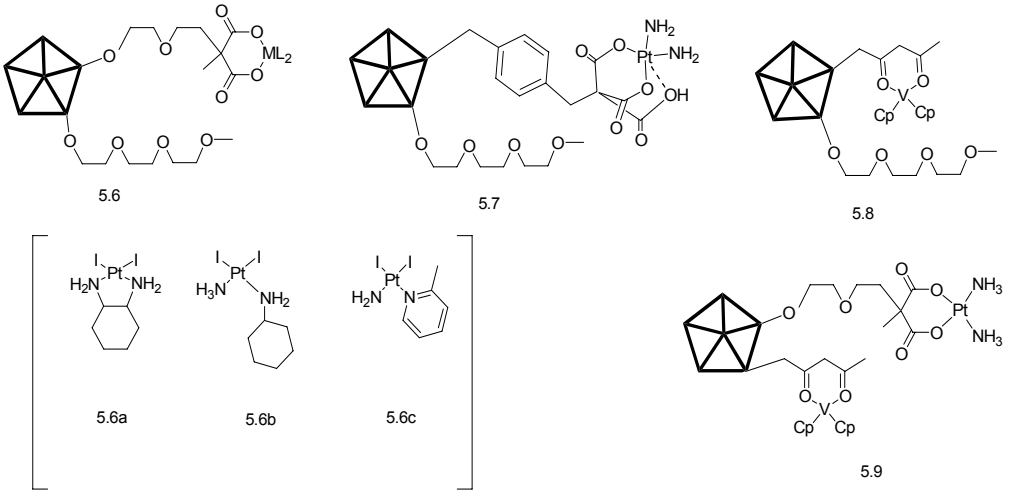

Figure 5.2 Proposed MGd-M conjugates (**5.6-5.9**) and precursors (**5.6a-c**).

Modification of proposed model compound **A1** into a useful therapeutic agent such as the proposed **5.6** can be envisioned as arising from analogs with a solubilizing PEG chain, synthesized via known routes.[252,253] Further improvements in efficacy may be attainable by the coordiation of therapeutic Pt moieties with demonstrated therapeutic activity, which can be envisioned as arising from dihalides such as **5.6a** (oxaliplatin precursor), **5.6b** (JM-216 precursor), and **5.6c** (ZD0473 precursor).

Thus, based upon the preliminary MGd-Pt results, a series of tri-PEG-linked MGd conjugates **5.6** and carboxylato-chelators **5.7**, appears synthetically justified. The readily derivitized tricarboxymethane[254] derivatives were of interest due to both their tri-coordinate nature, and the ability to readily convert them to conjugates in the ester state, then hydrolysis gives a coordinating species. A possible addional feature is that, on exposure to acidic conditions, the loss of a carboxylate renders the remaining malonate fragment a poorer coordinating species; thus it could be envisioned that under acidic cellular conditions, loss of carboxylate would render the Pt-Malonate more susceptible to hydrolysis, leading to greater release of Pt for chemotherapeutic activity.

A potentially fruitful area as well also involves studying in greater detail the relationship between the stability of the oxo-side tricoordinate MGd-Pt compounds **5.7** and in vitro efficacy. Such additional model studies with HPLC evaluation of hydrolysis rates may help uncover a substituent/hydrolysis rate correlation. To the extent this proves true, it would allowing the rates of hydrolysis of the putative new conjugates to be tailored for use with a given tumor or cell types.

Additionally, along these lines, increasing steric hindrance holds potential for Pt conjugates, worth investigating. While these tricoordinate compound presumably are more stable, possibly also worthwhile is effecting increased steric hindrance via linkers such as the 2,2-diethyl-1,3-dibromopropane spacer segment, as well as increasing malonate quaternary substitution.[255]

The MGd malonate chemistry developed to date has been for Pt conjugates. Vanadium conjugates may also hold significant promise as $Cp_2V(AcAc)$ was recently reported to suppress angiogenesis. As Cp_2V^{+2} coordinates readily to AcAc, MGd-V

conjugate **5.8** can be envisioned. The AcAc moiety, a conjugation system which theoretically does not interfere with the Pt-Malonate chemistry, this possibly could be elaborated to dual metal releasing agents, containing both $Pt(NH_2R)_2$ and Cp_2V **5.9**.

Further development of the quaternary amine platinum compounds, previously discussed in Chapter 4 also may prove atttractive. Derivatives particularly of the Brij® type of non-ionic detergent solubilizers (PEGylated C_{12}-C_{18} fatty alcohols), are attractive, with lipophilicity, aqueous solubility, and lower toxicity than ionic detergents. The quaternary amine platinum compounds, with a straightforward synthesis, even combinatorial for the initial model studies, could rapidly lead to the isolation of soluble lipophilic platinates with good activity, a goal that has so far proved unattainable.

In summary, this research has helped to lay a foundation of synthetic routes to additional MGd conjugates and potential Pt therapeutic agents. We had hoped to progress both further and faster in this work. Ultimately, we take satisfaction in having helped smooth the path for those who are to follow.

Appendix: Synthesis of Additional MGd-Pt Conjugate

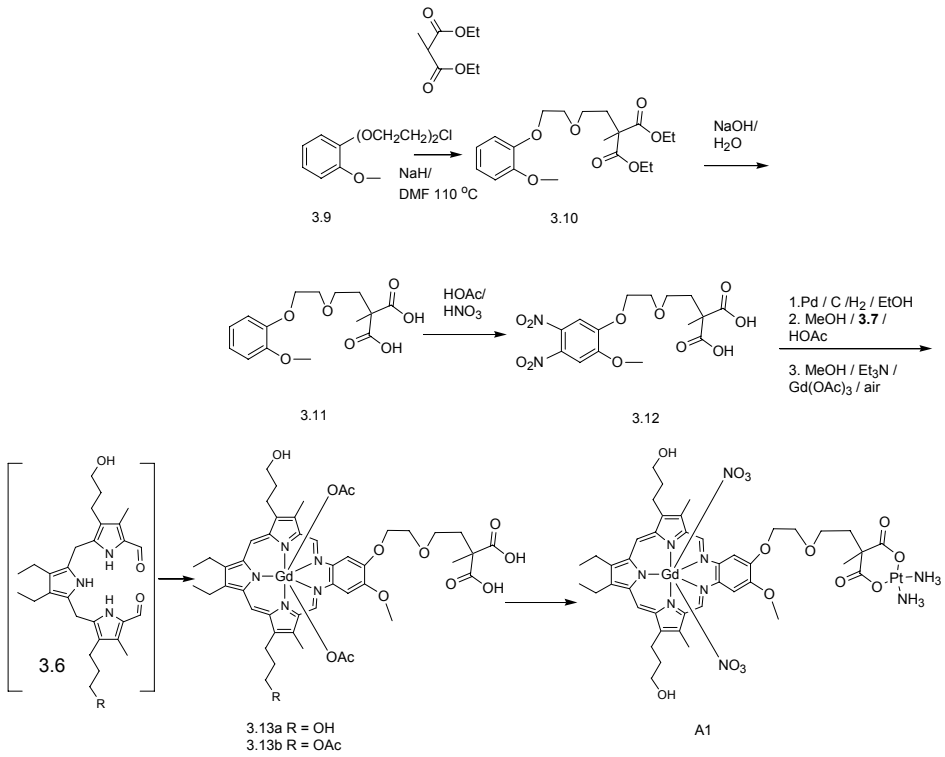

Scheme A1 Synthesis of MGd-Pt conjugate **A1**.

The activity of MGd-Pt conjugate **3.1** inspired the synthesis of MGd-Pt conjugates **A1** (Scheme A1). Due to the difficult purification of this final product due to low water solubility, discussion has been moved to this appendix.

For A1, the second conjugate, the previously reported halo-veratrole **3.9** was synthesized from guiaicol (Scheme A1).[256] Condensation with methyl diethylmalonate in the presence of NaH gave diester **3.10**. Hydrolysis under basic conditions was essentially quantitative. This gave the diacid **3.11** with no evidence of decarboxylation, a process

that is generally attributed to a thermal reaction.[257] Although decarboxylation during nitration was a concern, nitration of guiaicol acetate had been previously reported.[258] Nitration at 0-25 ^{o}C gave the dinitrobenzene-malonate **3.12** in 54% yield. The dinitrobenzene-malonate intermediate **3.12**, as in the synthesis of **3.1**, was reduced, cyclized and metallated, to the desired MGd malonates **A1**. The lower solubility of this non-PEGylated model compound proved to be an issue. The crude material **3.13a** (c.a. 70% HPLC assay, LRMS identification) was platinated, as with the prior MGd-malonate conjugate, by exchange of acetate for nitrate anion, followed by metallation to give the MGd-Pt conjugate **A1**. Purification was effected as the nitrate salt on C-18 with 10-100 mM KNO_3 in methanol. The material was characterized by MS, HPLC, HRMS and evaluated for stability.

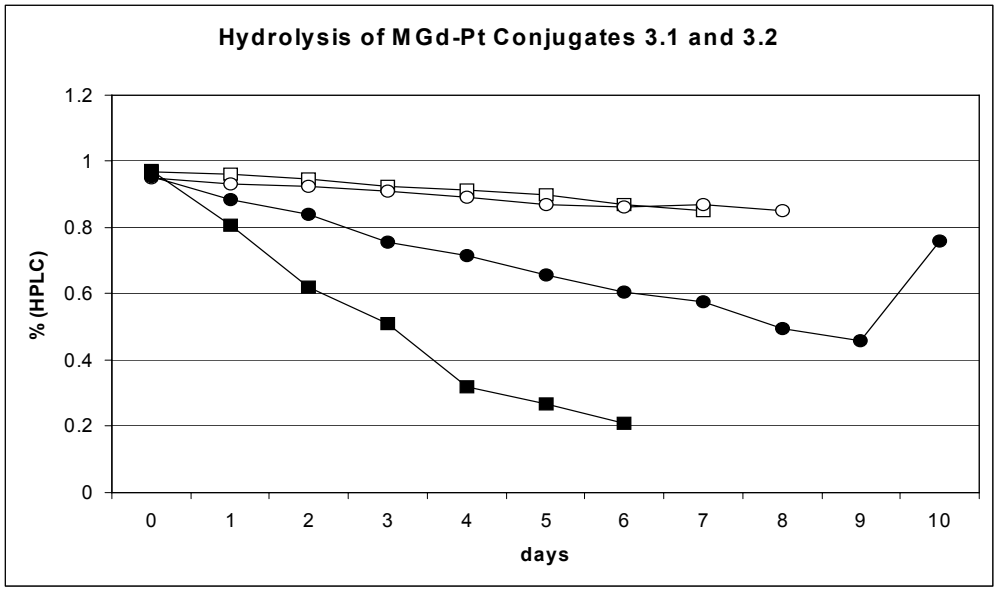

Figure A1 Hydrolysis Study of MGd-Pt conjugates 3.1 and 3.2 in methanol and phosphaete buffered saline (PBS). Methanol (**3.1** □, **3.2** ○), PBS (**3.1** ■, **3.2** ●).

Purification of the MGd-malonate acetate salt **3.13a** could not be effected as the nitrate salt on C-18 due to low solubility. The acetate salt could be purified on C-18 using MeOH and acetonitrile containing HOAc (1-2%), at high organic concentrations. This procedure gave a product which by HRMS analysis agreed with a product containing one esterified alcohol and a single acetate. It remained non-obvious which acid was esterified.

In HPLC stability studies, Figure A1, the hydrolytic profile of conjugate **3.1** demonstrated $t_{1/2}$ = 3 days (the above, additional, tertiary malonate model conjugate containing a PEG_2 linker, **A1** and a propyl linker conjugate were also prepared and both demonstrated an aqueous hydrolysis profile with $t_{1/2}$ = 9 days, the PEG conjugate Pt loss was confirmed as reversible on the addition of Pt-diaquo) The hydrolysis, as with the previous HPLC hydrolysis study, was reversible and the peak attributed to conjugate **A1** could be regenerated by the addition of "diaquo-Pt." Stirring the hydrolysis solution of **A1** (obtained on day 9) for one day at room temperature with excess "diaquo-Pt" resulted in the peak area at the retentiono time for conjugate **A1** incereasing from 45% to 76%, with a corresponding decrease in the peak seen to increase during the hydrolysis study.

While this latter guiaicol-type analogue demonstrated lower water solubility than MGd-Pt conjugate, this work has developed a flexible synthetic route to a scaffold for conjugation of MGd with Pt chemotherapeutic agents. The convergent synthetic scheme allows for variation of both malonate substitution to modify release rates and phenyl ring substitution to modify lipophilicity via solubilizing PEG spacers. This flexibility may allow combinatorial synthesis for tuning the Pt release rates as well as solubility and lipophilicity of the conjugates.

EXPERIMENTAL

Synthesis of 1-[2-(2-Chloro-ethoxy)-ethoxy]-2-methoxy-benzene 3.9.[259] To a solution of guiaicol (12.7 g, 102 mMol) and 1-Chloro-2-(2-chloro-ethoxy)-ethane (24 g, 128 mMol) was added NaOH (40 ml, 2.5 N). The solution was held at 70 ^{o}C for 24 hours. On cooling the solution was added to ice water (500 ml) and extracted with EtOAc:hexanes (2:1, 225 ml), washed with water, dried over $MgSO_4$, and evaporated to give an oil. The oil was extracted with hexanes (2 x 200 ml) to extract the product. The pooled hexanes were filtered through a bed of silica gel (50 ml) and the bed washed with hexanes (100 ml) and EtOAc (150 ml). The hexane fraction was discarded, and the EtOAc layer was evaporated to give the product as an oil (12g, 51%). HPLC (270nm): Tr 13.14 min; 53.33%. MS (CI) (M+H)+ = 231. ^{1}H NMR(400 MHz, $CDCl_3$) δ 6.83 (4), 4.18 (2H, t), 3.90 (2H, t) 3.83 (2H, t) 3.77 (2H, t). The crude product could be purified with difficulty by RP C-18 chromatography. This material contains residual bis-substituted product and the dihhalide. In preparative scale reactions the material was alkylated with excess methylmalonate. In preparative scale work purification is most easily effected at the dicarboxylic acid stage.

Synthesis of 2-{2-[2-(2-Methoxy-phenoxy)-ethoxy]-ethyl}-2-methyl-malonic acid diethyl ester. 3.10 To a suspension of NaH (60% in oil, 16.5 g, 410 mMol) in DMF (400 ml) was added methyldiethylmalonate (70 ml, 400 mMol). After the hydrogen evolution was complete 1-[2-(2-Chloro-ethoxy)-ethoxy]-2-methoxy-benzene (100 g, 450 mMol) was added. The solution was held at 110 ^{o}C for 24 h. On cooling the solution was added to water (1000 ml) and extracted with hexanes:EtOAc (2 x 200 ml) followed by washing with water (3 x 100 ml) and drying over $MgSO_4$. Purification by flash chromatography over silica gel (hexanes/EtOAc) provided the product as an oil (100 g,

79%). The crude material was of adequate purity for use in the next reaction. HPLC (269nm):Tr 14.68 min, 93.68%. ^{1}H NMR(400 MHz, $CDCl_3$) δ 1.21 (6H, t J = 7.2 Hz), 1.42 (3H, s), 2.19 (2H, t J = 7.8 Hz), 3.59 (2H, t J = 6.8 Hz), 3.75 (2H, t, J = 5.1 Hz), 3.83 (3H, s), 4.13 (6H, m), 6.89 (4H, m). ^{13}C NMR(100 MHz, $CDCl_3$) δ 13.8, 19.8, 34.9, 51.9, 55.7, 61.1, 67.2, 68.3, 69.1, 111.8, 113.9, 120.7, 121.3, 148.1, 149.5, 172.0. MS(EI) (M+H)+ = 369. HRMS(EI) calculated for $C_{19}H_{28}O_7$ 369.1913, found 369.1917. Anal. Calcd for $C_{19}H_{28}O_7$: C 61.94%; H 7.66%. Found C 61.26%; H 7.89%.

Synthesis of 2-{2-[2-(2-Methoxy-phenoxy)-ethoxy]-ethyl}-2-methyl-malonic acid. 3.11 To a solution of the diester (53 g, 147 mMol) in EtOH (250 ml) was added NaOH (200 ml, 2.5 N, 500 mMol). The solution was stirred overnight. The reaction was complete by tlc and the solution was added to water (400 ml) and washed with hexanes:EtOAc (200 ml 3:1). The aqueous layer was then acidified with HCl (3 N) and the aqueous layer extracted with EtOAc:DCM (2 x 200 ml, 3:1) which was back extracted with NaOH (2.5 N, 150 ml). The resulting aqeous solutin was acidified to pH = 2 with HCl (3N) and extracted with DCM (100 ml), dried over $MgSO_4$ and evaporated to give the product (15 g, 33% theo). HPLC (335nm): Tr 12.24 min, 91.11%. ^{1}H NMR(400 MHz, $CDCl_3$) δ 1.62 (3H, s), 2.30 (2H, t J = 5.1 Hz), 3.66 (2H, t J = 5.1 Hz), 3.75 (2H, m), 3.95 (3H, s), 4.06 (2H, m), 6.90-6.94 (4H, m). ^{13}C NMR(400 MHz, $CDCl_3$) δ 21.2, 36.1, 50.9, 55.7, 66.9, 67.4, 68.7, 111.7, 112.0, 120.9, 121.3, 147.9, 148.2, 176.6. MS (EI-) (M-H) 311 HRMS(EI) calculated for $C_{15}H_{19}O_7$ [M-1] 311.1494, found 311.1136. Anal. Calcd for $C_{15}H_{19}O_7$.$2H_2O$: C 51.87%; H 6.62%. Found C 52.84%; H 6.85%.

Synthesis of 2-{2-[2-(2-Methoxy-4,5-dinitro-phenoxy)-ethoxy]-ethyl}-2-methyl-malonic acid 3.12 A solution of the diacid (3.35g, 11 mMol) in HOAc (6 ml) was cooled to 10 ^{o}C and conc. HNO_3 (6 ml) was added solwly over 30 minutes. The solution was stirred for 2 hours, recooled to 8 ^{o}C and fuming HNO_3 (8 ml) was slowly

added. After 0.5 h at less than 10 ^{o}C additional fuming HNO_3 (4 ml) was added. After stirring overnight and being allowed to slowly warm to room temperature the solution was added to 100 cc crushed ice and centrifuged to give an oil. The aqueous layer was decanted and the remaining oil was partitioned between brine (50 ml) and EtOAc (75 ml). The organic layer was washed with water (4 x 50 ml). Evaporation gave the product as a yellow oil (2.52 g, 54%). HPLC (269nm): T_r 11.07 min, 88.20%. ^{1}H NMR(400 MHz, $CDCl_3$) δ 1.56 (3H, s), 2.26 (2H, t J = 5.1 Hz), 3.68 (2H, t J = 5.1 Hz), 3.78 (2H, m), 4.05 (3H, s), 4.21 (2H, m), 7.30 (1H, s), 7.39 (1H, s). ^{13}C NMR(100 MHz, $CDCl_3$) δ 20.6, 36.0, 57.5, 68.5, 69.6, 70.5, 108.3, 109.3, 137.1, 137.5, 152.3, 153.4, 175.7. MS (EI) (M)+ 402. HRMS(EI) calculated for $C_{15}H_{19}N_2O_{11}$ 403.0989, found 403.0987. Anal. Calcd for $C_{15}H_{18}N_2O_{11}$: C 44.78%; H 4.51%; N 6.97%. Found C 39.21%; H 2.38%; N 11.71%.

Synthesis of MGd-malonate. 3.13 To a solution of **3.12** (7.5 g, 18.6 mMol) in EtOH (200 ml 1:1) with 10% Pd/C (1.07 g.) was hydrogenated overnight at 40 psi. The resulting solution was filtered and added to a solution of **3.6** (9.21 g, 19.1 mMol) and HOAc (1 ml) in MeOH(600 ml). After heating at 50 ^{o}C for 8 h the red solution was evaporated. The resuidue was added to a solution of $Gd(OAc)_3$ (10.29 g, 25.7 mMol) and Et_3N (20 ml) in MeOH (600 ml) saturated with air in the dark at 50 ^{o}C for 8 h gave a deep green solution. The reaction was quenched by adding HOAc (30 ml) and the solution was filtered though celite and evaporated. The residue was washed with hexanes, toluene and Et_2O. The residue was then suspended in acetone and precipitate with the addition of hexanes. The product was dissolved in MeOH and precipitated with Et_2O (5x volume) to give the crude green solid product (16.45 g, 79%). Further purification was effected by dissolving the crude solid (1.15 g) in MeOH (10 ml), diluting with DCM (80 ml) and loading onto silica gel (50 cc). The silica gel was washed with

DCM/MeOH/HOAc solutions; 85/15/0, 85/15/1, 60/40/1. The first two washes reoved the soluble red by products, the third solution eluting the product from the silica gel. Evaporation of the product solution and tituration with Et_2O gave the green product (0.75 g, 65%). The solid was then dissolved in MeOH (1g/10 ml), diluting with an equal volume of NH_4OAc (100 mM) buffer, and loading on a tC-18 SPE cartridge (10 g). Elution with NH_4OAc (100 mM) buffer:acetonitrile solutions, 50:12 and 50:20 gave solutions containing impurities and the product respectively. The product fraction, after dilution with an equal volume of buffer was again loaded onto a fresh tC-18 column, washed with water, and the product eluted with acetonitrile:HOAc 95:5. The resulting solution was evaporated under high vacuum, dissolved in a minimal amount of MeOH and precipitated with Et_2O to give a green solid (0.23g, 20% yield overall). HPLC (470 nm): T_r 10.59 min, 96.20%. MS (EI+) (M-OAc)+ 999, 983 (EI-) 982. HRMS(EI+) calculated for $C_{45}H_{55}N_5O_{10}Gd$ 983.3185, found 983.3178. HRMS(EI-) calculated for $C_{45}H_{55}N_5O_{10}Gd$ 981.3039, found 981.3055. The predominant product by HRMS gave results in agreement with (M-OAc ester + H_2). A minor product also observed was in agreement by HRMS (EI-) with (M-OAc ester + H_2 +O_2): calculated for $C_{45}H_{55}N_5O_{12}Gd$ 1015.3080, found 1015.3087. Anal. Calcd for $C_{47}H_{58}GdN_5O_{13}$: C 53.34%; H 5.52%; N 6.62%. Found C 58.98%; H 5.68%; N 8.30.

Synthesis of MGd-Pt conjugate. 3.2 To a solution of **3.13** (260 mg, 0.23 mMol) in MeOH (10 ml) was added a solution of $(NH_3)_2Pt(H_2O)_2^{+2}(NO_3)_2^-$ (5 ml, 0.23 mMol) and stirring overnight gave the crude product. Purification was effected by adding the solution (1 ml) to KNO_3 (5 ml, 100 mM) and loading on a tC-18 SPE cartridge (500 mg). Elution with KNO_3 (100 mM):acetonitrile solutions, 100:24 and 100:40 gave solutions containing impurities and the product respectively. The product fraction, after dilution with an equal volume of buffer was was loaded onto a fresh tC-18 column, washed with water and the

product eluted with MeOH/ KNO_3 (10 mM, 95:5). The product solution was titurated with Et_2O to give a green solid (26 mg, 8%). HPLC (470 nm): Tr 9.92 min, 96.72%. HRMS(EI) calculated for C43H56N8O12PtGd 1228.294, found 1228.290. HRMS(EI) calculated for C43H57N8O12PtGd (M-NO3)+ 1229.293; found: 1229.292.

Bibliography

(1) Wei, W.-H.; Fountain, M., E.; Sessler Jonathan, L.; Magda, D., L,; Wang, Z.; Miller, R., A., Eds. *Texaphyrin Conjugates. Progress Towards Second Generation Diagnostic and Therapeutic Agents*; Springer: Dordrecht, 2005, 407-425.
(2) Wei, W.-H.; Fountain, M.; Magda, D.; Wang, Z.; Lecane, P.; Mesfin, M.; Miles, D.; Sessler Jonathan, L. *Org. Biomol. Chem.* **2005**, *3*, 3290-3296.
(3) Magda, D.; Lepp, C.; Gerasimchuk, N.; Lee, I.; Sessler, J. L.; Lin, A.; Biaglow, J. E.; Miller, R. A. *Int. J. Radiat. Oncol. Biol.* **2001**, *51*, 1025-1036.
(4) *Merriam-Webster Medical Dictionary*; Merriam-Webster: Springfield, 2002.
(5) Sessler, J. L.; Gebauer, A.; Weghorn, S. J., Eds. *Expanded Porphyrins*; Academic Press: San Diego, 2000; Vol. 2, 55-124.
(6) Sessler, J. L.; Johnson, M. R.; Lynch, V. *Journal of Organic Chemistry* **1987**, *52*, 4394-4397.
(7) Sessler, J. L.; Murai, T.; Lynch, V.; Cyr, M. *J. Am. Chem. Soc.* **1988**, *110*, 5586-5588.
(8) Sessler, J. L.; Cyr, M.; Murai, T. *Comments Inorg. Chem.* **1988**, *7*, 333-350.
(9) Sessler, J. L.; Mody, T. D.; Hemmi, G. W.; Lynch, V. *Inorg. Chem.* **1993**, *32*, 3175-3187.
(10) Hemmi, G. W. "Lanthanide complexes of the texaphyrin class of expanded porphyrins.," University of Texas, Austin, Ph.D., 1992.
(11) Mody Tarak, D. "The design, synthesis, and structural characterization of Schiff-base expanded porphyrins.," University of Texas, Austin, Ph.D., 1993.
(12) Sessler, J. L.; Hemmi, G.; Mody, T. D.; Murai, T.; Burrell, A.; Young, S. W. *Acc. Chem. Res.* **1994**, *27*, 43-50.
(13) Geraldes, C. F.; Sherry, A. D.; Vallet, P.; Maton, F.; Muller, R. N.; Mody, T. D.; Hemmi, G.; Sessler, J. L. *J. Magn. Reson. Imag.* **1995**, *5*, 725-729.
(14) Sessler, J. L.; Tvermoes, N. A.; Guldi, D. M.; Mody, T. D.; Allen, W. E. *J. Phys. Chem. A* **1999**, *103*, 787-794.
(15) Magda, D.; Gerasimchuk, N.; Lecane, P.; Miller Richard, A.; Biaglow John, E.; Sessler Jonathan, L. *Chem. Commun.* **2002**, 2730-2731.
(16) Sessler, J. L.; Kral, V.; Hoehner, M. C.; Chin, K. O. A.; Davila, R. M. *Pure Appl. Chem.* **1996**, *68*, 1291-1295.
(17) Sessler, J. L.; Mody, T. D.; Hemmi, G. W.; Lynch, V.; Young, S. W.; Miller, R. A. *J. Am. Chem. Soc.* **1993**, *115*, 10368-10369.
(18) Young, S. W.; Sidhu, M. K.; Qing, F.; Muller, H. H.; Neuder, M.; Zanassi, G.; Mody, T. D.; Hemmi, G.; Dow, W.; et al. *Invest Radiol.* **1994**, *29*, 330-338.
(19) Young, S. W.; Qing, F.; Harriman, A.; Sessler, J. L.; Dow, W. C.; Mody, T. D.; Hemmi, G. W.; Hao, Y.; Miller, R. A. *Proc. Nat. Acad. Sci. U S A* **1996**, *93*, 6610-6615, *Correction Proc. Nat. Acad. Sci. U S A*, 1999, 66**96**, 2569.

(20) Miller, R. A.; Woodburn, K.; Fan, Q.; Renschler, M. F.; Sessler, J. L.; Koutcher, J. A. *Int. J. Radiat. Oncol., Biol., Phys.* **1999**, *45*, 981-989.
(21) *Drugs in R&D* **2004**, *5*, 52-57.
(22) Alison, M. R. In *Encyclopedia of life sciences.*; Nature Pub. Group: London, 2002; Vol. 3.
(23) Kaufman, D. C.; Chabner, B. A. In *Cancer chemotherapy and biotherapy: principles and practice*; 3rd ed. ed.; Chabner, B. A., Longo, D. L., Eds.; Lippincott Williams & Wilkins: Philadelphia, 2001.
(24) Yunmbam, M. K.; Guo, Y. S.; Miller, M. R.; Yu, J. J. *Oncology Reports* **2004**, *11*, 833-838.
(25) Maruyama, K. In *Drug Delivery System*; CAS, 1999; Vol. 14, pp 433-447.
(26) Maeda, H.; Fang, J.; Inutsuka, T.; Kitamoto, Y. *International Immunopharmacology* **2003**, *3*, 319-328.
(27) Potgens, A. J. G.; Westphal, H. R.; de Waal, R. M. W.; Ruiter, D. J. *Biol. Chem.* **1995**, *376*, 57-70.
(28) Breier, G. In *Angiogenesis: from the molecular to integrative pharmacology*; Maragoudakis, M. E., Ed.; Kluwer Academic/Plenum: New York, 2000; Vol. 476.
(29) Gao, Z.; Lukyanov, A. N.; Singhal, A.; Torchilin, V. P. *Nano Letters* **2002**, *2*, 979-982.
(30) Shayan, R.; G., M. G. A. M.; Stacker, S. A. *Carcinogenesis* **2006**, *27*, 1729-1738.
(31) Krishna, R.; Mayer, L. D. *Anticancer Research* **1999**, *19*, 2885-2891.
(32) Au, J. L. S.; Jang, S. H.; Zheng, J.; Chen, C. T.; Song, S.; Hu, L.; Wientjes, M. G. *Journal of Controlled Release* **2001**, *74*, 31-46.
(33) Watanabe, J. *Yakubutsu Dotai* **1999**, *14*, 120-130.
(34) De Fabregas, B. R. *Revista del Instituto Nacional de Medicina Legal de Colombia* **1977**, *2*, 35-38.
(35) Milne, M. D. *Proc. Roy. Soc. Med.* **1965**, *58*, 961-963.
(36) Chaplin, D. J.; Hill, S. A.; Bell, K. M.; Tozer, G. M. *Seminars in radiation oncology* **1998**, *8*, 151-163.
(37) Terasaki, T. *Yakugaku zasshi. Journal of the Pharmaceutical Society of Japan* **1992**, *112*, 887-905.
(38) Denny, W. A. *Anti-cancer drug design* **1989**, *4*, 241-263.
(39) Tannock, I. F. *International journal of radiation biology and related studies in physics, chemistry, and medicine* **1986**, *49*, 335-355.
(40) Kessel, D.; Dougherty, T. J. *Reviews in Contemporary Pharmacotherapy* **1999**, *10*, 19-24.
(41) Mody, T. D.; Sessler, J. L. *Journal of Porphyrins and Phthalocyanines* **2001**, *5*, 134-142.
(42) Jiang, X.; Pandey, R. K.; Smith, K. M. *Tetrahedron Letters* **1995**, *36*, 365-368.
(43) Ghiggino, K. P.; Bennett, L. E.; Henderson, R. W. *Photochemistry and Photobiology* **1988**, *47*, 65-72.
(44) Derat, E.; Cohen, S.; Shaik, S.; Altun, A.; Thiel, W. *JACS* **2005**, *127*, 13611-13621.
(45) Benfrey, O. T.; Morris, P. J. T., Eds. *Robert Burns Woodward Artist and Architect in the World of Molecules*; Chemical Heritage Foundation: Philadelphia, 2001, 256-277, 302-342.

(46) Alberts, B.; Johnson, A.; Lewis, J.; Raff, M.; Roberts, K.; Walter, P. *Molecular Biology of the Cell*; 4 ed.; Garland Science: New York, 2002,p^pp P.
(47) Sanchez-Alcazar, J. A.; Khodjakov, A.; Schneider, E. *Cancer research* **2001**, *61*, 1038-1044.
(48) Policard, A. *C.R. Soc.Biol.* **1924**, *91*, 1423-1424.
(49) Bonnett, R. *Chemical Aspects of Photodynamic Therapy*; Gordon and Breach Science Publishers, 2000,p^pp P.
(50) Sternberg, E. D.; Dolphin, D. *Tetrahedron* **1998**, *54*, 4151-4202.
(51) Pandey, D. K.; Dougherty, T. J.; Smith, K. M. *Tetrahedron Letters* **1988**, *29*, 4657-4660.
(52) Byrne, C. J.; Morris, I. K.; Ward, A. D. *Aust. J. Chem.* **1990**, *43*, 1889-1907.
(53) Pandey, R. K.; Sihiau, F.-Y.; Dougherty, T. J.; Smith, K. M. *Tetrahedron* **1991**, *47*, 9571-9584.
(54) Luo, Y.; Chang, C. K.; Kessel, D. *Phochemistry and Photobiology* **1996**, *63*, 528-534.
(55) Dougherty, T. J.; Gomer, C. J.; Henderson, B. W.; Jori, G.; Kessel, D.; Korbelik, M.; Moan, J.; Peng, Q. *Journal of the National Cancer Institute* **1998**, *90*, 889-905.
(56) Pandey, R. K.; Zheng, G. *Porphyrin Handbook* **2000**, *6*, 157-230.
(57) Henderson, B. W.; Bellnier, D. A.; Greco, W. R.; Sharma, A.; Pandey, R. K.; Vaughan, L. A.; Weishaupt, K. R.; Dougherty, T. J. *Cancer Research* **1997**, *57*, 4000-4007.
(58) Marganon, P.; Gregoire, M.-J.; Scasnar, V.; Ali, H.; van Lier Johan, E. *Phochemistry and Photobiology* **1996**, *63*, 217-223.
(59) Leunig, M.; Richert, C.; Gamarra, F.; Lumper, W.; Vogel, E.; Jocham, D.; Goetz, A. E. *Br. J. Cancer* **1993**, *68*, 225-234.
(60) Moan, J.; Peng, Q.; Evensen, J. F.; Berg, K.; Western, A.; Rimington, C. *Photochemistry and Photobiology* **1987**, *46*, 713-721.
(61) Cunderlikova, B.; Bjorklund, E. G.; Pettersen, E. O.; Moan, J. *Photochemistry and Photobiology* **2001**, *74*, 246-252.
(62) Oenbrink, G.; Jurgenlimke, P.; Gabel, D. *Phochemistry and Photobiology* **1988**, *48*, 451-456.
(63) Nakae, Y.; Fukusaki, E.-i.; Kajiyama, S.-i.; Kobayashi, A.; Nakajima, S.; Sakata, I. *Journal of Photochemistry and Photobiology, A: Chemistry* **2005**, *172*, 55-61.
(64) Dubowchik, G. M.; Firestone, R. A. *Bioconjug. Chem.* **1995**, *6*, 427-439.
(65) El-Far, M.; Pimstone, N. In *Porphyrin Localization and Treatment of Tumors*; Doiron, D. R., Gomer, C. J., Eds.; Liss: NY, 1984; Vol. 170.
(66) Jori, G.; Cozzani, I.; Reddi, E.; Tomio, L.; Mandoliti, G.; Malvadi, G. In *Porphyrin Localization and Treatment of Tumors*; Doiron, D. R., Gomer, C. J., Eds.; Liss: NY, 1984; Vol. 170.
(67) Hirata, A. *Kanazawa Daigaku Juzen Igakkai Zasshi* **1990**, *99*, 618-633.
(68) Magda, D.; Miles, D.; Gerasimchuk, N.; Lepp, C.; Pharmacyclics, Inc.: US 6919327, 2005; Vol. 6919327.
(69) Ansel, H.; Allen, L. V. J.; Popovich, N. G. *Pharmaceutical dosage forms and drug delivery systems*; 7 ed.; Lippincott-Williams & Wilkins: Philadelphia, Pa., 1999,p^pp P.

(70) Iyer, S. S.; Anderson, A. S.; Reed, S.; Swanson, B.; Schmidt, J. G. *Tetrahedron Letters* **2004**, *45*, 4285-4288.
(71) Jayasuriya, N.; Bosak, S.; Regen, S. *JACS* **1990**, *112*, 5844-5850.
(72) Veronese, F. M.; Schiavon, O.; Pasut, G.; Mendichi, R.; Andersson, L.; Tsirk, A.; Ford, J.; Wu, G.; Kneller, S.; Davies, J.; Duncan, R. *Bioconjug. Chem.* **2005**, *16*, 775-784.
(73) Spinelli, S.; Pasini, A.; Menta, E.; Zunino, F.; Tognella, S. In *PCT Int. Appl.*; (Boehringer Biochemia Robin S.p.A., Italy): WO 5104895, 1989, p 57 pp.
(74) Kim, Y.-S.; Song, R.; Kim, D. H.; Jun, M. J.; Sohn, Y. S. *Bioorganic & Medicinal Chemistry* **2003**, *11*, 1753-1760.
(75) Furin, A.; Guiotto, A.; Baccichetti, F.; G., P.; Deuschel, C.; BertaniR.; Veronese, F. M. *European Journal of Medicinal Chemistry* **2003**, *38*, 739-749.
(76) Sessler, J. L.; Magda, D.; Mody, T.; Anzenbacher, P.; Carvalho, J.; (Board of Reagents, The University of Texas System, USA; Pharmacyclics, Inc.). WO 9962551, 1999, p 88.
(77) Hudecz, F.; Remenyi, J.; Szabo, R.; Koczan, G.; Mezo, G.; Kovacs, P.; Gaal, D. *Journal of Molecular Recognition* **2003**, *16*, 288-298.
(78) Kulkarni, R. P.; Mishra, S.; Fraser, S. E.; Davis, M. E. *Bioconjug. Chem.* **2005**, *16*, 986-994.
(79) McGraw, T. E.; Maxfield, F. R. In *Targeted drug delivery*; Juliano, R. L., Ed.; Springer-Verlag: Berlin, 1991; Vol. 100.
(80) Lloyd, J. B. In *Targeting of Drugs with Synthetic Systems*; Gregoriadis, G., Senior, J., Poste, G., Eds.; Plenum: New York, 1985; Vol. 113.
(81) Zhao, H.; Greenwald, R. B.; Reddy, P.; Xia, J.; Peng, P. *Bioconjug. Chem.* **2005**, *16*, 758-766.
(82) Hammer, N. D.; Sangwan, L.; Vesper, B. J.; Elseth, K. M.; Hoffman, B. M.; Barrett, A. G. M.; Radosevich, J. A. *J. Med. Chem.* **2005**, *48*, 8125-8133.
(83) Kessel, D.; Woodburn, K.; Henderson, B. W.; Chang, C. K. *Photochemistry and Photobiology* **1995**, *62*, 875-881.
(84) Sheulok, J. R.; Wade, M. H.; Lin, C.-W. *Photochem. Photobiol.* **1990**, *51*, 451-457.
(85) Woodburn, K. W.; Fan, Q.; Miles, D. R.; Kessel, D.; Luo, Y.; Young, S. W. *Photochem. Photobiol.* **1997**, *65*, 410-415.
(86) Ruck, A.; Diddens, H. In *The Fundamental Bases of Phototherapy*; Honigsman, H. J., G.; Young, A., Ed.; OEMF: Milano, 1996.
(87) Wood, S. R.; Holroyd, J. A.; Brown, S. B. *Photochem. Photobiol.* **1997**, *65*, 397-402.
(88) McMillin, D. R.; Shelton, A. H.; Bejune, S. A.; Fanwick, P. E.; Wall, R. K. *Coord. Chem. Rev.* **2005**, *249*, 1451-1459.
(89) Kessel, D.; Luguya, R.; Vicente, M. G. H. *Photochem. Photobiol.* **2003**, *78*, 431-435.
(90) Synytsya, A.; Kral, V.; Matejka, P.; Pouckova, P.; Volka, K.; Sessler, J. L. *Photochem. Photobiol.* **2004**, *79*, 453-460.
(91) Renschler, M. F.; Yuen, A. R.; Panella, T. J.; Wieman, T. J.; Dougherty, S.; Esserman, L.; Panjehpour, M.; Taber, S. W.; Fingar, V. H.; Lowe, E.; Engel, J. S.; Lum,

B.; Woodburn, K. W.; Cheong, W.-F.; Miller, R. A. *Proceedings of SPIE-The International Society for Optical Engineering* **1998**, *3247*, 35-39.
(92) Kessel, D. *Phochemistry and Photobiology* **1997**, *65*, 387-388.
(93) Berg, K.; Moan, J. *Phochemistry and Photobiology* **1997**, *65*, 403-409.
(94) Peng, Q.; Moan, J.; Ma, L. W.; Nesland, J. M. *Cancer research* **1995**, *55*, 2620-2626.
(95) Synytsya, A.; Kral, V.; Synytsya, A.; Volka, K.; Sessler, J. L. *Biochim. Biophys. Acta* **2003**, *1620*, 85-96.
(96) Du, H.; Fuh, R.-C. A.; Li, J.; Corkan, L. A.; Lindsey, J. S. *Photochem. Photobiol.* **1998**, *68*, 141–142.
(97) Bonnett, R. *The Chemical Aspects of Photodynamic Therapy*; Gordon and Breach Science Publishers, 2000,p^pp P.
(98) Luck, B.; Carlson, K.; Collier, T.; Sung, K.-B. *IEEE Potentials* **2004**, 14-17.
(99) Wang, X. F.; Herman, B., Eds. *Fluorescence Imaging Spectroscopy and Microscopy*; John WIley & Sons.: New York, 1996; Vol. 137.
(100) Bonnett, R. *The Chemical Aspects of Photodynamic Therapy*; Gordon and Breach Science Publishers, 2000,p^pp P.
(101) Coleman, M. A.; Lao, V. H.; Segelke, B. W.; Beernink, P. T. *Journal of Proteome Research* **2004**, *3*, 1024-1032.
(102) Woodburn, K. W. *J. Pharm. Exper. Ther.* **2001**, *297*, 888-894.
(103) Willis, R. C.; Lesney, M. S. *Modern Drug Discovery* **2003**, 29-32.
(104) Haughland, R. P. *Handbook of Fluorescent Probes and Research Products*; 9 ed.; Molecular Probes: Eugene, OR, 2002,p^pp P.
(105) Farris, R. E. In *Kirk-Othmer encyclopedia of chemical technology*; 3 ed.; Mark, H. F., Ed.; Wiley: New York, 1978-1984; Vol. 24.
(106) Lampidis, T. J.; Bernal, S. D.; Summerhayes, I. C.; Chen, L. B. *Cancer Research* **1983**, *43*, 716-720.
(107) Herr, H. W.; Huffman, J. L.; Huryk, R.; Heston, W. D.; Melamed, M. R.; Whitmore, W. F., Jr. *Cancer research* **1988**, *48*, 2061-2063.
(108) Haghighat, S.; Castro, D. J.; Lufkin, R. B.; Fetterman, H. R.; Castro, D. J.; Soudant, J.; Ward, P. H.; Saxton, R. E. *Laryngoscope* **1992**, *102*, 81-87.
(109) MacDonald, R. I. *Journal of Biological Chemistry* **1990**, *265*, 13533-13539.
(110) Fujita, S.; Toru, T.; Kitagawa, Y.; Kagiyama, N.; Momiyama, M. *Analytica Chimica Acta* **1997**, *339*, 289-296.
(111) Adamczyk, M.; Grote, J. *Bioorganic & Medicinal Chemistry Letters* **2000**, *10*, 1539-1541.
(112) Liebig, H. V. *Journal fuer Praktische Chemie (Leipzig)* **1913**, *88*, 26-48 (CAN 27:24353).
(113) Jochims, J. C.; Seegler, A. *Angew. Chem. Int. Ed. Engl.* **1967**, *6*, 174-175.
(114) N.A. *Methods in Enzymology* **1972**, *26*, 28-.
(115) Rosania, G. R.; Lee, J. W.; Ding, L.; Yoon, H.-S.; Chang, Y.-T. *J. Am. Chem. Soc.* **2003**, *125*, 1130-1131.
(116) Kessel, D. *Drugs of Today* **1996**, *32*, 385-396.
(117) Livesey, J. C.; Reed, D. J.; Adamson, L. F. *Radiation-protective drugs and their reaction mechanisms*; Noyes: Park Ridge, N.J., 1985,p^pp P.

(118) Sessler, J. L.; Tvermoes, N. A.; Guldi, D. M.; Mody, T. D. *J. Porphyrins Phthalocyanines* **2001**, *5*, 593-599.
(119) Khuntia, D.; Mehta, M. P. *Expert Rev. Anticancer. Ther.* **2004**, *4*, 981-989.
(120) Sessler, J. L.; Tvermoes, N. A.; Guldi, D. M.; Hug, G. L.; Mody, T. D.; Magda, D. *J. Phys. Chem. B* **2001**, *105*, 1452-1457.
(121) Tvermoes, N. A. "A mechanistic investigation of the experimental radiation sensitizer gadolinium(III) texaphyrin," University of Texas, Austin, Ph.D., 2000.
(122) Rockwell, S.; Donnelly Erling, T.; Liu, Y.; Tang, L.-Q. *International Journal of Radiation Oncology, Biology, Physics* **2002**, *54*, 536-541.
(123) Magda, D.; Gerasimchuk, N.; Lecane, P.; Miller, R. A.; Biaglow, J. E.; Sessler, J. L. *Chem. Commun.* **2002**, 2730-2731.
(124) Cameron, E.; Pauling, L. *Journal of the International Academy of Preventive Medicine* **1978**, *5*, 8-29.
(125) Cameron, E.; Pauling, L.; Leibovitz, B. *Cancer Research* **1979**, *39*, 663-681.
(126) Cameron, E.; Pauling, L. *Proceedings of the National Academy of Sciences of the United States of America* **1976**, *73*, 3685-3689.
(127) Cameron, E.; Pauling, L. *Oncology* **1973**, *27*, 181-192.
(128) Pauling, L.; Cameron, E. *Cancer and vitamin C*; Linus Pauling Institute of Science and Medicine: Menlo Park, Calif. (Norton, NY), 1979,p^pp P.
(129) Riviere, J.; Ravanat, J.-L.; Wagner, J. R. *Free Radical Biology & Medicine* **2006** *40*, 2071-2079.
(130) Gokhale, P.; Patel, T.; Morrison, M. J.; Vissers, M. C. M. *Apoptosis* **2006**, *11*, 1737-1746.
(131) Sane, A.-T.; Cantin Andre, M.; Paquette, B.; Wagner, J. R. *Cancer Chemother. Pharmacol.* **2004**, *54*, 315-321.
(132) Hvoslef, J.; Pedeersen, B. *Acta Chemica Scandinavica B* **1979**, *33*, 503-511.
(133) Ohmori, M.; Takagi, M. *Agric Biol Chem* **1978**, *42*, 173-174.
(134) Hirsch, J. *JAMA* **2006**, *296*, 1518-1520.
(135) Goldie, J. H.; Coldman, A. J. *Drug resistance in cancer : mechanisms and models*; Cambridge University Press: Cambridge, UK, 1988,p^pp P.
(136) Laing, N. M.; Tew, K. D. In *Encyclopedia of Cancer*; Bertino, J. R., Ed.; Academic Press: San Diego, 1997; Vol. 1.
(137) Chowdhary, S. A.; List, A. L. In *Encyclopedia of Cancer*; Bertino, J. R., Ed.; Academic Press: San Diego, 1997; Vol. 1.
(138) Cha, J. H.; Zou, M.-F.; Rasmussen, S. G. F.; Loland, C. J.; Schoenenberger, B.; Gether, U.; Newman, A. H. *J. Med. Chem.* **2005**, *48*, 7513-7516.
(139) Jaiswal, J. K.; Mattoussi, H.; Mauro, J. M.; Simon, S. M. *Nature Biotechnology* **2003**, *21*, 47-51.
(140) Li, C.; Winnard, P. T., Jr.; Tagaki, T.; Artemov, D.; Bhujwalla, Z. M. *JACS* **2006**, *128*, 15072-15073.
(141) Russell-Jones, G.; McTavish, K.; McEwan, J.; Rice, J.; Nowotnik, D. *Journal of Inorganic Biochemistry* **2004**, *98*, 1625-1633.
(142) Tosi, M. R.; Tugnoli, V. *Clinica Chimica Acta* **2005**, *359*, 27-45.
(143) Chari, R. V. J. *Adv. Drug Delivery Rev.* **1998**, *31*, 89-104.

(144) Woehrle, D.; Ardeschirpur, A.; Mueller, S.; Heuermann, A.; Graschew, G.; Schlag, P. *International Congress Series* **1992**, *1011*, 774-779.
(145) Kratz, F.; Beyer, U.; Schutte, M. T. *Critical reviews in Therapeutic Drug Carrier Systems* **1999**, *16*, 245-288.
(146) Antonello, A.; Tarozzi, A.; Morroni, F.; Cavalli, A.; Rosini, M.; Hrelia, P.; Bolognesi, M. L.; Melchiorre, C. *J. Med. Chem.* **2006**, *49*, 6642-6645.
(147) Sessler Jonathan, L.; Magda, D.; Mody Tarak, D.; Anzenbacher, P., Jr.; Carvalho, J.: US 6,207,660, 2001.
(148) Brunner, H.; Obermeier, H.; Szeimies, R. M. *Chem. Ber.* **1995**, *128*, 173-181.
(149) Brunner, H.; Maiterth, F.; Treittinger, B. *Chem. Ber.* **1994**, *127*, 2141-2149.
(150) Lottner, C., Bart, K.-C., Bernhart, G., Brunner, H. *J. Med. Chem.* **2002**, *45*, 2064-2078.
(151) Lottner, C.; Knuechel, R.; Bernhardt, G.; Brunner, H. *Cancer Letters (Amsterdam, Netherlands)* **2004**, *215*, 167-177.
(152) Song, R.; Kim, Y.-S.; Sohn, Y. S. *Journal of Inorganic Biochemistry* **2002**, *89*, 83-88.
(153) Song, R.; Kim, Y.-S.; Lee, C. O.; Sohn, Y. S. *Tetrahedron Letters* **2003**, *44*, 1537-1540.
(154) Lottner, C.; Bart, K.-C.; Bernhart, G.; Brunner, H. *J. Med. Chem.* **2002**, *45*, 2079-2089.
(155) Aronov, O.; Horowitz, A. T.; Gabizon, A.; Gibson, D. *Bioconjugate Chemistry* **2003**, *14*, 563-574.
(156) Sood, P.; Thurmond, K. B., II; Jacob, J. E.; Waller, L. K.; Silva, G. O.; Stewart, D. R.; Nowotnik, D. P. *Bioconjug. Chem.* **2006**, *17*, 1270-1279.
(157) Millet, R.; Urig, S.; Jacob, J.; Amtmann, E.; Moulinoux, J.-P.; Gromer, S.; Becker, K.; Davioud-Charvet, E. *J. Med. Chem.* **2005**, *48*, 7024-7039.
(158) Gibson, D.; Gean, K. F.; Katzhendle, J.; Ben-Shoshan, R.; Ramu, A.; Ringel, I. *Journal of Medicinal Chemistry* **1991**, *34*, 414-420.
(159) Appleton, T. G. *Coord. Chem. Rev.* **1997**, *166*, 313-359.
(160) Appleton, T. G.; Hall, J. R.; Neale, D. W.; Thompson, C. S. M. *Inorg. Chem.* **1990**, *29*, 3985-3990.
(161) Gibson, D.; Rosenfeld, A.; Apfelbaum, H.; Blum, J. *Inorganic Chemistry* **1990**, *29*, 5125-5129.
(162) Gandolfi, O.; Apfelbaum, H.; Blum, J. *Inorganica Chimica Acta* **1987**, *135*, 27-31.
(163) Appleton, T. G.; Hall, J. R. *Inorg. Chem.* **1972**, *11*, 112-117.
(164) Bitha, P.; Hlavka, J. J.; Lin, Y. I. In *Eur. Pat. Appl.*; (American Cyanamid Co., USA). EP304566, 1989, p 23 pp.
(165) Han, I.; Jun, M. S.; Kim, M. K.; Kim, J. C.; Sohn, Y. S. *Japanese Journal of Cancer Research* **2002**, *93*, 1244-1249.
(166) Lee, Y.-A.; Chung, Y.; Sohn, Y. *J. Inorganic Biochemistry* **1997**, 289-294.
(167) Gust, R.; Schnurr, B. *Monatshefte fuer Chemie* **1999**, *130*, 637-644.
(168) Rosenberg, B.; Van Camp, L. *Nature* **1969**, *222*, 385-386.
(169) Rosenberg, B.; Van Camp, L. *Cancer Research* **1970**, *30*, 1799-1802.
(170) Eastman, A. In *CisplatinChemisry and Biochemistry of a Leading Anticancer Drug*; Lippert, B., Ed.; Wiley-VCH: Zurich, 1999.

(171) Rosenberg, B.; Van Camp, L.; Krigas, T. *Nature* **1965**, *205*, 698-699.
(172) Mizumura, Y.; Matsumura, Y.; Hamaguchi, T.; Nishiyama, N.; Kataoka, K.; Kawaguchi, T.; Hrushesky, W. J.; Moriyasu, F.; Kakizoe, T. *Japanese journal of cancer research* **2001**, *92*, 328-336.
(173) Aggarwal, S. K. *Journal of Histochemistry and Cytochemistry* **1993**, *41*, 1053-1073.
(174) Lippert, B., Ed. *Cisplatin: Chemistry and Biochemistry of a Leading Anticancer Drug*; Wiley-VCH: Zurich, 1999.
(175) Khokhar, A. R.; Al-Baker, S.; Shamsuddin, S.; Siddik, Z. H. *J. Med. Chem.* **1997**, *40*, 112-116.
(176) Pasini, A.; Zunino, F. *Angew. Chem. Int. Ed. Engl.* **1987**, *26*, 615-625.
(177) Barzilay, G.; Hickson, I. D. In *Encyclopedia of Cancer*; Bertino, J. R., Ed.; Academic Press: San Diego, 1997; Vol. 1.
(178) Pil, P.; Lippard, S. J. In *Encyclopedia of Cancer*; Bertino, J. R., Ed.; Academic Press: San Diego, 1997; Vol. 1.
(179) Cleare, M. J.; Hoeschele, J. D.; Rosenberg, B.; Van Camp, L. In *U.S.*; (Research Corp., USA). US4657927, 1987; Vol. Division of U.S. Ser. No. 902,706, abandoned., p 7 pp.
(180) Gornet, J.-M.; Savier, E.; Lokiec, F.; Cvitkovic, E.; Misset, J. L.; Goldwasser, F. *Annals of Oncology* **2002**, *13*, 1315-1319.
(181) Canovese, L.; Cattalini, L.; Chessa, G.; Tobe, M. L. *J. Chem. Soc. Dalton Trans.* **1988**, 2135-2140.
(182) Yotsuyanagi, T.; Usami, M.; Yasuhiro, N.; Nagata, M. *Int. J. Pharmaceutics* **2002**, *246*, 95-104.
(183) Jerremalm, E.; Eksborg, S.; Ehrsson, H. *J Pharm Sci* **2003**, *92*, 436-438.
(184) Videhult, P.; Yachnin, J.; Jerremalm, E.; Lewensohn, R.; Ehrsson, H. *Cancer Letters (Shannon, Ireland)* **2002**, *180*, 191-194.
(185) Bloemink, M. J.; Reedijk, J. In *Metal Ions in Biological Systems (1996), 32(Interactions of Metal Ions with Nucleotides, Nucleic Acids, and Their Constituents)*, 1996.
(186) Fekl, U.; van Eldik, R. *Eur. J. Inorg. Chem.* **1998**, 389-396.
(187) Boreham, C. J.; Broomhead, J. A.; Fairlie, D. P. *Aust. J. Chem.* **1981**, *34*, 659-664.
(188) Appleton, T. G.; Berry, R. D.; Davis, C. A.; Hall, J. R.; Kimlin, H. A. *Inorg. Chem.* **1984**, *23*, 3514-3521.
(189) Reedijk, J. *Chem. Commun.* **1996**, 801-806.
(190) Corden, B. J. *Inorganica Chimica Acta* **1987**, *137*, 125-130.
(191) Suzuki, T.; Nishio, K.; Tanabe, S. *Current Drug Metabolism* **2001**, *2*, 367-377.
(192) Dethmers, J. K.; Meister, A. *Proceedings of the National Academy of Sciences of the United States of America* **1981**, *78*, 7492-7496.
(193) Ramstad, T.; Woollins, J. D. *Transition Met. Chem.* **1985**, *10*, 153-155.
(194) Hrubisko, M.; Balazova, E.; Ujhazy, V. *Neoplasma* **1984**, *31*, 649-653.
(195) Balazova, E.; Hrubisko, M.; Ujhazy, V. *Neoplasma* **1984**, *31*, 641-647.
(196) Bitha, P.; Child, R. G.; Hlavka, J. J.; Lin, Y. I. In *Eur. Pat.* ; (American Cyanamid Co., USA). EP185225B1, 1985, p 16 pp.

(197) Najajreh, Y.; Peleg-Shulman, T.; Moshel, O.; Farrell, N.; Gibson, D. *JBIC, Journal of Biological Inorganic Chemistry* **2003**, *8*, 167-175.
(198) Reithofer, M. R.; Valiahdi, S. M.; Jakupec, M. A.; Arion, V. B.; Egger, A.; Galanski, M.; Keppler, B. K. *J. Med. Chem.* **2007**, *50*, 6692-6699.
(199) Vassilian, A.; Bikhazi, A. B.; Tayim, H. A. *Journal of Inorganic and Nuclear Chemistry* **1979**, *41*, 775-778.
(200) Zeigler, C. J.; Silverman, A. P.; Lippard, S. J. *J. Biol. Inorg. Chem.* **2000**, *5*, 774-783.
(201) Schobert, R.; Biersack, B.; Dietrich, A.; Grotemeier, A.; Mu¨ller, T.; Kalinowski, B.; Knauer, S.; Voigt, W.; Paschke, R. *J. Med. Chem.* **2007**, *50*, 1288-1293.
(202) Mracec, M.; Mracec, M.; Simon, Z. *Revue Roumaine de Chimie* **1997**, *42*, 799-804.
(203) Simon, Z.; Holban, S.; Mracec, M.; Maurer, A.; Policec, S. *Revue Roumaine de Chimie* **1980**, *25*, 713-719.
(204) Simon, Z.; Mracec, M.; Maurer, A.; Policec, S.; Dragulescu, C. *Revue Roumaine de Biochimie* **1977**, *14*, 117-125.
(205) Witiak, D. T.; Rotella, D. P.; Filippi, J. A.; Gallucci, J. *Journal of Medicinal Chemistry* **1987**, *30*, 1327-1336.
(206) Rose, W. C.; Schurig, J. E.; Huftalen, J. B.; Bradner, W. T. *Cancer Treatment Reports* **1982**, *66*, 135-146.
(207) Rinke, K.; Grunert, R.; Bednarski Patrick, J. *Pharmazie* **2001**, *56*, 763-769.
(208) Yu, B.-Z.; Jain, M. K. *Biochim. Biophys. Acta* **1989**, *980*, 15-22.
(209) Blau, S.; Jubeh, T. T.; Haupt, S. M.; Rubinstein, A. *Critical reviews in Therapeutic Drug Carrier Systems* **2000**, *17*, 425-465.
(210) Kelso, G. F.; Porteous, C. M.; Coulter, C. V.; Hughes, G.; Porteous, W. K.; Ledgerwood, E. C.; Smith, R. A. J.; Murphy, M. P. *Journal of Biological Chemistry* **2001**, *276*, 4588-4596.
(211) Manetta, A.; Gamboa, G.; Nasseri, A.; Podnos, Y. D.; Emma, D.; Dorion, G.; Rawlings, L.; Carpenter, P. M.; Bustamante, A.; Patel, J.; Rideout, D. *Gynecologic oncology* **1996**, *60*, 203-212.
(212) Christman, J. E.; Miller, D. S.; Coward, P.; Smith, L. H.; Teng, N. N. H. *Gynecologic Oncology* **1990**, *39*, 72-79.
(213) Gamboa-Vujicic, G.; Emma, D. A.; Liao, S. Y.; Fuchtner, C.; Manetta, A. *J Pharm Sci* **1993**, *82*, 231-235.
(214) Turner, N.; Saunders, D. H. *Agr. Expt. Sta., Bull.* **1946**, *512*, 98-110.
(215) Dizman, B.; Elasri, M. O.; Mathias, L. J. *Jnl. Appl. Polymer Sci.* **2004**, *94*, 635-642.
(216) physchem.ox.ac.uk/MSDS/CE/cetylpyridinium_chloride.html 2007; Vol. 2007, p CPC has no exposure limits in MSDS.
(217) Holt, J. J.; Gannon, M. K. I.; Tombline, G.; McCarty, T. A.; Page, P. M.; Brighta , F. V.; Detty, M. R. *Bioorganic & Medicinal Chemistry* **2006**.
(218) Lippert, B.; Pesch, F. J.; Zanker, K. S.: DE 41 20 524 A1, 1992; Vol. DE 41 20 524 A1, p 6 pp.
(219) Chen, Z.; Woodburn, K. W.; Shi, C.; Adelman, D. C.; Rogers, C.; Simon, D. I. *Arteriosclerosis, thrombosis, and vascular biology* **2001**, *21*, 759-764.

(220) Lecane, P. S.; Karaman, M. W.; Sirisawad, M.; Naumovski, L.; Miller, R. A.; Hacia, J. G.; Magda, D. *Cancer Research* **2005**, *65*, 11676-11688.
(221) Grossweiner, L. I.; Bilgin, M. D.; Berdusis, P.; Mody, T. D. *Photochemistry and Photobiology* **1999**, *70*, 138-145.
(222) Modica-Napolitano, J. S.; Aprille, J. R. *Advanced Drug Delivery Reviews* **2001**, *49*, 63-70.
(223) Highsmith, S. *Biochemistry* **1986**, *25*, 1049-1054.
(224) Buchynskyy, A.; Kempin, U.; Vogel, S.; Hennig, L.; Findeisen, M.; Muller, D.; Giesa, S.; Knoll, H.; Welzel, P. *Eur. J. Org. Chem.* **2002**, 1149-1162.
(225) Lindsey, J. S.; North Carolina State University, 1998.
(226) Parker, C. A.; Rees, W. T. *Analyst* **1960**, *85*, 587-600.
(227) Lohse, J.; Nielsen, P. E.; Harrit, N.; Dahl, O. *Bioconjug. Chem.* **1997**, *8*, 503-509.
(228) Adamczyk, M.; Grote, J.; Moore, J. A. *Bioconjugate Chemistry* **1999**, *10*, 544-547.
(229) Bagchi, B. *Annu. Rep. Prog. Chem., Sect C.* **2003**, *99*, 127-175.
(230) Fery-Forgues, S.; Lavabre, D. *Journal of Chemical Education* **1999**, *76*, 1260-1264.
(231) Eaton, D. F. *Pure and Applied Chemistry* **1988**, *60*, 1107-1114.
(232) Guldi, D. M.; Mody, T. D.; Gerasimchuk, N. N.; Magda, D.; Sessler, J. L. *Journal of the American Chemical Society* **2000**, *122*, 8289-8298.
(233) Stehle, G.; Wunder, A.; Sinn, H.; Schrenk, H. H.; Schutt, S.; Frei, E.; Hartung, G.; Maier-Borst, W.; Heene, D. L. *Anti-Cancer Drugs* **1997**, *8*, 835-844.
(234) Magda, D. J.; Miller, R. A. *Abstracts of Papers, 226th ACS National Meeting, New York, NY, United States, September 7-11, 2003* **2003**, INOR-538.
(235) O'Dwyer, P. J.; Stevenson, J. P.; Johnson, S. W. *Cisplatin* **1999**, 31-69.
(236) Bernhardt, G.; Brunner, H.; Gruber, N.; Lottner, C.; Pushpan, S. K.; Tsuno, T.; Zabel, M. *Inorg. Chim. Acta* **2004**, *357*, 4452-4466.
(237) Aronov, O.; Horowitz, A. T.; Gabizon, A.; Fuertes, M. A.; Perez, J. M.; Gibson, D. *Bioconjugate Chemistry* **2004**, *15*, 814-823.
(238) Srinivasan, C.; Kluge, A. F.; Edwards, J. A. *JOC* **1977**, *42*, 3972-3974.
(239) Jung, M. E.; Lyster, M. A. *JOC* **1977**, *42*, 3761-3764.
(240) Ho, P. T.; Ngu, K. *Peptide Research* **1994**, *7*, 249-254.
(241) Lee, J.-W.; Park, J.-K.; Lee, S.-H.; Kim, S.-Y.; Cho, Y.-B.; Kuh, H.-J. *Anti-Cancer Drugs* **2006**, *17*, 377-384.
(242) Cleare, M. J.; Hoeschele, J. D. *Platinum Metals Review* **1973**, *17*, 2-13.
(243) Jung, Y.; Lippard Stephen, J. *Chemical Reviews* **2007**, *107*, 1387-1407.
(244) Lippard, S. J. In *Platinum and Other Metal Coordination Compounds in Cancer Chemotherapy*; Howell, S. B., Ed.; Plenum Press: NY, 1991.
(245) Kokotos, G.; Theodorou, V.; Constantinou-Kokotou, V.; Gibbons, W. A.; Roussakis, C. *Bioorg. Med. Chem. Letters* **1998**, *8*, 1525-1530.
(246) Craciunescu, D.; Doadrio, A.; Furlani, A.; Scarcia, V. *Chem.-Biol. Interactions* **1982**, *42*, 153-164.
(247) Henderson, W. A.; Schultz, C. J. *J. Org. Chem.* **1962**, 4643-4646.
(248) Paesen, J.; Quintens, I.; Thothi, G.; Roets, E.; Reybrouck, G.; Hoogmartens, J. *J. Chromatog. A* **1994**, *677*, 377-384.

(249) Jackson, J. E.; Soundararajan, N.; Platz, M. S.; Liu, M. T. H. *Journal of the American Chemical Society* **1988**, *110*, 5595-5596.
(250) Yutilov, Y. M.; Shcherbina, L. I. *Khimiya Geterotsiklicheskikh Soedinenii* **1987**, *5*, 639-645.
(251) Brown, D. J.; Grigg, G. W.; Iwai, Y.; McAndrew, K. N.; Nagamatsu, T.; Van Heeswyck, R. *Australian Journal of Chemistry* **1979**, *32*, 2713-2726.
(252) Honda, T.; Yoshida, S.; Arai, M.; Kaneko, S.; Yamashita, M. *Bioorg. Med. Chem. Letters* **2002**, *12*, 1925-1928.
(253) Selve, C.; Ravey, J.-C.; Stebe, M.-J.; El Moudjahid, C.; Moumni, E. M.; Delpuech, J.-J. *Tetrahedron* **1991**, *47*, 411-428.
(254) Lund, H.; Viogt, A. *Org. Syn. Coll. Vol.*, *2*, 594-596.
(255) Jamrozik, M.; Jamrozik, J. *J. f. prakt. Chemie.* **1986**, *328*, 327-330.
(256) Haeberle, N.; Eberle, O.; Mueller, F.; (Consortium fuer Elektrochemische Industrie G.m.b.H., Fed. Rep. Ger.): DE 3204953 A1, 1989.
(257) Maiella, P. G.; Brill, T. B. *J. Phys. Chem.* **1996**, *100*, 14352-14355.
(258) Cardwell, D.; Robinison, R. *J. Chem. Soc.* **1915**, *107*, 255-259.
(259) Voegtle, F.; Heimann, U. *Chemische Berichte* **1978**, *111*, 2757-2764.

VITA

Mark Fountain was born in Niceville, Florida on May 19, 1960, the son of Clarence Joseph Fountain, Jr. and Jane Kathleen Fountain After completing his work at Columbia High School, EastGreenbush, N.Y., in 1977 he went to the State University of New York (SUNY) in Plattsburgh. During this time he worked for Dr. Stuart Baum, and did research with Dr. Arnold Rheingold, and Dr. Jerome Supple. He received the degree of Bachelor of Science from SUNY Plattsburgh in December 1980. After completing his work at SUNY Plattsburgh in May 1981 he began graduate studies at the University of Maryland in Chemistry with Dr. Samuel Grim, from September 1981 to May, 1982. This was followed by graduate work at the University of Delaware in Organometallic Chemistry with Dr. Arnold Rheingold, from September 1982 to December 1985. He received the degree of Master of Science in December 1986 from the University of Delaware. He was employed as a pharmaceutical process development chemist with Johnson Matthey Pharmaceutical Materials in West Deptford, NJ from 1986 until 1995. In 1996 he moved to Epix Medical in Cambrdge, MA, also as a process development chemist where he remained for three years. He then returned to Johnson Matthey in 1999 for three years, first as a documentation specialist, then a technical services representative. Resigning this position in October 2001, he moved to Austin, married Michelle Ann Uretsky, and entered the Ph..D. program in Organic Chemistry at the University of Texas.

Permanent address: 2504 Greenland Lane, Austin, TX 78745

This dissertation was typed by Mark E. Fountain.